Design of Intratumoral Immunostimulant Formulations

By

Melissa Marie (Pressnall) Mihalcin

Submitted to the graduate degree program in Pharmaceutical Chemistry and the Graduate Faculty of the University of Kansas in partial fulfillment of the requirements for the degree of Doctor of Philosophy.

_____

Chair: Dr. Cory Berkland

_____

Dr. Laird Forrest

_____

Dr. John Stobaugh

_____

Dr. Jeff Krise

_____

Dr. Prajnaparamita Dhar

Date Defended: December 2, 2019

The dissertation committee for Melissa Marie (Pressnall) Mihalcin certifies that this is the approved version of the following dissertation:

Design of Intratumoral Immunostimulant Formulations

_____

Chair: Dr. Cory Berkland

Date Approved: December 2, 2019

Abstract

Cancer immunotherapy involves stimulation of the body's own immune system to fight cancer. Tumors possess myriad suppressive mechanisms that facilitate evasion of the immune system. Immunotherapy aims to stimulate immune cells to recognize and attack tumor tissue. While immunostimulatory agents have achieved some success in treating cancer, systemic toxicity remains a major concern. In particular, systemic exposure to immunostimulants can activate immune cells outside of target tissues, which can potentially induce side effects or autoimmune reactions. In the treatment of solid tumors, intratumoral (IT) therapy offers unique benefits as an anti-cancer strategy, especially in the ability to bypass obstacles of trafficking, tumor penetration, and severe adverse events associated with systemic delivery. IT administration of immunostimulants, for example, can work synergistically with checkpoint inhibitors making a nonresponsive 'cold' tumor 'hot' by recruiting and activating tumor infiltrating lymphocytes. Unfortunately IT administration does not necessarily preclude the manifestation of systemic adverse events; therapy transport out of the tumor and back into systemic circulation can lead to similar adverse events as seen with systemic exposure. While many researchers have worked to optimize the efficacy of immunostimulants, few have approached delivery design with the consideration of drug retention after IT administration. This dissertation sought to explore delivery strategies for two negatively charged immunostimulants, polyI:C and CpG, which are potent toll-like receptor 3 (TLR3) and TLR9 agonists, respectively. Both compounds exhibit strong induction of interferons, leading to a proinflammatory environment after binding to TLRs, thus generating memory and tumor-specific T cells. Both TLR3 and TLR9 are located intracellularly; thus negatively-charged polyI:C and CpG macromolecules must be internalized by immune cells in order to be efficacious. To achieve both goals of increased retention and intracellular delivery, polycations were selected as a delivery tool. Polycations have historically been employed for intracellular delivery of nucleic acid material. This dissertation suggests that electrostatics can aid in injection site retention through interactions with highly negatively charged extracellular matrix. In chapter 2, polylysine, at a range of molecular weights, was evaluated for its ability to complex with

immunostimulants and subsequently activate TLR(s). Chapter 3 presented a novel idea utilizing Glatiramer Acetate (GA), better known as Copaxone® as a delivery tool for immunostimulants. GA is a highly positively-charged polypeptide and is currently an FDA-approved therapy for multiple sclerosis. In this work, we generated small nanoparticles known as polyplexes, which form when mixing positively-charged GA and negatively-charged immunostimulant(s) (polyI:C or CpG). Together from chapters 2 and 3, we found that the relationship between complexation and TLR activation depends on the strength of the interaction in the polyplex. In a tumor model of head and neck squamous cell carcinoma, GA polyplexes were able to decrease tumor burden as compared to the vehicle controls. Therefore, this dissertation demonstrates that using polycations to complex with immunostimulant(s) is a promising approach to effectively deliver therapies and stimulate a local immune response.

Acknowledgements

I would first like to thank my advisor, Dr. Cory Berkland. I am so grateful that you took me into your group and for the opportunity to work with you. Thank you for providing the resources and space for me to develop into an independent scientist. You are a wonderful example of a scientist and a human being. Thank you for always challenging me, being patient with me, and having faith in me even in the times when I didn't. I am especially thankful for your ability to lead and command with kindness and light-heartedness. Thank you for everything you have done for me and taught me over the years.

I am also appreciative of the support from my committee members: Dr. Laird Forrest, Dr. John Stobaugh, Dr. Jeff Krise, and Dr. Prajna Dhar. I am grateful for your time and encouragement over the years. To Dr. Stobaugh- thank you so much for your support and kindness through a transition time in my graduate career. Your support and faith in me encouraged me to keep fighting and I am so grateful.

I would also like to thank the Pharmaceutical Chemistry department. You all took a leap of faith accepting a student from a small-town college who barely knew how to pipette. I am so grateful you did because overall, this has been an incredible experience getting to learn from and work with some of the best pharmaceutical scientists. I am so honored to be included in the KU Pharm Chem family. I am also so thankful to all the administrative staff in the department, particularly Nancy Helm, Michelle Huslig, and Nicole Brooks. I am incredibly grateful to the department for the chance to participate in planning GPEN 2016 in Lawrence, KS and then for financially supporting me to attend GPEN 2018 in Singapore. It was a truly amazing experience to network and explore a beautiful country.

Thank you to all the past and present group members I have had the chance to work with: Lorena Napolitano, Chad Pickens, Chris Kuehl, Joshua Sestak, Stephanie Johnson, Danny Griffin, Jimmy Song, Aric Huang, Mary Duncan, Jian Qian, Sebastian Huayamares, Kyle Apley, Aparna Raghavachar, Fah Chueahongthong, Justin Ruffalo, Jon Whitlow, Bryce Stottlemire, Dakota Even, Matt Christopher, Martin Leon, Brad Sullivan, and Nashwa El-Gendy. It was wonderful working with so many intelligent, kind, and uplifting people. Thank you especially to Aric Huang and Chad Groer whose collaboration was essential for the animal work in chapter 3.

Thank you to the all the amazing friends who have been a huge part in making the last 5.5 years so enjoyable. KU Pharm Chem allowed me to meet and make lifelong friends. To our best friends Chris and Cassie Kuehl, we love you so much and are so grateful for your friendship and the countless adventures together. To my best friend and first friend in Lawrence, Lorena Napolitano, you are such a blessing to my life, and I love you so much! Thank you for both your scientific support and friendship which truly helped me get through graduate school. To my fitness coaches Mitch Moore and Kyle Thatcher, thank you for teaching me a sport that was the perfect outlet for stress, and I have come to love!

To my workout partner in crime, Brett Leonard, thank you for constantly pushing and encouraging me both in weightlifting and in life, and for becoming one of my best friends. Thank you to Barlas Buyuktimkin, Chad Pickens, and Josh Sestak for being not only great scientific mentors, but also wonderful friends. Thank you to everyone else in "the gang" who made my time here in Lawrence a wonderful adventure!

Thank you to my family who were constantly supportive and loving. To my in-laws Mike and Janet Mihalcin, and Matt, Nikki, Makiah, Jon, Angela, and Kristin Mihalcin, thank you for your love and encouragement over the past years. To my sister, Kelsey Pressnall, thank you for reminding me of what I am capable of and for your love and encouragement. I cannot go without thanking the humans that made me who I am, Brian and Robin Pressnall. Thank you for the sacrifices you made to make sure I had every opportunity I needed to be successful. Thank you for raising me to understand the value of hard work, respect, and kindness.

To the most incredible and handsome man on the planet, my husband, Jason Mihalcin, I am the luckiest woman alive to have such a supportive and patient partner. Thank you for being there for me through my toughest battles. Thank you for taking care of everything especially in the months leading up to the defense. Thank you for pushing me, for reminding me of my strength to persevere, for keeping me sane, and for your unconditional, and unfailing love.

Finally, I thank God for the blessings he has given me. I hope that I can use this PhD to serve in ways that glorify God.

Melissa (Pressnall) Mihalcin

December 2, 2019

Table of Contents

Chapter 1:

Intratumoral Delivery of Cancer Therapeutics: Biophysical Considerations for Therapies in Clinical Trials

1. Introduction

Recent clinical successes of intratumoral (IT) therapy have stimulated a wave of new clinical trials investigating IT therapies both alone, and in tandem with other immuno-oncology agents. IT therapy offers unique benefits as an anti-cancer strategy, especially in the ability to bypass obstacles of trafficking and tumor penetration.[1] Severe adverse events associated with systemic delivery of cancer immunotherapies[2-3] can be avoided by delivering small doses IT.[4] IT administration of immunostimulants, for example, can work synergistically with checkpoint inhibitors making a nonresponsive 'cold' tumor 'hot' or by recruiting and activating tumor infiltrating lymphocytes.[4-6] Intuitively, the design of IT therapies is significantly different than that of systemic cancer medications, as these localized interventions aim for retention at the administration site or draining lymph nodes with limited systemic exposure. In this review, we highlight transport mechanisms involved in IT delivery and recent clinical trials while elucidating relationships between biophysical characteristics of the formulation with efficacy.

1.1 A Brief History of IT Therapy

Merck's acquisition of Immune Design sparked a new wave of activity around the already building tide of IT therapy. Leading up to its acquisition, Immune Design had disclosed two IT immunotherapies, G100 and ZVEC-IL12.[7-8] G100 is a stable oil-in-water emulsion containing glucopyranosyl lipid A (GLA), a potent toll-like receptor 4 (TLR4) agonist that induces activation of local dendritic cells (DCs) to elicit broad, patient-specific anti-tumor immune responses.[8] Notably and importantly for the broad consideration of IT immunotherapies, G100 exhibited abscopal effects - the shrinkage of even non-injected tumors.[9] This highly promising therapy received orphan drug designation by the U.S. Food and Drug Administration (FDA) and European Medicines Agency (EMA) for follicular non-Hodgkin's lymphoma, further highlighting IT interventions as a compelling therapeutic approach.[10] Moving forward, G100's efficacy was even more pronounced when applied in combination with Merck's anti-PD1 checkpoint inhibitor, Keytruda®, alongside radiation therapy.[8]

The first successful IT cancer therapy was performed over 100 years ago by Dr. William Coley on patients with inoperable solid tumors. Coley noticed a patient with an inoperable egg-sized sarcoma on the face was completely cured after suffering a severe infection from a failed skin graft. He proposed that by introducing a bacterial infection at the site of the patient's tumor, an immune response against the tumor might be generated. This intervention proved an unprecedented success, and Coley went on to treat many more patients with bacterial-derived heat-killed toxins. Coley's Toxins became one of the first examples of cancer immunotherapy.[11-12] With the introduction of radiation and chemotherapy, Coley's toxins largely faded into the background and are no longer in use. Since Coley's seminal work, very few IT cancer therapies have been approved in humans, but many have been investigated in clinical trials.

Among the few IT therapies available today, the Bacillus Calmette-Guerin (BCG) instilled transurethral for patients with bladder cancer can be considered an IT therapy of sorts, which applies the very same concepts first laid out by Coley. First used nearly 40 years ago, no other treatment for bladder cancer has surpassed the success of BCG treatment.[13] Imiquimod, a TLR7 agonist, is the only other FDA-approved IT therapy for cancer. Imiquimod is topically applied to genital warts or basal cell carcinomas[14]. Today, there are many more agents being investigated for IT delivery that exploit the immune system, including pathogen associated molecular patterns (PAMPs), monoclonal antibodies (mAbs), cytokines, small molecules, viral and gene therapies, and autologous cells.[15]

Despite scientific advances in the field of oncology, generally, cancer mortality rates have decreased only marginally over the past three decades.[16] The major persisting barriers for effectiveness and toxicity in cancer immunotherapies stem from delivery and transport constraints, as well as off-target adverse events. Systemically delivered therapeutics encounter countless obstacles on their journeys to tumor tissue that lead to a very small fraction of the compound reaching the tumor while much of it remains in circulation throughout healthy tissues.[17] Reaching the tumor alone is not a sufficient criterion for dictating efficacy with a therapeutic agent. The drug must penetrate the tumor where it will ultimately encounter the TME, which often differs drastically from healthy tissue. While IT administration of therapeutic agents can

overcome some of the concerns of systemic delivery, we must consider the TME and its potential retention, clearance, and modification mechanisms.

1.2 Tumor Microenvironment

The TME is heterogeneous between patients, tumor types, and often even within individual tumors, making generalities about transport difficult to ascertain. Overall, tumor tissue is physically distinct from normal tissue in that it has poorly organized vasculature with inconsistent vessel diameters and more prevalent branching.[18] Further, tumor cell distance from blood vessels results in restriction of oxygen supply and hypoxia in portions of the tumor.[19] This roughly organized vasculature and hypoxic setting creates a microenvironment with increased fluid leakage and elevated interstitial fluid pressure (IFP). These conditions support decreased uptake of therapeutic molecules, which is correlated with poor prognosis in some cases.[20] The lack of proper vasculature for gas exchange and delivering nutrients leads to areas of hypoxia within a tumor.[21-22]

When delivering a drug systemically, distribution to all cells in a tumor is dependent on the distance between vascular beds. The compound may have to penetrate a tumor up to 200 μm to reach all of its targeted cells.[23] Moreover and compared to the extravascular space in healthy tissue, tumors tend to have higher extracellular matrix density lacking functional lymphatic vessels. This dense network causes increased interstitial fluid pressure which further limits interstitial diffusion and the drainage of fluid from the tissue.[20, 24] Together, dense but leaky vasculature and limited lymphatic drainage may contribute to enhanced permeability and retention of tumor tissue, however, this phenomena has not been fully supported in human tumors.[25-26] These conditions can decrease uptake of circulating therapeutic molecules, which is correlated with poor prognoses in some cases.[20]

While intracellular pH in tumors and normal tissue is similar, extracellular pH can be more acidic in tumors.[27] Increased extracellular acidity and anerobic glycolysis alters the pH gradients found in the TME versus healthy tissue.[27-28] Evidence suggests that higher acidity may increase tumor cell invasion and

metastatic potential while also aiding evasion of immune surveillance.[29-30] For drugs that rely on ionization-dependent diffusion, the extracellular pH may cause the drug to become charged, preventing diffusion across membranes.[25, 27]

Tumor tissue contains myriad immune-suppressive signals and mechanisms that allow malignant cells to proliferate undetected by the immune system. T-regulatory cells are attracted to the tumor by chemokines and aid in suppressing antigen presenting cells (APCs) that may otherwise stimulate a response against tumor antigens.[31] Additionally, tumor cells can secrete anti-inflammatory and regulatory cytokines that facilitate cancer growth and directly prevent dendritic cell (DC) activation. Tumor cells can also limit the expression of co-stimulatory molecules (MHC II, CD80, CD86), potentially inducing anergy or senescence in infiltrating T cells.[31-32] At the other extreme, overstimulation can cause T cell exhaustion from chronic exposure to tumor antigen.[33] Finally, tumor cells can also downregulate the expression of tumor antigen over time, evading recognition by cytotoxic T-lymphocytes (CTLs). Cytotoxic T lymphocyte antigen 4 (CTLA-4) and programmed death ligand 1 (PD-L1) pathways are both exploited by tumors. While engaging different mechanisms, both induce immunosuppressive signals through cytokines that reduce proliferation or cause apoptosis of T-cells.

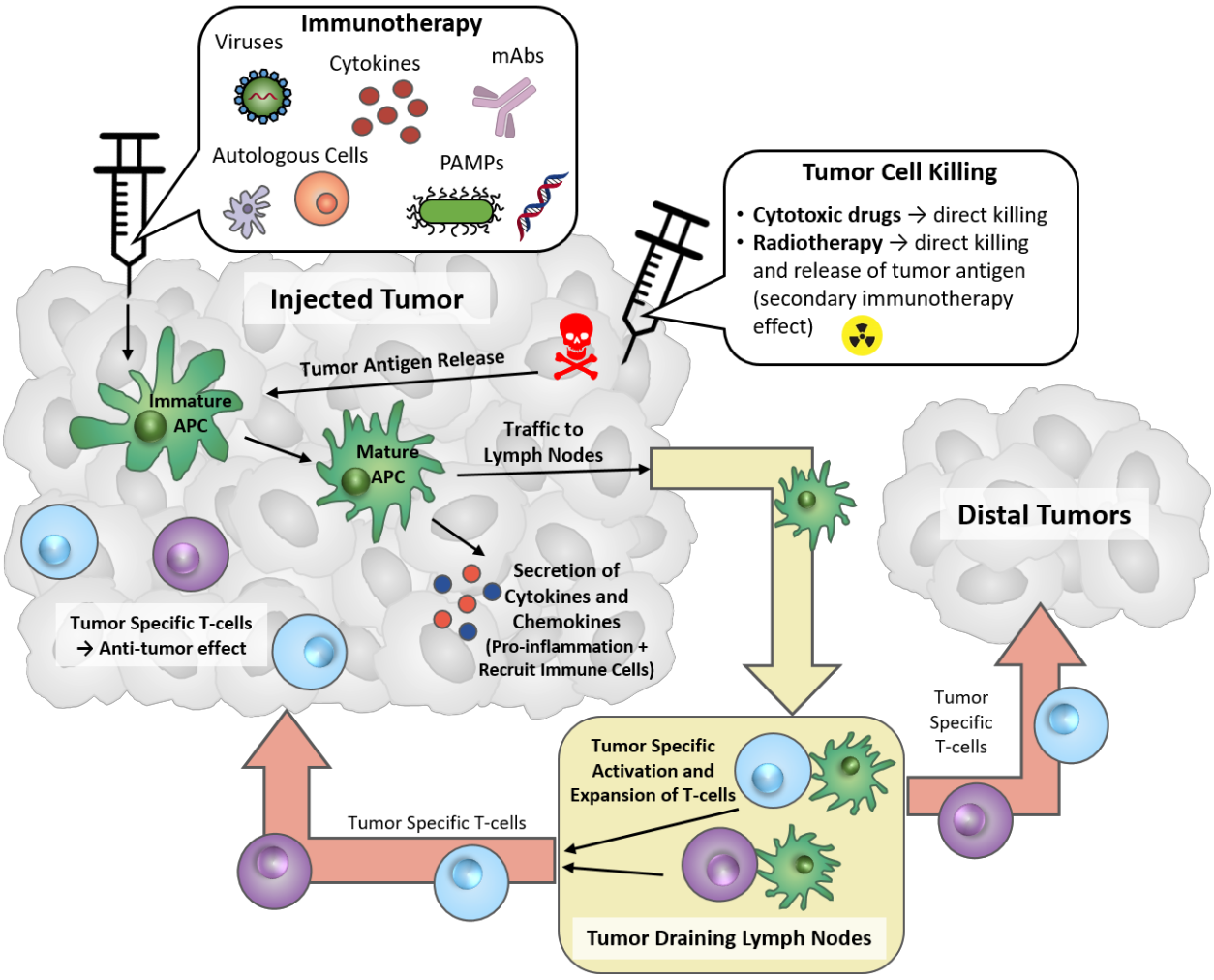

Figure 1. Concept of intratumoral (IT) immunotherapy with an abscopal effect. Injection with immunotherapy can activate an innate immune response leading to systemic effects due to circulating immune cells.

1.3 Overcoming the TME (Immune mechanism of immunostimulants)

Traditional cancer treatments like chemotherapy and radiation aim to directly kill tumor cells and the mechanism of action is not directly limited by the TME. On the other hand, clinical studies indicate the suppressive environment within the tumor can be overcome by immunostimulants. Immune cells can be activated by immunostimulants in the presence of tumor antigen, traffic to lymph nodes, and then create tumor antigen specific T cells via cross presentation (**Figure 1**). These antigen-specific T cells can then circulate back to the tumor or to distal tumors and instigate tumor cell killing. The activation of the innate immune response creates a pro-inflammatory environment and can result in recruitment additional immune

cells to the tumor. Some of the actives used in cancer therapy that will be reviewed in this article are listed in **Table 1**.

Table 1. Strategies to treat cancer.

Category	Mechanism	Cells Types Involved	Refs
Pathogen-Associated Molecular Patterns (PAMPs)	• Binding toll-like receptors (TLRs), RIG-I-like receptors (RLRs), NOD-like receptors (NLRs), and cell membrane components • Downstream signaling leading to innate immune response	Immune cells, cancer cells	34
Cytokines	• Binding to specific cell-surface glycoproteins • Downstream signaling leading to innate immune response • Direct anti-proliferative activity	Immune cells, cancer cells	35
Viruses and Plasmids	• Interaction of viral surface proteins with cell surface proteins • Target cancer cells by exploiting pathways, receptors, and mechanisms that promote tumor growth • Viruses can be used to infect cancer cells or as vehicles for gene delivery • Cell death *and* downstream signaling leading to innate immune response	Immune cells, cancer cells	36
Monoclonal antibodies (mAbs)	• Binding to specific protein on surface of tumor or immune cell • Checkpoint blockades inhibit immune suppression • Other mAbs can mark cells for death or aid in immune activation	Immune cells, cancer cells	37
Small Molecules	• Extra and Intracellular targets, must diffuse or transport through cell membrane • Cytotoxins → Cause damage to various cell functions • Targeted drugs → disruption of specific pathways critical for tumor cell progression	Cancer cells, rapidly dividing cells	38-39

1.4 Intratumoral Transport

Identifying and targeting dysregulated immune mechanisms within the TME is key, but an understanding of transport in the TME is also crucial for the design of IT cancer therapies. With IT injection,

transport considerations can be simplified to the major themes of molecular transport within the TME, exfiltration from the TME, cellular uptake, and binding to intra- and extra- cellular proteins (**Figure 2**). IT transport mechanisms are influenced by various factors that affect the retention or transport out of the tumor of the anti-cancer therapy (**Table 2**).

Transport of molecules through normal extracellular matrix is based on both diffusion along a concentration gradient as well as advective convection (or bulk transport of mass) along a pressure gradient.[18] Conversely in the TME, transport of anti-cancer agents after intratumoral administration are governed by diffusion, as elevated IFP makes the bulk IT pressure gradient negligible.[40-41] Close to blood vessels, however, where IFP can exceed that of the vascular fluid, a gradient is created and intravasation of the therapeutic agent out of the tumor can occur by diffusion and advective transport.

Though the blood vessels represent an escape route for the therapeutic agent, the abnormal and poorly organized vascular architecture characteristic of the TME increases retention at the tumor cells that are distant from the vessels, as compared to normal tissue.[42] The absence of lymphatics in the TME increases IFP and reduces the elimination or drainage of the agent before its anti-cancer action, improving IT retention.[43-44] Despite the relatively ineffective lymphatic drainage in the TME, it still represents the major route for metastasis and a route of escape for the IT therapeutic.[45] Therefore, angiogenesis, which seeks to normalize tumor vasculature leading to increased blood flow and reduced IFP, can result in a decrease in retention time when enhanced within the tumor.[46-48] Vascular permeability could have a negative effect on tumor retention time if encumbered, but this characteristic is insignificant in most tumors because blood vessel fenestrations are present and confound its effects.[49-50]

Densely packed collagen fibers are characteristic of the TME, and they pose transport resistance, which results in an increase in intratumoral retention.[18, 51] Fibrillar collagen and high IFP, among other TME characteristics, contribute to a high mechanical solid stress in the tumor.[52] This stress results in an effect on retention similar to that of IFP. Cellular packing density is also a relevant factor; loosely packed tumor cells enable fast, thorough penetration by the therapeutic agent, increasing retention at tumor.[53] However, the inverse can be the case where densely packed cells decrease drug retention as well. Finally,

cellular uptake or binding of the therapy can occur by passive diffusion, active transport, or other mechanisms depending on molecular properties.

Drug features such as molecular size, charge, and other properties (**Table 2**) influence intratumoral residence time. Water soluble molecules diffuse more easily in the TME resulting in a lower retention in the tumor,[54] but increases in hydrodynamic radius can reverse these effects. It is critical to balance size such that a therapeutic or its carrier is small enough to diffuse through the TME while avoiding clearance through lymphatic drainage.[55] Drug diffusion and retention deep inside the tumor mass is largely affected not only by the molecular size but also binding kinetics and affinity.[54] Molecular charge may also be exploited such that the acidic extracellular pH in the tumor has a positive impact on the retention. The plethora of factors that influence TME transport offer unique opportunities for the targeted delivery and retention of drugs in the IT space such that the exploitation of these abnormalities can be harnessed to maximize therapeutic effect.

Table 2. Factors affecting transport of therapy out of the tumor after intratumoral injection.

Tumor tissue factors	**Phenomena**
Microvascular permeability	Decreases retention at tumor, but insignificant where blood vessel fenestration is present
Abnormal vascular architecture	Increases retention at the tumor
Absence of lymphatics	Increases retention at the tumor
Interstitial fluid pressure (IFP)	Increased IFP increases retention time at the tumor but decreases it close to vessels
Solid stress elevation	Increases retention within the tumor, but decreases the retention close to vessels
Angiogenesis	Decreases retention at the tumor
Physicochemical factors	**Phenomena**
Concentration gradient	Increases diffusion out of tumor, decreasing retention
Water solubility	Water soluble agents diffuse easily in the TME, decreasing retention in tumor
Extracellular pH	Effect on retention at tumor depends on the carcinogenic agent's molecular properties (pI, pKa)
Fibrillar collagen	Increases retention at tumor
Cellular packing density	Low packing density increases retention at tumor

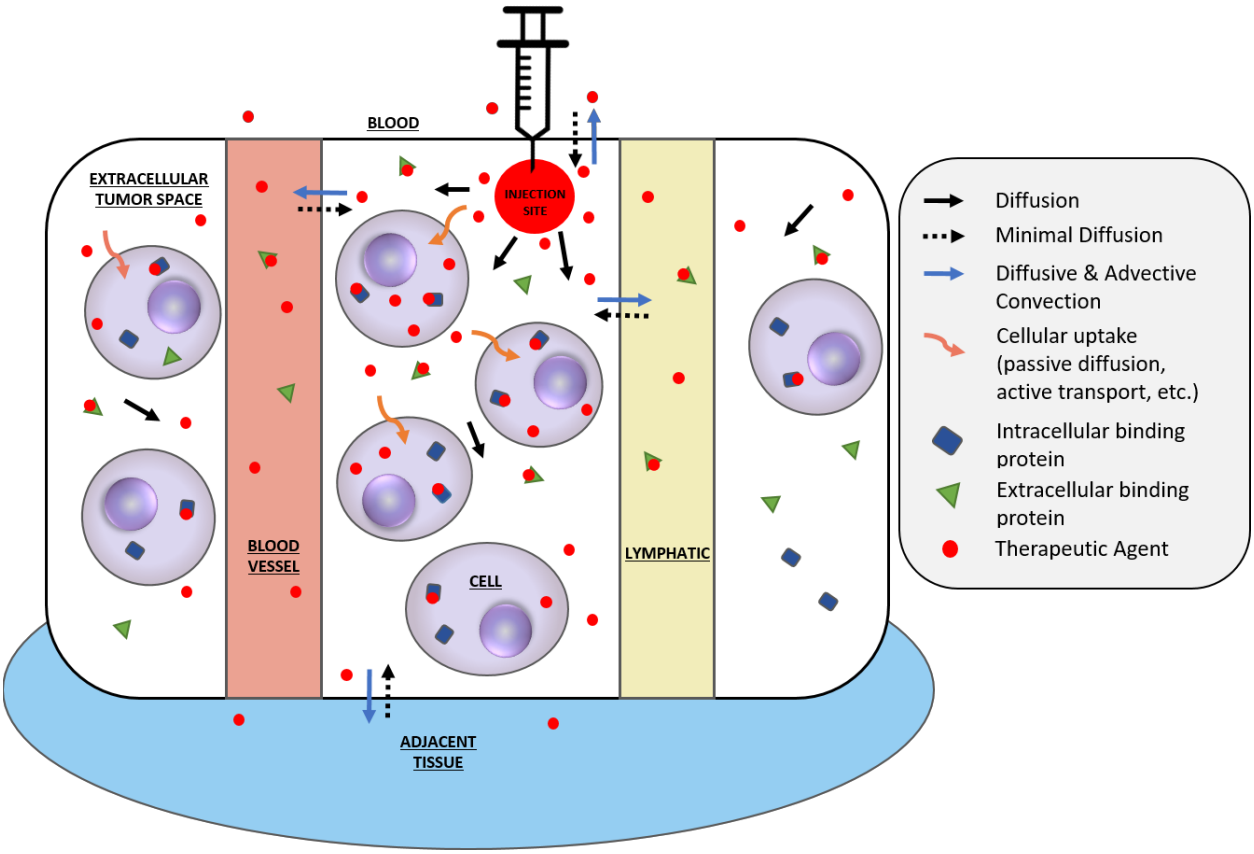

Figure 2. Representative transport and kinetic processes in intratumoral injection therapies. The therapeutic agent can diffuse through the TME, enter the cell, be bound by extracellular or intracellular proteins, unbind them, or leave the tumor into blood vessels, lymphatics, peripheral blood or adjacent tissue by diffusion and advective convection. Diffusional transport the agent back into the tumor is expected to be minimal.

2. Current Cancer Therapies

2.1 Radiation

Radiation therapy employs highly focused energy to kill or damage tumor cells.[56-58] It works by damaging the DNA of tumor cells to prevent their proliferation and cause cells to die. The goal of radiation therapy is to direct waves to cancer cells while limiting exposure to normal cells. Radiation therapy can be used to treat tumors alone, but it is also employed in combination with other cancer treatments, such as chemotherapy, immunotherapy, and surgery.[57-59] For instance, radiation can be used to shrink the tumor before surgery or to eliminate residual tumor cells post-surgery. Radiation therapy can be local, externally

or internally, where the radiation source is from an external machine or from a radioactive source placed at or near the tumor. Contrastingly, systemic radiation therapy involves taking a radioactive drug taken orally or IV, allowing the drug to be distributed throughout the body and target towards tumor cells. The type of radiation therapy given to patients may depend on a variety of factors, including the type of cancer, the size of the tumor, and the proximity of the tumor to radiation sensitive normal tissues. Despite efforts to minimize radiation damage to non-cancerous normal tissues, damage to normal tissues is inevitable, leading to side effects such as fatigue, hair loss, and skin irritation.

2.2 Chemotherapy

Cancer therapy was dominated by surgery and radiation until the 1960s when a plateau in survival rates for advanced cancers was finally overcome with the addition of chemotherapeutical drugs with these treatments. Chemotherapies are cytotoxic anti-cancer agents that target quickly proliferating cells non-selectively; both normal and cancer cells are subject to their mechanism of action.[60] These agents can be classified according to their many varied cytotoxic mechanism as alkylating agents, platinum compounds, antimetabolites, anthracyclines, topoisomerase inhibitors, tubulin-binding drugs, and tyrosine kinase inhibitors.

The administration routes for chemotherapy include intravenous, intramuscular and oral. The most common route of administration is intravenous, given the fact that most chemotherapeutic drugs exhibit poor oral bioavailability. Chemotherapy drugs undergo metabolism in the liver followed by excretion via the kidney or bile, but the metabolism differs among patients, mostly due to genetics. Patients with faster metabolisms may process and excrete the agents too rapidly to benefit from therapeutic effects, while those with slow metabolism have an excessive amount of drug reach their bloodstream, which makes them suffer the side effects more.[61] All chemotherapy patients, however, will suffer from some degree of consequences from systemically administered, non-selective cytotoxic action.

2.3 Immunotherapy

Cancer immunotherapy stems from Coley's seminal work and harnesses the body's own immune mechanisms to fight cancer. Though the first immunotherapies can be traced back over a century ago, it is only in the last decade that scientists have made significant progress in creating immunogenic cancer therapeutics as alternatives to traditional treatments like chemotherapy and radiation. Today, several therapies have been approved to treat broad types of cancer.[62] The major classes of immunotherapies include checkpoint inhibitors, oncolytic viruses, cell-based immunotherapies, cytokines and adjuvants.[63-64] Immune checkpoint inhibitors block the checkpoint receptors to prevent tumor cells from escaping immune system attacks, resulting in enhanced anti-tumor responses. Ipilimumab (Yervoy®), an antibody against cytotoxic T-lymphocyte antigen-4 (CTLA-4), is the first approved and most notable immune checkpoint inhibitor that significantly increased the survival of metastatic melanoma patients.[65-66] Other major inhibitors include the antibodies of programmed cell death protein-1 (PD-1) (e.g. Keytruda) or its ligand (PD-L1) (e.g. Imfiazi).[66] However, the use of these inhibitors are commonly associated with immune-related adverse events (irAEs) and toxicities as a consequence of over activation of T-lymphocytes.[67] Oncolytic viruses (OVs) fight cancer by both infecting the cancer cells and stimulating anti-tumor immune responses, and can be engineered with optimized tumor selectivity. The oncolytic herpesvirus talimogene laherparepvec (T-Vec) is the first approved OV for the treatment of advanced melanoma, but its toxic side effects caused by genetic manipulation still remain a safety concern.[68] Cytokines, often combined with the use of adjuvants to boost the efficacy, are immunomodulators that enhance the host anti-tumor immune responses. Interferon-α and interleukin-2 are two types of cytokines that have been approved for the treatment of several types of leukemia and melanoma.[69] Anther branch of immunotherapy includes adjuvants, which are substances that mimic the natural microbial ligands and are added to vaccines to improve immunogenicity. Cervarix, an approved vaccine for human papillomavirus (HPV) contains an adjuvant called AS04 that includes a TLR4 agonist-based system.[70]

Cellular immunotherapies, including adoptive cell transfer, enhance the tumor antigen presentation to the immune cells and improves the efficiency to target or kill tumor cells. One form of this rapidly emerging immunotherapy called chimeric antigen receptor T (CAR-T) therapy involves autologous T cells engineered to be specific for antigens expressed on the tumor. Typically, this therapy also requires a pre-conditioning treatment of lymphodepletion prior to infusion of the cells for increased T cell expansion. The first CAR-T cell therapy, Kymriah was approved by the FDA less than two years ago, in 2017 for the treatment of B-cell precursor acute lymphoblastic leukemia (ALL) that is refractory or in the second or later relapse. Kymriah, or tisagenleceucel, is a CD19 directed autologous T cell containing co-stimulation zone 4-1BB (CD137). The second and only other approved CAR-T cell therapy, Yescarta (axicabtagene ciloleucel) was approved by the FDA only a few months after Kymriah. Yescarta is also a CD19 directed CAR-T cell but differs structurally from Kymriah. Yescarta is approved for use in adults with relapsed or refractory diffuse large B-cell lymphoma (DLBCL). While CAR-T cell therapy dominates the adoptive transfer cancer immunotherapy another therapy called Provenge or sipuleucel-T was the first cancer vaccine to be FDA approved. Provenge is comprised of autologous T cells selective for prostate acid phosphatase (PAP) that is expressed in 95% of prostate cancers.[71-72] The most common adverse reactions to Provenge include fever, and fatigue. Provenge, interestingly, does not seem to cause CRS as CAR-T cell therapies do. For all these T–cell-based therapies, insufficient cell trafficking, tumor microenvironment, inhibitory cytokines, and regulatory T-cells are still obstacles for the efficacy of the therapies.[73]

Together, the explosion of immunotherapeutic breakthroughs illustrates the immense promise of using the immune system to fight cancer, but each of the examples carry substantial risks as a consequence of systemic exposure. Adjuvants and TLR agonists can trigger intense immune anaphylaxis that resembles that of sepsis. CAR-T technologies have been extensively reported to leave patients susceptible to off-target toxicities. These unmitigated dangers highlight the importance of new strategies for treating cancer that can act in safer, more specific fashion. Leveraging the TME through IT administration is one such compelling approach to this problem, and in this review we will assess the state of these developing technologies.

3. IT Therapies in Clinical Trials

Traditional cancer research has focused on the development of cytotoxic drugs that target cancerous cells with higher degrees of specificity. Today, many approaches are seeking to harness the power of the immune system to stimulate anti-tumor responses. Particularly with IT immunotherapy, the aim is to employ the tumor as its own vaccine.[4] A major benefit of IT immunotherapy is the potential to achieve an abscopal response due to generation of circulating anti-tumor immune cells **figure 1**. While many types of IT therapies are in progress for clinical trials, we will mainly discuss trials with posted or published data and we will only briefly consider the clinical therapies yet to produce results. Highlights of recent and upcoming clinical trials of IT therapies are reflected in **table 3.**

3.1 Pathogen-Associated Molecular Patterns

Pathogen-Associated Molecular Patterns (PAMPs) are non-self molecules that inherently activate innate immune responses. PAMPs are recognized by pattern recognition receptors (PRRs) including toll-like receptors (TLRs), nucleotide-binding oligomerization domain (NOD)-like receptors, RIG-I-like receptors (RLR), stimulator of interferon genes (STING) receptors, and C-type lectin receptors (CLR).[74] For example, motifs from bacterial infection can be detected and swiftly acted against when unmethylated CpG DNA binds to TLR9 on the endosomal membrane of cells to induce immune activation.[75-76] Multiple CpG structures have been developed to ligate this pathway, and many elicit different (albeit robust) immune responses. Some approaches have multimerized CpG or even modified it as closed loops in favor of increased stability and efficacy.[5, 77-78] Derivatives of lipopolysaccharide (LPS) sourced from gram negative bacteria are another class of PAMP that stimulates an immunity through binding TLR4 on the outer cell membrane.[8] Several other agonizing pathways are under investigation in cancer immunotherapy including mimics of pathogen infection, RNA or DNA, which bind to TLR3, TLR7/8, RIG-I receptors, or STING receptors.[4, 74] Finally, attenuated bacteria itself has been explored in IT immunotherapy; intravesicalar BCG for bladder cancer is one of the few "intratumoral" immunotherapies that is currently FDA approved.[79]

PAMP immunotherapies are some of the first developed for IT administration. However, since these motifs are formulated to mimic components of bacterial and viral pathogens (which the human body is primed to elicit efficient and robust immunity against), many of these candidates pose a high probability for significant adverse events (AEs) when these PAMPs are able to leak into systemic circulation. For example, several trials investigating SD-101, a CpG oligodeoxynucleotide, in combination with other anti-cancer modalities have resulted in a 100% AE rate that includes detriments seen in authentic pathogen infections such as sepsis. It seems that PAMPs alone act as a major driver of AEs (as opposed to combination therapy implements); one trial studying G100, a synthetic TLR4 agonist, led to an AE incidence greater than 80%.

3.1.1 Tumor Retention Mechanism of PAMPs

The mechanism of PAMPs is dependent on receptor binding which triggers downstream signaling cascades to promote innate immune responses. Receptors for PAMPs are located on both extra- and intracellular membranes of immune cells (depending on the mechanism). An ideal IT therapy incorporating PAMPs should both be formulated to target these receptors and retain at the injection site. While IT administration can reduce the side effects associated with systemic administration, immunostimulatory molecules can still leak out of the tumor and cause AEs as if they were injected systemically.

Unmethylated CpG oligonucleotides are PAMPs that mimic bacterial DNA and trigger an innate immune response upon binding to TLR9. PF-3512676 is a class B, linear CpG formulated as a sodium salt with a molar mass of 8204 g/mol.[80] The formulation of PF-3512676 is proprietary, however, we presume it is un-modifed, water-soluble, negatively charged, and does not form higher order structures.[81] Clinical trial results are promising with IT administration in B-cell lymphoma and mycosis fungoides but interestingly a higher percentage of AEs were experienced in mycosis fungoides patients receiving the same dose.[82] The differences between the AEs could be a result of therapy retention diversity due to the extreme heterogeneity in vasculature of tumors across different types and locations. In a phase 2 study with lymphoma patients, an increased dose resulted in similar efficacy but more than doubled the percentage of AEs, likely a result of increased systemic exposure.[83] Another presumably unmodified and soluble CpG therapy, SD-101, is a

class C CpG. While the structural and formulation information is proprietary, CpG class C is known to form dimers. In IT trials, SD-101 exhibited promising abscopal effects, however, there were 100% grade 1-2 AEs, and a high incidence of AEs at grade 3 or above including some severe AEs (SAEs).

Many approaches have utilized structurally modified CpG ODNs to increase immunogenicity and stability. IMO-2125 exploits an interesting design in its two strands of class C CpG linked at the 3' end consisting of an 11-mer of CpG on each flanking end to allow formation of intermolecular structure that deters intramolecular interaction.[78, 84] Favorable potency may be retained by the exposed 5' ends which are pertinent for CpG's binding mechanism.[76, 84] This variant is formulated as a sodium salt with a molecular weight of 7712 g/mol and likely forms dimers.[76, 85] IMO-2125 has been granted fast track designation and orphan drug designation by the FDA and has shown promising results in early trials with fewer AEs than other most other IT TLR agonists. Additionally, this modified CpG therapy reaps increased TLR9 activation over unmodified CpG likely due to increased metabolic stability from the chemical linkage of the 3' ends.[84]

Another consideration for CpG based therapies is the type of backbone. In nature, CpG has a phosphorodiester (PO) backbone, however, synthetic CpG is often made with a phosphorothioate (PT) backbone to increase its stability *in vivo* to enhance potency.[86] The creators of MGN1703 purport that the PT backbone is to blame for toxic side effects seen when injecting this variant of CpG, however.[87] They developed a covalently-closed loop of CpG with its native PO backbone in attempts to avoid PT-associated toxicity and enhance the stability that hinders the use of native PO. Similarly, CMP-001 is a CpG class A with the native PO backbone that is modified to assemble into quarduplexes.[5, 76] Clinical results for both of these compounds are pending, and they may provide an interesting precedent for future trials employing modified and native backbones of CpG.

One method to boost potency by increasing intracellular PAMP delivery is formulation with a polycationic carrier. PAMPs whose receptors are intracellular (like TLR9, TLR3, and RIG-I) may benefit from a cationic carrier or particulate formulation for attraction to cell surfaces and increased APC uptake, respectively. Two such TLR3 agonist candidates, Hiltonol and BO-112, include polyI:C formulated with polycations for improved intracellular delivery potential. This strategy may also increase retention at the

injection site and minimize systemic exposure due to increased size and electrostatic interactions at the site of injection. In the most recent update of an IT BO-112 clinical trial, patients exhibited only mediocre overall response rate (ORR) and high percentage of AEs, however, patients saw increase in immune circulating cells and no BO-112 was detected in the blood post injection indicating injection site retention.[88] According to a patent describing its formulation, BO-112 is an aqueous composition at pH 2.7-3.4 with glucose or mannitol in an optimal particle size range of 45-85 nm and zeta potential between 40-45 mV.[89] Optimal size of particles for APC uptake and processing is estimated to be ~100 nm, similar to that of authentic viruses.[90] The N/P ratio for the polyI:C/PEI complex is between 2.5-4.5 and the PEI MW is between 17.5-22.6 kDa.[89] IT Hiltonol (polyI:C:LC) showed preliminary success in a single patient on both local and distal tumor sites however systemic side effects or AEs were not reported.[91] Hiltonol is formulated with carboxymethylcellulose (CMC), a hydrophilic, negatively charged material, in an aqueous saline solution. The molar ratio of PO4 groups to the ε amino group of the lysine in polyIC:LC is 1:1 which corresponds to an excess of ε amino groups which may contribute to further complexing with CMC.[92] The polylysine used ranges from 13-35 kDa.[92] As intracellular delivery is critical for agonists with intracellularly located TLRs, formulation with a polycation addresses the attraction to cell surfaces and aids in tumor retention.

RIG-I agonist candidate, MK-4621 is a synthetic RNA oligonucleotide that alone caused 100% grade 1-2 AEs and 48% grade 3-4 AEs in a (terminated) IT clinical trial in solid tumors.[93] Upcoming trials plan to use a complex of MK-4621 with a PEI variant (JetPEI).[94] It will be interesting to learn whether the complexation of negatively charged RNA with positively charged JetPEI will increase retention and intracellular delivery while decreasing systemic toxicity or AEs in comparison to uncomplexed MK-4621.

Another strategy for improving efficacy and retention is formulation into an emulsion. An optimized TLR4 agonist, G100 is a glucopyranosyl Lipid A (GLA) derivative with a single phosphate group and six C_{14} acyl chains formulated in a squalene emulsion.[95] The emulsion contains the excipients squalene, egg phosphatidyl choline (PC), DL-α-tocopherol, and Poloxamer 188.[96] The particle/droplet size has been reported to be 82.7- 111 nm[95-98] and zeta potential measurements -17 mV.[90] Because TLR4 is located on

the surface of the cell, intracellular uptake is not necessary for the mechanism of a TLR4 agonist. Rather, formulation efforts should focus on accessibility of the agonist as well as drug release, and local retention. For lipid emulsions, retention in tumor tissue is optimal for cationic materials, and in a size range of 120-250 nm.[99-100] Research has indicated that the formulation of GLA has critical effects on TLR activation and that *in vitro* data does not translate well to *in vivo* results.[98] GLA-SE (G100) resulted in greater immune activation than GLA formulated as an aqueous nanosuspension in various mouse models as well a human skin explant model.[98] Efficacy of GLA itself could be highly dependent on GLA density within a particle or droplet which is dictated by formulation and would need to be optimized in humans.

A more rudimentary approach to immunotherapy is the use of live attenuated bacteria. IT Clostridium novyi-NT trials are in progress but too early on to draw comparisons.[101] IT BCG resulted in no better than stable disease and all patients experienced AEs or SAEs. BCG is a gram positive, rod shaped bacterium. In the case of the TICE BCG vaccine, the average length of the bacterium is 2.36 μm and a width of 0.474 μm but there is evidence of micro-aggregates approximately 30-50 nm in diameter.[102] BCG are negatively charged but can be positively charged at lower pH's as the pI depends on the method of preparation.[102] BCG is recognized by TLR4 and TLR2 through its mycobacterial components like cell wall skeleton and peptidoglycan but also TLR9 through its bacterial DNA.[103] More research is needed to evaluate transport of bacterial candidates after IT injection.

Overall, it is apparent that unmodified TLR agonists lead to a greater AE incidence than those structurally modified or formulated with a cationic carrier. For example, research by Lynn et. al. studied TLR 7/8 agonists attached to polymer scaffolds in a variety of structures and concluded that particle formation was critical for improved local retention and innate activation.[104] TLR agonists comprised of DNA or RNA motifs are naturally negatively charged. Since extracellular space and cell membranes are also negatively charged, IT administration of these compounds is not conducive to retention. While the rationale for formulating with a cationic carrier has historically been to aid in cell penetration for intracellular TLR delivery, it is likely that net positively charged formulations could further benefit from retention through electrostatic interactions at the injection site. Such interactions could feasibly limit

systemic exposure and mitigate the AEs commonly associated with PAMP immunotherapies. Further exploration of the optimal physiochemical properties for retention and efficacy would be vital for the research of future IT therapies incorporating PAMPs.

3.2 Cytokines

Cytokines play an important role in cell signaling and are major regulators of immunity. Therefore, these immunological signals have drawn interest for their immunostimulatory function to potentially activate immune system and encourage the destruction of cancer cells.[105-106] Several types of cytokines have been investigated as immunotherapies (**table 3**). Granulocyte-Macrophage Colony Stimulating Factor (GM-CSF) is a growth factor that stimulates hematopoietic stem cells to differentiate into dendritic cells, granulocytes, and monocytes – cells capable of potentiating robust immune responses through antigen processing and presentation.[107] GM-CSF is a prominent stimulatory agent being used to promote the activation, maturation, and migration of immune cells to collectively elicit anti-tumor action. Where results are posted, trials administering GM-CSF exhibited AEs lower than 15% with tumor size reduction rates exceeding 85%.

IL-2 is a cytokine with an alternate immunostimulatory mechanism that has also been widely explored in cancer. IL-2 activates cytotoxic effector cells and causes them to proliferate.[108] The T cell expansion that ensues in the presence of IL-2 has the potential to promote an anti-tumor response that overcomes the senescent microenvironment typically established by tumors.[109] IL-2 does not seem to be as safe as GM-CSF; trials commonly report systemic AEs in greater than 50% of patients. However, one Phase 2 trial exploring Proleukin (intratumoral IL-2) exhibited an 85% complete remission (CR) rate in tumor metastases, suggesting high potential for the efficacy of this T cell-stimulating signal when directed to the tumor microenvironment.

Intratumoral cytokine immunotherapies extend far beyond GM-CSF and IL-2 regimens alone. Recombinant alpha-interferon has been administered intralesionally in patients with prostate cancer to

achieve a 30% CR rate.[110] Tumor Necrosis Factor-α (TNFα) has been intratumorally injected while co-administering subcutaneous IFN-a2b for advanced prostate cancer as well. Notably, TNFα leakage into the systemic circulation was observed after just 2 hours of injections, and this leakage may have contributed to AEs. Systemic exposure with IT cytokines is intuitively common, as these proteins are largely soluble and small (<70 kDa).[111] Recombinant human interleukin-12 (rhIL-12) in six head and neck squamous cell carcinoma (HNSCC) was detected in the plasma 30 minutes after the IT injection with a half-life of 7.2 h.[112] Such systemic exposure is troubling, as a phase 2 study that used a similar treatment regimen on 10 patients HNSCC resulted in high toxicities.[113]

Cytokines elicit signaling cascades by acting in step with other directive signals, so cocktail approaches and combination therapies have also been attempted, but with limited success. One study investigated a multikine solution (combination of natural interleukins) that was injected IT or peritumorally in patients with HNSCC in combination with intravenous cyclophosphamide, intraoral indomethacin, and oral zinc.[114] Components of the multikine solution included IL-2, IL-1α, IL-1β, GM-CSF, IFNα, TNFα, TNFβ, IL-3, IL-4, IL-6, IL-8, IL-10, and macrophage inflammatory protein 1α. Tumors accumulated an elevated number of CD4+ T cells and natural killer cells, and the treatment resulted in a 16.7% CR rate. Notably, however, this high-powered cocktail led to 8.3% of patients developing sepsis and Wegener granulomatosis, suggesting systemic exposure.

3.2.1 Tumor Retention Mechanisms of Cytokines

Generally, cytokines in cancer immunotherapy work by stimulating effector cells at the tumor site and rely on the host to initiate an immune response against the tumor.[106] Ideally, the cytokines should localize at the tumor to avoid systemic toxicity, and therefore, it is important to consider the dosage concentration, dosage schedule, and route of administration. IT administration typically lacks the severe side effects associated with systemic therapies; however, AEs may occur if there is leakage of the IT treatment to the systemic circulation.

Recombinant human GM-CSF is a 14-35 kDa glycoprotein with 127 amino acids.[115] It is composed of four bundles of α-helices and is non-spherical with dimensions of 20 Å by 30 Å by 40 Å.[116] Since GM-CSF is a white-blood cell growth factor that promotes the recruitment and activation of dendritic cells and monocytes, this cytokine has been studied for use in cancer immunotherapy as an immunostimulatory adjuvant to induce anti-tumor immunity.[117] Of note, although the GM-CSF have been investigated as an immunostimulant for its anti-tumor properties, there is emerging evidence that GM-CSF can potentially stimulate tumor growth and metastasis in certain cancers.[107] Nevertheless, it is important to limit systemic toxicity associated with cytokine therapies. The severe AEs observed in malignant mesothelioma patients given intralesional infusion of 2.5-10 mg/kg/day GM-CSF may be a result of systemic exposure.[118] Conversely, lower dosage, daily injections of 15-50 μg or 400 μg GM-CSF given to melanoma patients produced milder side effects, likely due to lower systemic exposure.[119-120] The lower AEs seen in these studies may have resulted from a combination of the lower dosage concentration, or a difference in the location and morphology of tumors associated with the cancer type (i.e. mesothelioma vs melanoma).

Human IL-2 has a molecular weight of 15.5 kDa and is comprised of 133 amino acids.[108] IL-2 has a hydrodynamic radius of ~3 nm.[121] Interestingly, IL-2 can be immuno- stimulatory or suppressive by activating cytotoxic effector cells or regulatory T (Treg) cells, respectively.[108] These contrasting effects are due to differences IL-2 receptor expression patterns; where $CD8^+$ T and natural killer cells express high levels of IL-2Rβ (CD122) and IL-2Rγ (γ_c), while Treg cells express high levels of IL-2Rα (CD25) and only intermediate levels of CD122 and γ_c.[108] Typically, high doses of IL-2 is immunostimulatory and generates an anti-tumor immune response, while low doses of IL-2 are used for immunosuppression. Similar to the effects seen with IT GM-CSF injections, patients with melanoma[122-123] responded better to IT IL-2 treatment compared to patients with HNSCC[124], which may be reflective of differences in tumor morphology between melanoma and HNSCC. Moreover, the modification of the IL-2 protein to be conjugated to 6-7 kDa poly-ethylene glycol (PEG) chains increases the drug's solubility, improves its half-life, and reduces off-target immunogenicity, which translated into better patient responses.[125-126] Additional studies have interestingly demonstrated that the PEGylation lowered the drug's affinity for the receptors on Treg cells to a greater

extent than the receptors on CD8+ T cells, which resulted in a more favorable CD8+ T cell activation over Tregs.[127]

One method to limit the systemic exposure of cytokines is to include a tumor-targeting domain onto the therapy. For instance, IL-4(38-37)-PE38KDEL is a chimeric protein composed of modified IL-4 and a truncated form of *Pseudomonas* exotoxin (PE), which can target and bind to IL-4 receptor-positive glioblastoma cells.[128] Likewise, IL13-PE38QQR (IL13PE) is a chimeric protein of IL-13 conjugated to truncated PE and binds to IL-13 receptors on malignant glioma cells.[129] The IL-2-based immunokine (darleukin) and the TNFα-based immunokine (fibromun) further incorporate a diabody derived from the L19 antibody to introduce fibronectin binding functionality which capitalizes on overexpression in tumors.[130] With the absence of the Fc region on the diabody fragment of the antibody, the molecule does not interact with FcRn and has a more limited half-life as such. Nonetheless, its smaller size allows for better penetration and distribution in the tumor. The combination therapy of darleukin and fibromun (called daromun) resulted in AEs that were limited to local injection site reactions.[131] This was likely due to the antibody-cytokine fusion format of the treatment, which improves the cytokine residence time on the injected tumor and allows for the build-up of local cytokine concentration, thereby minimizing systemic AEs.

In summary, cytokines offer the promise of stimulating immunity in the presence of tumors to indirectly promote an anticancer response. Cytokines are by nature small and water-soluble, which potentially confounds their retention within the TME. Several clinical approaches have sought to address these detriments, but the continued development of strategies for the IT administration of cytokines within the TME will undoubtedly optimize efficacy while minimizing AEs. These strategies should continue to seek modification strategies that do not impede receptor binding or penetration within the tumor.

3.3 Viruses and plasmids

Oncolytic viruses selectively replicate in tumor cells, causing tumor cell destruction while sparing normal healthy cells.[132] Oncolytic viruses have been investigated in clinical studies for their ability to preferentially infect and kill cancer cells. A variety of virus types have been designed to be oncolytic and have been investigated for intratumoral therapy, including adenovirus, enterovirus, herpes simplex virus, parvovirus, measles (Rubeola) virus, reoviruses, and vaccinia virus classes.[133-143]

Viruses both replicative (oncolytic) or non-replicative (non-oncoyltic), can be used as vectors to carry and deliver foreign DNA into cells with high gene transfer efficiency.[144] For instance, talimogene laherparepvec (T-VEC/Imlygic®) was approved by the Food and Drug Administration (FDA) and European Medicines Agency (EMA) in 2015 for the treatment of melanoma lesions. This modified oncolytic herpes simplex virus-1 can selectively replicate in cells and will destroy infected tumor cells.[145]

Viruses have been used to express pro-inflammatory cytokines to reap the same benefits as exogenous formulations. Several IT viral-based therapies have been designed to express factors such as GM-CSF[146-147], interferon (IFN)-γ [148-149], tumor necrosis factor-α (TNFα) [150-152], or IL-12.[153] Suicide genes have also been delivered, such as the bacterial gene called *E. coli* purine nucleoside phosphorylase (PNP), which can convert fludarabine into the anti-cancer agent fluoroadenine.[154] Further, the herpes simplex kinase thymidine kinase (HSV-TK) has been used to incorporate ganciclovir into a toxic phosphorylated compound.[155-157]

Although less commonly investigated, another tool for gene delivery includes the use of plasmids. Plasmids are sometimes administered alone but are likewise used in tandem with a variety of techniques that can enhance gene transfer efficiency such as electroporation or in complex with cationic carriers. For instance, a phase 1 clinical study investigated the IT injection of 50 μg of IL-12 plasmid cDNA in patients with cutaneous or subcutaneous metastases.[158] Plasmids may be delivered with the assistance of electroporation to make the cell membrane permeable to the plasmid DNA. For example, electroporation

was used to help deliver tavokinogene telseplasmid (tavo), a 6215 bp plasmid that encodes for the p35 and p40 subunits of the human IL-12 protein, in metastatic melanoma patients.[159-160]

Cationic lipids or cationic polymers are also known to improve gene delivery into tumors by inserting through cell membranes.[161] Examples of this approach is evident in the use of DC-Chol liposomes to form DNA-lipid complexes called lipoplexes[162] or the use of polyethylenimine polymers to form DNA-polymer complexes called polyplexes.[71, 163-165]

3.3.1 Tumor Retention Mechanisms of Viruses and Plasmids

Generally, viruses can be found between 20 and 500 nm in diameter.[166] Oncolytic viruses direct the killing of tumor cells through cell lysis by infecting tumor cells. Subsequent viral replication, as well as the induction of an immunogenic response triggered by the release of tumor cell fragments upon cell lysis further compound their effects.[132] Oncolytic viruses can be modified to improve their affinity for tumor cells while limiting infection in healthy cells by deleting viral genes that will not affect the ability of the virus to replicate in cancer cells, but will inhibit viral replication in normal cells.[132] For instance, when an adenovirus infects a normal cell, the cell expresses the tumor suppressor proteins and the cell undergoes cell-cycle arrest or apoptosis, preventing the virus from replicating. The E1B 55-kDa gene in wild-type adenoviruses encodes for a protein that inhibits the tumor suppressor protein p53 and allows viral replication to occur. Therefore, adenoviruses that have the E1B 55-kDa gene deleted (such as OsNYX-015) would have inhibited viral replication in cells with normal p53 function. However, many tumor cells lack functional p53, which allows the E1B 55-kDa gene-deficient viruses to replicate within the tumor and lyse the cells. A similar mechanism is used with adenoviruses with the E1A gene deletion (such as DNX-2401). E1A binds and inhibits the cellular tumor suppressor protein pRB that is expressed functionally in normal cells but is mutated and non-functional tumor cells. Therefore, these E1A gene-deleted viruses can selectively replicate and destroy tumor cells, while avoiding replication in normal cells. Similarly, HSV-1716 is a herpes simplex virus (HSV) type 1 (155 – 240 nm in diameter) with a RL1 gene deletion.[139, 167] This gene encodes for the ICP34.5 protein, which inhibits the double-stranded RNA-activated protein

kinase (PKR) protein, a protein that is involved in inhibiting RNA translation and thereby preventing the synthesis of viral protein.[168] The deletion of the RL1 gene allow for selective replication in tumors with the defective anti-viral PKR pathway. The vaccina virus vvDD-CDSR has been mutated to have the viral genes encoding vaccinia growth factor (VGF) and thymidine kinase (TK) deleted[143]. These proteins are essential to viral replication, so their deletion prevents the virus from replicating in normal cells. However, viral replication in tumor cells is possible due to their upregulation of growth factors and nucleotides.

Viruses can also be designed to specifically target tumor cells by exploiting alterations in cell surface receptors compared to normal healthy cells. For instance, in addition to the E1A gene deletion, DNX-2401 also has an RGD-motif engineered into the fiber H-loop.[135] This motif enhances tumor infectivity/cell entry by allowing the virus to utilize the $\alpha_v\beta_3$ and $\alpha_v\beta_5$ integrins enriched on tumor cells. The coxsackievirus a21 (CVA21) (~31 nm in diameter) can bind to intracellular adhesion molecule 1 (ICAM-1) and decay acceleration factor (DAF) proteins that are highly expressed on certain tumor cells.[169] The live-attenuated measles virus Edmonston-Zagreb vaccine strain (120-250 nm in diameter)[170] can bind to CD46 that are expressed by some cancer cell lines, making these cells a preferred target.[141]

The use of these oncolytic viruses as a monotherapy was generally well-tolerated with mild AEs such as injection site pain, fever, fatigue, chills, and flu-like symptoms. However, they have shown varying success, where a few treatments led to some clinical responses and others to no clinical responses with limited evidence of abscopal effects. A common lack of abscopal effects by oncolytic viruses may suggest poor immune activation outside of the primary tumor destruction that occurs as a function of the virus itself.

Better clinical responses were observed with the incorporation of transgenes into oncolytic viruses for cancer gene therapy. An effective cancer gene therapy requires the delivery therapeutic genes into tumors and regulation of gene expression within the tumor microenvironment. A common mode of gene transfer is by using a viral vector. As such, the incorporation of transgenes in replicative or non-replicative viruses have been designed and used in clinical studies. For instance, FDA approved T-Vec is an attenuated herpes simplex virus, type 1 (HSV-1) (155-240 nm) that was engineered to express human GM-CSF. T-Vec is ICP34.5-deficient (similar to HSV-1716), allowing selective replication in tumor cells.[171] Of note, a

comparison between intratumoral T-vec and subcutaneous GM-CSF in patients with unresectable stage IIIB/C/IV melanoma in a phase 3 trial showed a higher efficacy for T-vec compared to GM-CSF alone.[172] Specifically, the T-vec-treated compared to the GM-CSF alone treated patients had a higher median overall survival (OS, 23.3 months vs 18.9 months), durable response rate (DRR) (19.3% vs 1.4%) ORR (31.5% vs 6.4%), CR (16.9% vs 0.7%), and partial response (PR, 14.6% vs 5.7%), and disease control rate (DCR) (76.3% vs 56.7%). Common AEs with T-vec treatment include fatigue, chills, pyrexia, nausea, and flu-like illness. However, T-Vec-treated patients had higher instances of grade 3 or 4 AEs compared to GM-CSF-treated patients (11.3% vs 4.7%), which include fatigue, flu-like illness, injection site pain, vomiting, cellulitis, dehydration, deep vein thrombosis, and tumor pain.

TNFerade uses an interesting technique for the localized delivery of TNFα. TNFerade is a replication-deficient adenovirus type 5 that carries a transgene encoding human TNFα. However, a radiation-inducble Egr-1 promoter gene was placed upstream to the TNFα cDNA, allowing for control the time and location of TNFα delivery through the use of radiation therapy. Ad-RTS-hIL-12 is an adenoviral vector that was engineered for the controlled expression of IL-12. This involves the use of the RheoSwitch Therapeutic System®, which requires the oral activator veledimex to induce IL-12 expression.[153] These inducible systems allow the regulation of gene expression, allow for control of when to activate the production of the gene product.

The popularity of using adenoviruses as a method of gene transfer may be a result of the ability to achieve high viral titers, low instances of severe AEs observed in vaccinations with unmodified adenoviruses, and higher packaging capacity of genetic information compared with other viruses such as the retrovirus.[173] However, limitations include the development of immunogenicity against adenoviruses that may make repeated treatments ineffective and the limited insert capacity for the length of the coding sequence.

Aside from using viral vectors, genes have been introduced into cells through plasmids, which can overcome the limitations associated with viral vectors. For instance, the EGFR antisense DNA is a plasmid of pNGVL1-U6-EGFRAS was prepared in phosphate-buffered saline.[162] We estimate this plasmid to be

about 9600 base pairs; the pNGVL vector (also called pUMVC) is 9287 bp, human U6 promoter is 241 bp, and EGFRAS is 39 bp.[162, 174-175] The IL-12 plasmid cDNA (pNGVL3-mIL12) which was given at 50 μg, was also prepared in saline (0.76 mL).[158] Since the efficacy of these therapies require their entry into cells, the negatively charged nature of plasmid DNA would likely make it difficult for DNA to pass through the negatively charged cell membranes.

One method to facilitate the entry of plasmids into cells would be to use electroporation. The application of short electric pulses creates temporary pores or holes in the membrane, increasing cell permeability.[176] In addition, the applied electric field drives the negatively charged DNA that are on the anode end to migrate towards the cell on the cathode end, where the DNA accumulates and interacts with the plasma membrane. The DNA enters the cells as endosome-like vesicles. After the application of the electric pulses, the cell membrane naturally reseals. For instance, electroporation was used to help deliver tavo, a 6215 bp IL-12 plasmid. Clinical responses were fairly similar between treatment the naked IL-12 plasmid cDNA and tavo with electroporation; however, a direct comparison cannot be made due to their difference in plasmid design, study design, and dosage regime.

Another method to facilitate plasmid DNA entry into cells is by formulating the plasmids with cationic polymers to create polyplexes similar to those employed for PAMP immunotherapies. The polyplex system masks the negatively charged DNA to feasibly allow the positively-charged polyplexes to bind the negatively-charged cell surface of the host mammalian cell and enter through endocytosis.[161] For example, mixing BC-819 (a plasmid DNA that encodes for the A fragment of diphtheria toxin under the control of a H19 gene promoter), with PEI formed polyplexes 80-90 nm in size.[177] Also, CYL-02 (a plasmid that encodes for the DCK-UMK fusion protein, which phosphorylates and activates the pro-drug gemcitabine) was prepared in 5% w/v glucose with a PEI nitrogen to DNA phosphate (N/P) ratio of 8 to 10. No particle size information was provided for CYL-02; however, we estimate that the polyplexes may be around 45 nm based on another reported polyplex with N/P of 8-10 that was made with JetPEI, which appears to be the same JetPEI used to make CYL-02.[178]

Together, we surmise that the use of electroporation or cationic polymers will continue to allow for better potency compared to the injection of naked plasmid DNA alone. Furthermore, the use of these non-viral gene therapies eliminates the drawbacks of using viral gene therapies, such as the immunological inactivation of adenoviruses and limited insert capacity. However, the non-viral vectors may have non-specific targets (does not distinguish transfection between tumor and normal cells) and lower transfection efficiencies compared to viral vectors.

3.4 Monoclonal antibodies

Monoclonal antibodies (mAbs) have shown promising therapeutic efficacy as cancer treatment (**table 3**). Immunostimulatory mAbs can target antigens expressed on the surface of tumor cells and induce cytotoxic T lymphocyte (CTL) responses to result in tumor cell death.[165] A major class of therapeutic antibodies are immune checkpoint inhibitors (ICIs), which target the receptors of inhibitory signaling pathways to reverse immune suppression and reactivate immune-mediated antitumor responses.[179]

Antibodies targeting CTLA-4 and PD-1/PD-L1 have demonstrated broad activation of tumor-specific T cells by blocking negative-feedback mechanisms of the immune system. The most common administration route of these mAbs is systemic[180], however, systemic delivery of mAbs is known to potentially induce many immune-related adverse events (irAE), and only 20-30% of patients respond to this treatment. IT administration of mAbs has been suggested in attempts to retain mAbs in the tumor microenvironment and reduce systemic exposure and associated inflammatory side effects.[181]

Ipilimumab (Ipi), a human IgG1 that targets CTLA-4, was the first approved immune checkpoint inhibitor for advanced melanoma, and has significantly improved the overall survival rate associated with this disease.[182] Systemic Ipi administration is commonly associated with a low response rate and life threatening toxicities, which has prompted the exploration of IT delivery. A phase 1 ongoing clinical trial is testing a combinatorial immunotherapy using IT injection of autologous CD1c (BDCA-1) myeloid dendritic cells, ipilimumab, and the PD-L1 blocking mAb, avelumab. Another phase 1 study of IT

ipilimumab combined with IL-2 for advanced melanoma found that it was well-tolerated and generated responses in both injected and non-injected lesions in a majority of patients.[183] T-cells were activated within the tumor and in the draining lymph nodes, indicating IT administration enhanced the local anti-tumoral responses and also induced distal effects.

CD40 is a member of the TNF receptor family expressed on the surfaces of APCs and B cells. The CD40 ligand, CD154, is mainly expressed by activated T cells and B cells. CD40 ligands assist T cell activation and differentiation, which results in increased tumor-specific antigen presentation and the production of CTLs. Despite its potential synergy with other forms of anticancer therapy, the use of CD40 agonists has been associated with toxicities including cytokine release syndrome, thromboembolic events, and tumor angiogenesis. Collectively, these detriments substantiate CD40 ligands as candidates for IT immunotherapy to refine their delivery profiles. ADC-1013 is a human IgG1 agonistic CD40 antibody that has been investigated in human via both IT and IV administration in advanced solid malignancies. Although the main delivery method of ADC-1013 has been IV, a phase I trial for IT administered ADC-1013 in patients with advanced solid tumors has shown safety and B cell expansion after treatment, which could be related to the antitumor efficacy.[184-185]

3.4.1 Tumor Retention Mechanisms of Monoclonal Antibodies

The administration of immune checkpoint inhibitors including CTLA-4, PD-1 and PD-L1 downregulates the suppression of T cells and improves their activation. Binding of co-stimulatory receptors such as CD40 and OX40 is important for turning non-immunogenic ("cold") tumors "hot". These co-stimulatory receptors are mainly expressed on APCs, and when activated, the presentation of tumor antigens is increased and cytokines are released to improve the activation of anti-tumor T cells. Immunostimulatory mAbs are commonly administered as IV infusions, but so far only a small fraction of cancer types are successfully treated by mAbs. Severe irAEs have been prevalent with these therapies. irAEs are mostly attributed to be induced by the inhibition of immune checkpoints that are naturally in-place to prevent autoimmunity. Therefore, when checkpoints are inhibited outside of the TME, autoimmune responses can

ensue. The small size of mAbs (~10 nm) is a likely contributor to rapid clearance and dispersion out of an injection site and into systemic circulation.[186]

Local administration of immunotherapeutic mAbs can restrain immune responses to the tumor site and minimize unwanted systemic activation of the immune system by reducing leakage from the tumor. So far there are a limited number of slow-release systems for injected antibodies that largely use emulsions or micro/nano-formulations. Anti-CD40 has been conjugated to immunostimulatory poly(γ-glutamic acid) nanoparticles to successfully improve localization of the mAb as the nanoparticle minimized systemic cytokine release.[187] However, the coupling of anti-CD40 to polylactide nanoparticles did not show an improvement of anti-tumor activity.[188] Other anti-CD40 formulations based on mineral oil or dextran-based microparticles have shown the capacity to activate tumor-specific T cell responses and significantly decrease the AEs compared to systemic infusion, but the microparticles caused overly severe local inflammation.[189]

AEs including local inflammation and pain at the injection site are most commonly observed for the IT clinical trials investigating mAbs. One of the critical concerns of IT administration is the dispersion of the antibody following injection. Local administration of antibodies has shown increased accumulation in the tumor-draining lymph nodes, which may assist in generating anticancer immunity.[190] ADC-1013 has been optimized through the use of Fragment Induced Diversity (FIND) technology to improve binding affinity.[191] This optimization makes it possible to achieve high efficacy with very low doses. To further facilitate TME retention, mAbs can be engineered to accumulate in the tumor site. Antibodies with a high isoelectric point can be better retained in the TME as it is more acidic than normal tissues. Also, antibodies with increased binding affinities at lower pH are known to increase the activation of antitumor responses.[192]

Together, IT antibody delivery offers the potential for increased potency with mitigated risk. As antibodies are produced as highly specific, high-affinity proteins, colocalization with the TME where cognate receptors abound should facilitate IT retention. Alternate approaches formulating these biologics with particles and emulsions may also favor retention, however more work should be done to strike a tolerable balance between anti-tumor immunostimulation and uncontrollable local inflammation.

3.5 Small Molecules

Small molecule drugs have provided the most storied historical benefit for immuno-oncology therapies over many decades. Compared to large molecules that often have long half-life and poor tissue penetration, small molecules have the advantage of an <24hr half-life and can more readily cross cellular membranes. Together, these properties aid with intermittent dosing that can reduce toxicity and side effects. Small-molecule oncology drugs invoke various mechanisms like checkpoint inhibition, immunomodulation, and cytotoxic chemotherapy.

One of the most extensively studied and widely utilized chemotherapy drug is cisplatin. Cisplatin [cis-diammineplatinum dichloride] has been used to treat lung, bladder, and head and neck cancers. Significant systemic toxicity has been a limiting factor for further use, and thus IT formulations have been investigated. Currently there are several cisplatin-based IT delivery systems in clinical trials. INT230-6 is a supermolecular complex of cisplatin, vinblastine, and an amphiphilic penetration enhancer that assists dispersion in tumors and diffusion into tumor cells. Intratumoral injections of INT230-6 for solid tumors resulted in an 80% CR rate.[193]

3.5.1 Tumor Retention Mechanisms of Small Molecules

Small molecule drugs are versatile for therapeutic design because of the ease of modification, intervention and formulation, and the flexibility for better management of AEs that is conferred by a relatively short half-life. In contrast to large-molecule therapies like mAbs, which primarily target extracellular ligands and receptors, small molecules have enhanced vascular permeability that can target intracellular components with potentially faster penetration and homogenous distribution into solid tumors that can achieve greater response rates. Chemotherapeutics were designed to rapidly interrupt cancer cell proliferation through multiple mechanisms. Alkylating agents like cisplatin bind DNA through covalent bonds and prevent DNA replication. Anti-metabolites like gemcitabine resemble nucleobases by their structure, and once incorporated into DNA, inhibit the enzymes involved in DNA synthesis.[194]

One of the most critical challenges in the development of small molecule antitumoral drugs is the rapid plasma and tumor clearance due to their small size and molecular weight. Therefore, therapeutic molecules have been widely applied as IV infusion in free, unmodified forms. However, as IT injection these compounds are commonly modified into a prodrug or formulated with large molecules and carriers to improve retention. Several delivery systems are under clinical trials including polymer-drug conjugates, liposomal carriers, and polymeric micelles.[195] The performance of these formulations can be affected by multiple physicochemical characteristics including particle size, composition, stability, and surface properties. The particle size and surface charge have shown large influence on the cellular uptake and tumor distribution. It has been observed that particles with size <200nm are able to penetrate and distribute into tumors after IT injections.[196] Many polymeric formulations of cisplatin are sized 60 to 450 nm.[197-199] The composition of the delivery system includes non-toxic, non-immunogenic, biodegradable, and biocompatible polymers like PEG and PLGA, to support a controlled-release system while minimizing the dispersion into systemic circulation. The formulation developed by Chen et al. has shown an extended release and higher maximum-tolerated dose (MTD) than the free cisplatin, as well as significantly tumor suppression effect for HNSCC.[200] In the trials of Celecoxib, hydrophobic vitamin D was used as a carrier to potentially solve the low solubility issue of the drug and increase the depot effect at the tumor site. However, extensive hydrophobicity might increase non-specific serum protein binding, which can be avoided by PEGylation to provide a hydrophilic surface that can prevent access of proteins.

Small molecule drugs enter tumors mainly through non-selective diffusion and passive targeting, so an ideal form of these molecules is likely nonionized to fully enable conductive diffusion. The acidic microenvironment of tumor tissue causes chemoresistance against weak-base drugs, which become protonated and positively charged upon entering the tumor and are less membrane permeable. Alkylation drugs including Cisplatin (pH 3.5-5.5) and Gemcitabine (pH 2.7-3.3) remain nonionized and have higher cytotoxicities at lower pH. The effect of surface charge on nanoparticles has been investigated on many nano-sized formulations as well. It was observed that positively charged particles retain in the tumor at higher concentrations compared to the surrounding tissue[201] and diffuse out at a slower rate in comparison

to anionic particles.[202] Together this observation is attributed to the electrostatic interactions with negatively charged proteoglycans of the tumor neovasculature. For highly charged particles like gemcitabine hydrochloride and PV-10, a disodium salt, the electrostatic interactions might be a significant limitation to their mobility within the tumor, which could affect the efficacy of IT injections.

As small molecules are largely unhindered by the transport phenomena that dictate the distribution of other classes we have discussed in this review, chemical modifications can serve to selectively impede egress from the TME. Non-specific binding of small molecules to tumor cells or the extracellular matrix components can enhance the retention within the tumor. Ligand-receptor binding also delays clearance. Polymerization and complexation of small molecules enables their retention and depot-release within the TME. Tuning the charge properties of small molecules has also shown to aid intracellular penetration of these compounds as well as retention in the tumor. IT delivery of small molecules is appealing because the lower specificity of these candidates' mechanism can be overcome by the physical retention of their presence at the TME. However, in cancers where multiple tumor sites are present, it may not always be feasible to elect this strategy as an abscopal effect is unlikely when the immune system is not invoked.

4. Conclusion

This review set out to emphasize the impact of therapy biophysical characteristics on safety and efficacy by associating IT cancer therapies currently in clinical trials with their respective characteristics or formulations. While depending on the mechanism of action and target, it may be said that therapies with modifications to the active or those formulated to be more than aqueous demonstrated increased safety profiles. For intratumoral delivery, one theory could be that formulation or design of therapy that is larger, or particulate in nature may be connected to increased safety due to increased injection site retention. Overall, this review was intended to help future researchers realize the importance of design when considering an IT cancer therapy. Current cancer therapy strategies are vast in type and mechanism

therefore the target and function have to be the primary consideration in the design, however, the physiological and immunological properties of the TME can be harnessed when designing an IT therapy.

Category	Agent	Combination	Tumor Histotype	Trial ID[status]	Phase	Available Results	Reported Adverse Events	Refs
PAMPs	Tilsotolimod/IMO-2125	Ipilimumab	Melanoma	NCT02644967[A]	Phase 1/2	38% ORR, 71% DCR, 10% CR, 28% PR, 33% SD *major expanding T-cell clones found to be shared in responding local and distant lesions.	25% irAEs[+], hepatitis, gastritis, guillain-barre syndrome, clolitis, neutropenia.	203
	SD-101	Ipilimumab, radiation	Low-grade lymphomas	NCT02254772[C]	Phase 1/2	14% PR, 14% SD, 86% PD,	100% AEs, 11% SAEs (neutropenia/sepsis)	204
	SD-101	Pembrolizumab	Head and neck squamous cell carcinoma	NCT02521870[A]	Phase 1/2	22% ORR, 26% SD, 30% PD, 22% non-evaluable, 48% DCR	7% AEs[+], 32% SAEs, >20% AEs[˚]	62
	SD-101	Radiation	Low-grade B-cell lymphomas	NCT02266147[C]	Phase 1/2	24% PR, 3% CR, 83% Reduction of distal tumors	100% AEs[˚], 28% AEs[+] mostly flu like symptoms	205
	PF-3512676/Agatolimod/CpG 7909	Local Radiation	Low-grade lymphomas and mycosis fungoides (MF)	NCT00185965[C]	Phase 1/2	In lymphoma patients: At treated site: 47% CR, 40% PR, 13% SD Excluding treated site(distal only): 26.7% ORR, 20% PR, 53% SD In MF patients: 35.7% ORR	In lymphoma patients: 33% AEs[˚] flu-like symptoms In MF patients: 100% AEs[˚] injection site reactions, chills, fever, myalgia, arthralgia	82
	PF-3512676/Agatolimod/CpG 7909	Local Radiation	Low-grade lymphomas	NCT00880581[C]	Phase 2	23% PR, 63% SD, 13% PD	73% AEs	83
	Hiltonol/ polyIC:LC		embryonal rhabdomyosarcoma	NCT01984892[T]	Phase 2	1 patient only but saw reduction of tumor		91
	B0-112/ polyI:C+polyalkyleneimine	Pembrolizumab (with or without)	Solid tumors	NCT02828098[A]	Phase 1	(At 10 weeks) Combination therapy: 58% DCR, 17% ORR Monotherapy: 88% increase in circulating immune cells, 46% increase in immune gene expression *No BO-112 was found in the blood.	Monotherapy: 53% AEs[˚] Combination: 67% AEs[˚]	88
	G100/GLA-SE		Merkel Cell Carcinoma	NCT02035657[C]	Phase 1	40% PR, 10% CR, 50% PD *responders had increased inflammation and infiltration of CD8+ and CD4+ T cells as well as evidence of global immune activation.	>80% AEs[˚]	206
	G100/GLA-SE	Radiation	Soft Tissue sarcoma	NCT02180698[A]	Phase 1	Induced local and systemic immune changes	Nothing higher than grade 2	207
	G100/GLA-SE	Pembrolizumab, rituximab, (with or without)	Follicular Non-hodgkins lymphomas	NCT02501473[R]	Phase 1/2	Reported best response: 45% PR, 33% SD, 22% pending, PRs also saw up to 56% shrinkage of distal tumors. *CD4+ and CD8+ T cell tumor infiltration		208

	MK4621/RGT100		Solid Tumors	NCT03065023[T]	Phase 1/2	At data cutoff best response was 27% SD *PK shows minimal systemic exposure	100% AEs[°] (pyrexia, fatigue, headache, nausea), 48% AEs[+], 53% irAEs	93
	BCG	Ipilimumab and isoniazid	Metastatic melanoma	NCT01838200[T]	Phase 1	Low dose group: 33% PD, 66% SD High dose group: 100% PD	100% AEs, 67% SAE in low dose group, 50% SAE in high dose group, DLT met at higher dose group	209
	Clostridium novyi- NT			NCT01924689[C]	Phase 1	1 patient only. Saw reduction in tumor size/destruction of tumor	Pain	210
Cytokine	GM-CSF		malignant mesothelioma			2.5-10 µg/kg/day for 8 weeks 7.1% had local tumor necrosis, 7.1% had response at a distal tumor, 57.1% had tumor progression during treatment, and 71.4% had tumor progression after 2 months.	AE[+]: 14.3% pain, 14.3% malaise, 7.1% dyspnea Not graded AE: 7.1% neurologic, 7.1% angina, 7.1% peripheral edema, 7.1% rash, 50% increased alkaline phosphatase Treatment promoted neutrophil agglutination, which can cause vascular plugging	118
	GM-CSF		Melanoma		Phase 1	15–50 µg/day 61.5% SD, 30.8% PD, 7.7% PR 23.1% PR in non-injected lesions Responding patents had increased numbers of CD4+ T cells and Langerhans' cells, and increased IL-2R expression on T cells		119
	GM-CSF		cutaneous melanoma metastases			400 µg/day for 5 days, and repeated after 21 days 85.7% of patients had reduced tumor size, 71.4% of patients had reduced number of cutaneous metastases injected and non-injected tumors had increased infiltration of monocytes/macrophage, and CD4+ and CD8+ T-cells	Mild drowsiness and local erythema at the injection sites	120
	GM-CSF	interleukin (IL)-12	metastatic melanoma		Phase 1/2	150 ng GM-CSF on day 1 followed by subcutaneous administration of 3 000 000 IU of IL-2 on days 3-7 (5 days) at every 3 weeks	AE[0]: 18.8% fever, 12.5% arthralgia AE[+]: 6.3% fever	211

						25% PR, 25% minimal response, 56% SD for 3-6 months, and 18.8% PD		
	Interleukin-2 (IL-2)		head and neck squamous cell carcinoma		Phase 1	200 U - 4 × 10^6 U/day 5.6% PR, 58.3% SD, 27.8% PD, 8.3% unevaluable	MTD: 2 × 10^6 U/day AE^0: 69.4% fever, 13.9% anemia, 8.3% nausea, 30.6% hepatic toxicity, 8.3% cardiac toxicity, 8.3% pulmonary toxicity, 13.9% neurologic toxicity AE^+: 2.8% fever, 8.3% hepatic toxicity, 8.3% cardiac toxicity, and 2.8% metabolic toxicity	124
	IL-2 (Proleukin)		advanced melanoma	NCT00204581[C]	Phase 2	6-12 MIE/d 3 times a week 78.7% CR, 0.7% PR, 16.3% SD, and 4.3% PD No responses in distant untreated metastases	AE^0: ~98% inflammatory injection site reaction, ~79% injection site pain, 58% fever, 36% fatigue, and 34% nausea	122
	IL-2 (Proleukin)		soft-tissue melanoma metastases		Phase 2	Intralesional 85% CR in metastases, 6% PR, 3% PD, and 3% of the metastases were not assessable No responses observed for untreated metastases	AE^0: 100% local erythema and slight welling, 55% fever, 58% flu-like symptoms, 67% pain, 46% fatigue, 41% nausea/vomiting, 17% stomach pain, 8% headache AE^+: 4% headache	123
Antibody + cytokine	Ipilimumab and Interleukin-2		Melanoma	NCT01672450[C]	Phase 1	67% patients had local response, 89% patients had abscopal response 40% ORR: 30% irPR, 10% irSD, 60% irPD Some of the responders had increased frequency of CD8+ T cells expressing IFNγ, Tbet, granzyme-B and/or perforin, which may be evidence of a systemic immune response	AE^0: 33.3% chills, 50% fatigue, 41.7% flu-like symptoms, 58.3% pain at injection site AE^+: 8.3% hyponatremia, 41.7% ulceration at injection site	182
Cytokine	PEG-IL-2		head and neck squamous cell carcinoma			200,000 U of PEG-IL-2 3 times a week for 4 weeks 6% CR, 35% SD, and 47% PD	Swelling and redness near the injection site with no systemic toxicity	126
	PEG-IL-2		basal cell carcinoma			Perilesional 3000 – 1,200,000 IU PEG-IL-2	Local pain, swelling, and erythema	125

						66% CR, 25% PR, and 8.4% SD		
Cytokine	interferon-α (IFN-α)		Prostate cancer		Phase 1	30% CR	Mild systemic effects of chills, fever, and malaise	110
Cytokine	Tumor Necrosis Factor-α	IFN-a2b	Advanced prostate cancer		Phase 1	Quad-weekly intratumoral 160 mg/m^2 Tumor Necrosis Factor-α and subcutaneous 5×10^6 IU IFN-a2b 44.4% SD, and 55.6% PD TNFα leakage into the systemic circulation was observed after 2 hrs after injection	AE°: 50% fever and chills, 30% headaches, 30% nausea, 20% hepatotoxicity, 10% hair loss	212
Cytokine	recombinant human interleukin-12 (rhIL-12)		head and neck squamous cell carcinoma		Phase 1	Weekly injection of 100 or 300 ng of rhIL-12 per kg body weight 40% tumor size reduction in one patient, but no PR or CR responses IL-12 was detected in the plasma 30 mins after injection with a half-life of 7.2 h. The treatment increased plasma IFNγ and IL-10 levels.	AE°: 100% fever, 33% itching at site of injection All patients had lymphopenia before treatment. After the first injection, 60% had AE^+ of lymphopenia	112
Cytokine	recombinant human interleukin-12 (rhIL-12)		head and neck squamous cell carcinoma		Phase 2	Weekly injeciton of 100 or 300 ng of rhIL-12 per kg body weight DLT: 300 ng/kg No measurable changes in tumor due to short treatment period Dose-dependent plasma IFNγ and IL-10 increments were detected	AE°: 20% myalgia, 50% fever, 50% lymphopenia AE^+: 20% elevation of the ratio of amino alanine transferate/aspartate amino transferase, 10% fatigue, 10% metabolic acidosis, 40% lymphopenia	113
Cytokine	multikine solution (combination of natural interleukins: IL-2, IL-1α, IL-1β, GM-CSF, IFNα, TNFα, TNFβ, IL-3, IL-4, IL-6, IL-8, IL-10, and macrophage inflammatory protein 1α)	IV cyclophosphamide, intraoral indomethacin, and oral zinc	head and neck squamous cell carcinoma			16.7% CR and 25% PR Tumors had elevated number of CD4+ T-cells and natural killer cells	16.7% had minor AE of headaches and palpitations. 8.3% developed sepsis and Wegener granulomatosis	114
Cytokine	IL-4(38-37)-PE38KDEL (IL-4-toxin)		recurrent malignant high-grade gliomas			4-8 day infusion period (0.3-0.6 mL/h) of 0.2 – 6 μg/mL	AE°: 11.1% headache, 11.1% anomia, 11.1% dysphasia, Grade 2/3: 22.2% weakness, 11.1% nausea, 22.2% seizures	213
Cytokine	IL13-PE38QQR (IL13PE)		patients undergoing tumor resection for		Phase 1/2	No clinical response reported, Drug remained distributed in tumor	31% headache, 16% hemiparesis, 11% fatigue	129

			recurrent malignant glioma					
Antibody / Cytokine fusion	L19IL2 + L19TNF		Malignant Melanoma, Skin	NCT02076633[C]	Phase 2	28.3% CR in lesions and 68.1% non-CR (values include both targeted and non-target lesions)	AE^{0}: ~63% injection site reaction, 59% fever, 50% headache, 36.4% edema, 36.4% erythema, 27.3% chills, 22.7% rash, 22.7% nausea/vomiting, 18.2% vertigo. AE^{+}: ~10% injection site reaction	131
Viral (oncolytic)	Onyx-015		recurrent head and neck cancer		Phase 1	no ORR observed Evidence of tumor necrosis in injected tumors	AE^{0}: 21% fever, 9% nausea, 6% chills, 6% flu syndrome, 6% diarrhea, 6% tumor pain	133
Viral (oncolytic)	Onyx-015	cisplatin and 5-fluorouracil	recurrent squamous cell cancer of the head and neck		Phase 2	53% ORR with 27% CR and 36% PR	AE°: injection site pain, mucous membrane disorder, and flu-like symptoms AE^{+}: 16% injection site pain, 8% mucous membrane disorder, 5% syncope, 5% kidney failure, 5% facial endema, 3% anorexia	134
Viral (oncolytic)	DNX-2401 (Formerly Known as Delta-24-RGD-4C)		Recurrent Malignant Glioma	NCT00805376[C]	Phase 1	Tumor reductions in 72% of patients Tumor analysis showed signs of inflammation, tumor infiltration by CD8+ and T-bet+ cells, and transmembrane immunoglobulin mucin-3 downregulation, and tumor cell death	All AE°: 63% headache, 41% nausea, 22% speech disorder, 21% hemiparesis, 32% insomnia, 30% confusional state, 30% peripheral edema All AE^{+}: 5% headache, 19% speech disorder, 11% hemiparesis, 3% convulsion, 5% muscular weakness, 3% visual field defect. Drug-related AE°: 3% headache, 3% nausea, 3% confusional state, 3% vomiting, and 3% pyrexia	135
Viral (oncolytic)	Coxsackievirus A21 (CVA21, CAVATAK)		Malignant Melanoma	NCT01227551[C]	Phase 2	ORR was 28.1% with a 1-year survival rate of 19.3%.	AE°: mild fatigue, chills, injection site reactions, and fever	136
Viral (oncolytic)	HF10		Pancreatic cancer		Phase 1	1×10^{6} p.f.u. for 3 days 66.7% SD or PR, and 33.3% PD Blood levels of NK cells increased, and histological staining showed CD4+ cells, CD8+ cells, and macrophages infiltration in the tumor	No AEs	137
Viral (oncolytic)	HF10	Erlotinib and gemcitabine	Pancreatic cancer		Phase 1	1×10^{6} pfu - 1×10^{7} pfu of HF10 in combination with daily 100 mg	No AEs	137

						oral erlotinib and weekly 1000 mg/m^2 gemcitabine administration 33.3% PR, 44.4% SD, and 22% PD CD4+ and CD8+ cells infiltration were observed around the cancer tissue		
Viral (oncolytic)	HSV1716		recurrent malignant glioma		Phase 1	No marked improvements. Most patients had initial tumor stability followed by tumor progression	No AEs	139
Viral (oncolytic)	Parvovirus H-1 (ParvOryx; H-1PV)		Glioblastoma Multiforme	NCT01301430[C]	Phase 1/2	Progression-free survival of 27% at 6 months and an overall survival (OS) of 72% Treatment induced antibody formation and triggered T cell responses. Tumor analysis showed markers of virus replication, microglia/macrophage activation, and cytotoxic T cell infiltration	Reduced consciousness, complications caused by hydrocephalus, and occlusion of ventricular catheters due to high protein levels in the cerebrospinal fluid	140
Viral (oncolytic)	measles virus Edmonston-Zagreb vaccine strain	IFNα	Cutaneous T cell lymphoma		Phase 1	83.3% of the treated tumors regressed and distant non-injected lesions improved in 40% of patients. Patients had higher levels of anti-measles antibody titers. Local viral activity with positive staining for MV nucleoprotein (NP), an increase of the interferon γ (IFN-γ)/CD4 and IFN-γ/CD8 mRNA ratios and a reduced CD4/CD8 ratio	AE: erythema and itching at the injection site	141
Viral (oncolytic)	pelareorep (REOLYSIN®)	gemcitabine	advanced pancreatic adenocarcinoma		Phase 2	9% PR, 67.6% SD, and 14.7% PD	AE°: 8% anemia, 5% neutropenia, 9% thrombocytopenia, 24% diarrhea, 29% nausea, 24% vomiting, 62% fatigue, 51% chills/flu-like symptoms, 33% edema, 56% fever, 6% AST increase, 33% anorexia/weight loss, and 44% dyspnea AE$^+$: 27% anemia, 27% neutropenia, 6% thrombocytopenia, 9% fatigue,	142

							6% AST increase, and 6% dyspena	
Viral (oncolytic + vector; chemosensitizing)	vaccinia virus vvDD-CDSR (also called JX-929 or vvDD)		breast, pancreas, colon, or melanoma cancer		Phase 1	No clinical response observed vvDD genome was observed in blood 15 minutes after injection and was dose-dependent, Treatment induced the production of neutralizing antibodies against the virus, Observed vvDD replication and spread to non-injected tumors.	AE°: 88.2% of patients developed delayed symptoms of fever, malaise and/or pain AE⁺: pain	143
Viral (oncolytic + vector)	Talimogene laherparepvec		unresectable stage III-IV melanoma	NCT00769704[C]	Phase 3	T-vec-treated compared to the GM-CSF treated patients had a higher median OS (23.3 months vs 18.9 months), DDR (19.3% vs 1.4%) ORR (31.5% vs 6.4%), CR (16.9% vs 0.7%), and PR (14.6% vs 5.7%), and DCR (76.3% vs 56.7%)	AE°: 49% fatigue, 49.3% chills, 43.2% pyrexia, 36.3% nausea, 30.1% flu-like illness, 27.4% injection site pain, 20.2% vomiting, 3.7% cellulitis, 2.4% dehydration, 0.4% deep vein thrombosis, 6.2% tumor pain, AE⁺: 1.7% fatigue, 0.7% flu-like illness, 1% injection site pain, 1.7% vomiting, 2.1% cellulitis, 1.7% dehydration, 1.7% deep vein thrombosis, 1.7% tumor pain	172
Viral (oncolytic + vector)	ONCOS-102 (previously called CGTG-102 and Ad5/3-D24-GMCSF)	cyclophosphamide	Malignant Solid Tumour	NCT01598129[C]	Phase 1	Short-term increase in serum pro-inflammatory cytokines IL-6 and IL-8 RECIST 1.1 criteria: 40% SD and 60% PD at 3 months; 100% PD at 6 months PET response criteria: 10% stable metabolic disease and 40% progressive metabolic disease Viral genome in serum detected by quantitative real-time PCR at 6 and 24 hours post-treatment Treatment increased CD8+ T cell infiltration in 91.7% of patients and promoted the up-regulation of PD-L1 in the tumor in 18.2%	100% patients with AE°: flu-like symptoms, pyrexia, and fever 50% patients with AE⁺: pyrexia, increased alkaline phosphatase (ALP), increased aspartate aminotransferase (AST), proteinuria, hyponatremia, anaemia, fatigue, oedema peripheral, and dyspnoea	146
Viral (oncolytic + vector)	Pexa-Vec			NCT01387555[C]		$1x10^8 – 1x10^9$ pfu Modified Choi response rate: 62% ORR, mRECIST responses: 3.6% CR, 10.7% PR, 35.7% SD	100% AE°: fever, rigors, nausea, vomiting 12-24 hours post-treatment AE⁺: 6% (1/16 patients given $1x10^9$ pfu) lymphopenia	147

						Pexa-vec genome found in the blood hGM-CSF protein was quantifiable in the plasma on day 5, Humoral immune response resulting in antibody-mediated complement-dependent cytotoxicity was observed in 67% of patients		
Viral (non-oncolytic + vector)	TG1042 (Adenovirus-interferon-γ)		cutaneous lymphomas		Phase 2	Local tumor regression in 53% patients and a regression in non-injected, distant lesions in 27% patients, Elevated serum levels for IL-6, IL-10, IFN-γ, and neopterin	AE°: 65% chills, 60% injection site pain, 55% lymphopenia, and 45% fever. AE+: 46.7% lymphopenia, 13.3% chills, 6.7% high fever, 6.7% injection site pain, and 6.7% pruritus at the injection site	214
Viral (non-oncolytic + vector)	TG1042 (Adenovirus-interferon-γ)		Primary Cutaneous B-cell Lymphoma	NCT00394693[C]	Phase 2	5×10^{10} viral particles (vp) per lesion into up to six lesions treated simultaneously on days 1, 8 and 15; no treatment on fourth week 85% ORR: 54% CR, 31% PR CD8+ T lymphocytes and of TIA-1+ cytotoxic T-cells in lesions injected with TG1042	100% AE°: fatigue, headache, pyrexia, injection site irritation, chills, flu-like illness, injection site erythema, and injection site pain, 7.7% AE+: 7.7% increased lipase	149
Viral (non-oncolytic, vector)	TNFerade	5-FU, Cisplatin and radiation	Esophageal Cancer	NCT00051480[C]	Phase 2	4×10^8 - 4×10^{11} PU of TNFerade in combination with daily IV 1000 mg/m^2 5-fluorouracil and 75 mg/m^2 cisplatin 29% pathologic complete response (pCR)	AE: 83% nausea 83%, 75% fatigue 75%, 63% vomiting, 58% mucosal inflammation, 54% diarrhea, 50% fever, 46% dehydration, 42% anorexia, and 42% dysphagia, AE related to TNFerade biologic: 54% fatigue, 38% fever, 29% nausea, 21% esophagitis, 21% vomiting, 21% chills	152
Viral (non-oncolytic, vector)	TNFerade	Radiation therapy	soft tissue sarcoma		Phase 1	$4 \times 10^9 - 4 \times 10^{11}$ particle units (PU) 15.4% CR, 69.2% PR, and 7.7% SD Patients had low levels (<15 pg/mL) of serum TNFα	AE°: 50% chills, 43% fever, 36% fatigue, 21% flu-like symptoms.	151

Viral (non-oncolytic, vector)	TNFerade	5-fluorouracil and radiation therapy	advanced pancreatic cancer		Phase 1/2	4×10^9 to 1×10^{12} particle units (PU) every week for 5 weeks, along with 50.4 Gy radiation and 5-fluorouracil (5-FU) 200 mg/m^2 daily over 5.5 weeks 2% CR, 6% PR, 8% minor response, 24% SD, 38% PD, and 16% non-evaluable	MTD of 4×10^{11} PU AE$^+$: 18% abdominal pain, 16% biliary obstruction, 12% GI bleeding, 12% deep vein thrombosis, 12% cholangitis, 4% pulmonary emboli, 4% pancreatitis, and 2% cholangitis	150
Viral (vector)	INXN-2001 (Ad-RTS-hIL-12)	INXN-1001 (Veledimex)	Melanoma	NCT01397708[C]	Phase 1/2	Increase in serum IL-12 and IFNγ was observed, Increase in CD3+ and CD8+ T cells were detected in analyses of PBMCs	Related AEs: 78.6% chills, 78.6% pyrexia, 71.4% fatigue, 71.4% nausea	153
Viral (non-oncolytic + vector; chemosensitizing)	Ad/PNP	fludarabine monophosphate	Head and Neck Cancer	NCT01310179[C]	Phase 1	75 mg/m^2 fludarabine: 83.3% PR and 16.7% SD 15 or 45 mg/m^2 fludarabine: 67% SD and 33% PD	100% any AE°: 100% injection site symptoms, 66% fatigue, 66% non-injection site pain, 50% nausea/vomiting/diarrhea, 42% flu-like symptoms/chills, 42% facial edema/pitting edema, 42% dizziness, 42% dyspnea, 42% any AE$^+$: 8% dehydration, 8% pericardial effusion, 8% cardiac tamponade, 8% pain, 8% nausea/vomiting, 8% bacteremia, 8% partial seizure, 8% lower ext. weakness, 8% chronic wound infection Treatment-related AE°: 83% injection site pain, 50% injection site drainage/itching/burning, 50% fatigue, 42% flu-like symptoms, Treatment-related AE$^+$: 16.7% including 8.3% decreased lymphocyte count, 8.3% pain at the injection site	154
Viral (non-oncolytic + vector)	TK99UN adenoviral vector encoding herpes simplex virus thymidine kinase (*HSV-TK*) gene (Ad.TK)	intravenous ganciclovir or oral valganciclovir	Hepatocellular Carcinoma	NCT00844623[C]	Phase 1	60% SD and 40% PD Thymidine kinase (TK) expression in the tumor detected in all patients that received a dose of $> 10^{12}$ viral particles (vp) and was absent after 9 days	Definite treatment-related AEs: 62% fever, 62% flu-like symptoms, 44% lymphopenia, and 12% injection site pain Probable treatment-related AEs: 38% abdominal pain, 38% leukopenia, 19% thrombocytopenia, 19% anemia, 12% vomiting	155

							Possible treatment-related AEs: 31% encephalopathy, 31% edema, 12% diarrhea, 12% ascites, 6% hyperbilirubinema, 6% hypertransaminasemia, 6% itching	
Viral (non-oncolytic + vector)	adenoviral vector (Adv.RSV-tk) expressing the herpes thymidine kinase gene	Ganciclovir (GCV)	metastatic colorectal adenocarcinoma in the liver		Phase 1	68.8% SD and 31.3% PD	AE°: 18.8% hepatic toxicity (elevations of serum alanine aminotransferase (ALT) and/or aspartate aminotransferase (AST)), 18.8% leucopenia AE⁺: 6.3% thrombocytopenia, 31.3% grade 2-3 fevers	156
Viral (non-oncolytic + vector)	adenoviral vector (Adv.RSV-tk) expressing the herpes thymidine kinase gene	Ganciclovir	Recurrent Malignant Brain Tumors		Phase 1		Toxicity at 2×10^{12} VP 76.9% AEs: seizures, IT hemorrhage, rash, hemiparesis, thrombocytopenia, lethargy, confusion, hyponatremia, fever, leukocytosis, increased CSF protein and liver enzymes	157
Plasmid	Plasmid IL-12		Cutaneous or subcutaneous metastases		Phase 1	Among analyzed patients: 45.5% SD and 54.5% PD, 41.7% PR in treated tumor, no reduction in non-treated lesions No IL-12 or IFNγ was detected in patient serum	16.7% local AE°, 50% systemic AE°: 8.3% night sweats, 8.3% nasal congestion, 8.3% diarrhea, 8.3% dyspepsia, 16.7% fatigue, and 8.3% tachycardia 8.3% systemic AE⁺: 8.3% pulmonary embolism	158
Plasmid	IL-12p DNA (which is also Tavokinogene Telseplasmid (tavo))	Intratumoral Electroporation	Malignant Melanoma	NCT00323206[C]	Phase 1	Increased local expression of IL-12 and IFNγ but no increased levels in the serum 76% of the analyzed injected lesions had over 20% necrosis. 29% of the patients had increased lymphocyte infiltration in the tumors 53% SD or objective regression in distant tumors	100% AE°: 100% transient pain during electroporation, 100% hemorrhage around treatment site	160
Plasmid	EGFR antisense DNA with DC-Chol Liposomes		Head and Neck Cancer	NCT00009841[C]	Phase 1	29% ORR, which include 11.8% CR and 17.6% PR Responding patients had increased EGFR and lower STAT3 expression in the tumors compared to the patients with PD	11.8% TEAE°: 11.8% injection site pain/swelling and 5.9% localized edema	162

Plasmid	DTA-H19		Pancreatic Neoplasms	NCT00711997[C]	Phase 1/2			
Plasmid	DTA-H19		Intermediate risk nonmuscle invasive bladder cancer		Phase 2	64% recurrence-free at 3 months. 45% and 40% recurrence-free rate at 1 and 2 years, respectively. 33% complete ablation of tumor with no new lesions at 3 months, 20% lesion still present and new tumors formed.	74.5% AE: 29.8% dysuria, hematuria, and urinary urgency; 17% gastrointestinal disorders, 14.9% infection disorders, 12.8% musculoskeletal disorders, 23% general disorders (asthenia, fatigue, chills, etc.) 4.3% AE^{+}: 2.1% myocardial infarction, and 2.1% hyperkalemia 23.4% possibly drug-related AE	163
Plasmid	CYL-02	Gemcitabine	Pancreatic Adenocarcinoma	NCT01274455[C]	Phase 1	CYL-02 was detected in the blood with no active excretion by the kidneys into the urine CYL-02 DNA and the expression of therapeutic mRNA was detected in the tumor after 1 month of treatment 95% inhibition of tumor progression 2 months after treatment, 91% of the metastasis-free patients had no new tumor development, 71% progression of distant tumors	AE°: 30.0% neutropenia, 35.0% anemia, 25.0% thrombocytopenia, 45% fever, 65% anorexia/nausea, 20% abdominal pain, 5% acute pancreatitis, 15% pruritus, 5% foot and hand syndrome, 10% hyperlipasemia, 30% increased ASAT, and 35% increased ALAT 10% AE^{+}: fever	164
	Ipilimumab	IL-2 (IT)	advanced melanoma	NCT01672450[C]	Phase 1	Generated responses in both injected and non-injected lesions in the majority of patients. Activated T-cells found in the tumor and draining lymph nodes.	Well-tolerated	182
	ADC-1013		Advanced solid tumors	NCT02379741[C]		PK detectable for 75 µg/kg deep tumors IT injections. Administration of a CD40 agonistic antibody into liver metastases is not optimal from a safety perspective; therapeutic ratio is more favorable for injections into superficial than into deep (i.e. liver) metastases	~20% Grade 2 and 3 TEAEs 83% TEAEs° *Mainly- pyrexia, nausea, vomiting, fatigue, flu-like symptoms, chills, malaise 22% TEAEs^{+} 33% SAEs DLT reached at 400 µg/mL, 1 patient (5%) has cytokine release syndrome	184
	TTI-621	Monotherapy; PD-1/PD-L1 Inhibitor; PEG INF-a2a; T-Vec, radiation	Relapsed and Refractory Solid Tumors and Mycosis Fungoides	NCT02890368[R]	Phase 1	91% (21/22) local lesion reduction and systemic effects	Well tolerated, with all TEAEs being grade 1 or 2	215

Small molecules	INT230-6 (supermolecular complex containing Cisplatin)	anti-PD1	surface of the skin (melanoma, head and neck, lymphoma, breast) and tumors within the body	NCT03058289[R]	Phase 1-2	Up to 80% CR with generation of antigen-specific CD8 T-cells	Grade 1 or 2 pain at the injection sites were reported	
	Cisplatin/Epinephrine injectable gel	Paclitaxel and Carboplatin	Recurrent or Refractory Head and Neck Cancer	NCT00002659[A] NCT00022217[N]	Phase 3 Phase 2	35% response rate for patients, 19% CRs and 10% PRs for target tumor responses		216
	Para-toluenesulfonamide (PTS)		Non-small cell lung carcinoma (NSCLC), severe malignant airway obstruction (SMAO)	NCT03448146[C]	Phase 3	ORR 30 days post-treatment was 100% (33.3% CR and 66.7% PR), 50% OSR at 5 years post-treatment	64% AE°, 7.9% SAE	217-218
	Gemcitabine		Locally advanced Pancreatic Adenocarcinoma	NCT01834170[C]	Phase 1	No patients experienced downstaging of tumor. Survival rate at 6 months was 92% vs. 48% and at 1 year 42% vs 21% for IT gemcitabine vs control. There was a trend for higher median OS in the IT gemcitabine group (274 vs. 177 days; P: 0.1 on log rank analysis).	No AEs	219
	PV-10 (Rose Bengal disodium)		metastatic melanoma	NCT02693067[R]	Phase 1 Phase 2	51% ORR among injected lesions, 26% CR Chemoablation observed at distal lesions Saw increase in cytotoxic T cell responses	Well tolerated	220-222
	PV-10	pembrolizumab	metastatic neuroendocrine tumors	NCT02557321[R]	Phase 2	19% ORR (vs 3.7% ORR for Keytruda)		223
	PV-10		in-transit melanoma metastases		Phase 2	Per treatment episode analysis: 78.1% ORR (30.5% CR, PR 47.6%) 87.9% Clinical benefit (CR+PR+SD). With sequential PV-10 treatments: 42% CRR, 87% ORR on an intention to treat analysis. The median follow-up duration was 22 months and the median overall survival was 25 months from first PV-10 treatment.	100% AE° *Mainly- injection site pain, oedema, blistering, erythema 3.6% AE+ *treatment site ulceration, cellulitis, and photosensitivity	224

Category	Therapy/Alternative Names	Description of Active	Characteristics and Formulation information	Mechanism Engaged	NCTs	Refs
PAMPs	Tisotolimod/IMO-2125	CpG class C derivative, TLR9 agonist	• Two strands of CpG linked at the 3' ends • Likely forms dimers • MW 7712 Da • Formulated as a sodium salt	• Intracellular TLR binding • Exposed 5' ends increases potency	NCT03052205 NCT02644967 NCT03445533	85
	SD-101	CpG class C, TLR9 agonist	• Proprietary investigational • CpG class C has one or more TCG elements close to or at the 5' end of the ODN and a palindromic sequence containing multiple CpG motifs • CpG alone is negatively charged	• Intracellular TLR binding	NCT02254772 NCT03007732 NCT03831295 NCT02521870 NCT03410901 NCT02927964 NCT02266147 NCT03322384	225
	PF-3512676/ Agatolimod/CpG 7909	CpG class B, TLR9 agonist	• MW 7698.212 Da • Class B CpG is usually linear and does not form higher order structures alone • CpG alone is negatively charged • AFM measurements of CpG class B: 1.2 x 8.7 nm	• Intracellular TLR binding	NCT00185965	81
	CMP-001	CpG class A derivative with native DNA backbone (PO)	• MW 9691.2 Da • Assembles into higher order structures • AFM measurements: 1.1 x 10-17 x 25-90 nm	• Intracellular TLR binding	NCT03507699 NCT03084640 NCT03983668 NCT02680184 NCT03618641	81, 225
	MGN1703/Lefitolimod	CpG derivative, native DNA backbone (PO)	• Dumbbell shaped • 28 base pair double-stranded middle section flanked by two single-stranded loops containing 30 nucleotides • Approximate MW 32 kDa	• Intracellular TLR binding	NCT02668770	77, 87, 226
	Hiltonol/polyI:C-LC	TLR3 agonist	• Complexed with polylysine (PLL) • Optimal PLL MW 28 kDa but ranges 13-35 kDa • Formulated with carboxymethylcellulose (CMC) • In an aqueous saline solution • Net positively charged	• Intracellular TLR binding	NCT02423863 NCT01976585 NCT03262103 NCT01984892	92
	BO-112/ polyI:C+polyalkyleneimine	TLR3 agonist	• Complexed with PEI • PEI MW between 17.5-22.6 kDa • Zeta potential 38 mV at pH 3.1 • 45-85 nm particles • polyI:C/PEI ratio between 2.5-4.5 • Aqueous formulation with glucose or mannitol	• Intracellular TLR binding	NCT02828098	89, 227

	G100/GLA-SE	GLA derivative, TLR4 agonist	• Single phosphate groups and six C_{14} acyl chains • Formulated in a squalene in water emulsion • Contains egg phosphatidyl choline (PC), DL-α-tocopherol, and Poloxamer 188 • Particle size 82.7-111 nm • Zeta potential -17 mV	• Extracellular TLR binding	NCT02035657 NCT02180698 NCT03742804 NCT02501473 NCT03915678 NCT02406781 NCT03982121 NCT02387125	90, 95-98, 228
	CV8102	TLR7/8 and RLR agonist	• ssRNA- 547 nucleotides • Complexed with cationic peptide (Cys-Arg12-Cys) that is disulfide-crosslinked	• Intracellular TLR and RLR binding	NCT03291002	229-230
	MK4621/RGT100 (upcoming trials formulate with JetPEI)	RIG-I agonist	• Cyclic dinucleotide • No structural information provided • Newer formulation are complexing with JetPEI which is a linear PEI with 1-3 positive charges on the nitrogen species.	• Intracellular TLR binding	NCT03739138 NCT03065023	74
	Motolimod/VTX-2337	TLR8 and NOD agonist	• MW 458.6 g/mol • No charge	• Intracellular TLR binding	NCT03906526	
	MIW815/ADU-S100	STING agonist	• Synthetic cyclic dinucleotide • Formulation unknown	• Intracellular binding	NCT03172936 NCT02675439 NCT03937141	
	MK-1454	STING agonist	• Synthetic cyclic dinucleotide • Formulation unknown	• Intracellular binding	NCT03010176	
	BCG	Derivative of BCG bacteria	• Live, attenuated BCG • Gram positive, rod shaped • Average length 2.36 µm, width 0.474 µm, volume 0.389 μm^3 or 0.906 µm diameter • Vaccine contains loosely aggregated cells often but not always • TICE substrain isoelectric point is 4.4	• Mock bacterial infection	NCT03928275 NCT01838200	102, 231
	Clostridium novyi-NT	Derivative of clostridium bacteria	• Gram positive, contain flagella, spore forming • Length of oval shape- 1 µm	• Mock bacterial infection	NCT01924689	210, 232
Cytokine	Granulocyte-Macrophage Colony Stimulating Factor (GM-CSF)	white blood cell growth factor	• 14-35 kDa glycoprotein • 127 amino acids • 20 Å by 30 Å by 40 Å	• Immunostimulatory cytokine	NCT00600002	115-116
	IL-2	Immune cell signaling molecule	• 15.5 kDa and is comprised of 133 amino acids • 18 MIU recombinant human IL-2 (Proleukin®, Chiron, Ratingen, Germany) was dissolved in 6 ml	• Immunostimulatory cytokine	NCT03233828 NCT00204581 NCT01480323 NCT00600002	108, 123

			glucose (5%) prepared with albumin (0.2%) solution		NCT01672450	
	PEG-IL-2	Modified immune cell signaling molecule	• Covalent addition of 6–7 kDa poly-ethylene glycol (PEG)	• Immunostimulatory cytokine		125-126
Antibody and cytokine	Ipilimumab and IL-2	Immune cell signaling molecule and checkpoint inhibiting antibody	• Ipilimumab: 148634.914 g/mol g·mol−1 • The real size of an antibody molecule is about 10 nm	•	NCT01480323	186
Cytokine/ toxin	IL-4(38-37)-PE38KDEL	Immune cell signaling molecule conjugated to a toxin	• amino acids 38–129 of IL-4, fused via a peptide linker to amino acids 1–37, which in turn is fused to the PE38KDEL toxin • PE38KDEL is composed of amino acids 253–364 and 381–608 of PE, with KDEL (an endoplasmic retaining sequence), at positions 609–612.	• Bind to IL-4 receptors on tumors • Pseudomonas exotoxin (PE) is a cytotoxic agent	NCT00797940 NCT00014677	128
Cytokine/ toxin	IL13-PE38QQR (IL13PE)	Immune cell signaling molecule conjugated to a toxin	• IL-13 conjugated to truncated PE	• Bind to IL-13 receptors on tumors	NCT00064779	129
Cytokine	darleukin (L19-IL2) and fibromun (L19-TNFα) L19 (a human monoclonal antibody fragment) fused to an immunocytokine	Combinatio n of immune cell signaling molecules	• Darleukin: interleukin-2 (IL-2) is fused to a human single-chain variable fragment (scFv) that recognizes L19. • Fibromun: tumor necrosis factor-α (TNFα) fused to scFv that recognizes L19	• Bind to L19 on tumors • immunostimulatory cytokine	Darleukin: NCT01253096 Daromun (Darleukin and Fibromun): NCT02076633 NCT02938299 NCT03567889	233
Oncolytic virus	ONYX-015	Adenovirus	• E1B 55-kDa gene deleted • 90 - 100 nm diameter	• Destroy tumor cells		234
Oncolytic virus	DNX-2401	Adenovirus	• E1A gene deletion • RGD-motif engineered into the fiber H-loop	• RDG-motif allow interaction with $\alpha_v\beta_3$ and $\alpha_v\beta_5$ integrins enriched on tumor cells • Destroy tumor cells	NCT00805376 NCT02798406 NCT02197169 NCT01956734	135
Oncolytic virus	Coxsackievirus A21 (CVA21)	coxsackievir us	• ~31 nm in diameter	• Bind to intracellular adhesion molecule 1 (ICAM-1) and decay acceleration factor (DAF) proteins on tumor cells	NCT01227551 NCT00438009 NCT00235482 NCT00832559 NCT02307149	169

Oncolytic virus	HF10	Herpes simplex virus-1 (HSV-1)	• *Loss of expression of UL43, UL49.5, UL55, UL56, and LAT* • *Overexpression of UL53 and* UL54 • 155 – 240 nm in diameter	• Destroy tumor cells	NCT02428036 NCT01017185 NCT03153085 NCT03252808 NCT02272855 NCT03259425	167, 235
Oncolytic virus	HSV-1716	Herpes simplex virus	• RL1 gene deletion • 155 – 240 nm in diameter	• Destroy tumor cells	NCT00931931 NCT02031965	
Oncolytic virus	H-1 parvovirus (H-1PV, ParvOryx)	parvovirus	• 180–250 Å in diameter	• Destroy tumor cells	NCT02653313 NCT01301430	139, 167, 236
Oncolytic virus	measles virus Edmonston-Zagreb vaccine strain	measles virus	• 120 – 250 nm in diameter	• Bind to CD46 that are expressed by some cancer cell lines • Destroy tumor cells		141, 170
Oncolytic virus	Pelareorep (REOLYSIN®)	reovirus	• Unmodified oncolytic reovirus • Type 3 Dearing strain	• Destroy tumor cells • Mechanism unclear, may be related to Ras signaling	NCT00528684 NCT02723838	142, 237
Oncolytic virus	vvDD-CDSR	Vaccina virus	• Vaccinia growth factor (VGF) and thymidine kinase (TK) deleted	• Destroy tumor cells	NCT00574977	143
Oncolytic virus + vector	Talimogene laherparepvec (T-VEC); Imlygic™		• ICP34.5-deficient • ICP47-deficient • 155 - 240 nm in diameter	• Destroy tumor cells • Expresses GM-CSF for immunostimulation	NCT00289016 NCT02014441 NCT00769704 NCT03747744	167
Oncolytic virus + vector	ONCOS-102 (previously called CGTG-102 and Ad5/3-D24-GMCSF)	Adenovirus	• Serotype 5 adenovirus • Placing the Ad3 fiber knob into the Ad5 backbone results in an Ad5/3 chimera • 24 bp deletion in Rb binding site of E1A for cancer cell restricted replication • Armed with granulocyte-macrophage colony-stimulating factor (GM-CSF)	• Serotype 3 fiber knob allow enhanced gene delivery to cancer cells • Destroy tumor cells • Expresses GM-CSF for immunostimulation	NCT01598129 NCT03514836 NCT03003676	146, 238
Oncolytic virus + vector	Pexa-Vec (JX-594)	Vaccina virus	• Wyeth strain vaccinia modified by insertion of the human GM-CSF and Lac-Z genes into the vaccinia TK gene region under control of the synthetic early-late promoter and p7·5 promoter, respectively. • Virion morphology and size: Enveloped, biconcavecore with two lateral bodies, brick-shaped to pleo-morphic virions,~360x270x250 nm in size • Diluted in bicarbonate-buffered saline	• Replication and hGM-CSF transgene • Destroy tumor cells	NCT01329809 NCT01387555 NCT01169584 NCT00554372 NCT02562755 NCT01171651 NCT02977156 NCT03294083 NCT00429312 NCT00625456	147, 239-240

Non-oncolytic virus + vector	TG1042 (Adenovirus-interferon-γ)	Adenovirus	• Nonreplicating (E1 and E3 regions deleted) • Adenovirus type 5 (group C) vector • Containing a human IFN-γ cDNA insert under cytomegalovirus promoter control	• Expresses IFN-γ	NCT00394693	[148]
Non-oncolytic virus + vector	TNFerade Biologic (AdGVEGR.TNF.11D)	Adenovirus	• Replication-deficient adenoviral vector that expresses tumor necrosis factor-α (TNFα) under the control of a radiation-inducible Egr-1 promoter	• Expresses TNFα	NCT00051467 NCT00051480	[150-151]
Viral vector	INXN-2001 (Ad-RTS-hIL-12) with oral activator INXN-1001 (Veledimex)	Adenovirus	• Expresses human IL-12	• Expresses human IL-12	NCT01397708 NCT02423902 NCT03679754 NCT02026271 NCT03330197 NCT03636477 NCT04006119	
Non-oncolytic virus + vector	adenoviral vector expressing *E. coli* PNP (Ad/PNP) and IV fludarabine therapy	Adenovirus	• Loaded with a bacterial gene called E. coli purine nucleoside phosphorylase (PNP)	• PNP converts fludarabine to anti-cancer agent fluoroadenine	NCT01310179	[154]
Non-oncolytic virus + vector	adenoviral vector (Adv.RSV-tk) expressing the herpes thymidine kinase gene with IV Ganciclovir (GCV)		• Adenoviral vector allow high transgene expression and high transduction efficiency of both dividing and non-dividing cells • Suicide gene transfer • GCV is a synthetic nucleoside analogue that competes with deoxyguanosine triphosphate as a substrate for DNA polymerase in dividing cells and produces cell death	• Expression of herpes simplex virus thymidine kinase (HSV-tk) allow phosphorylation of GCV, forming cytotoxic GCV-triphosphate	NCT00844623	[156]
Plasmid	IL-12 plasmid cDNA (pNGVL3-mIL12)		• Formulated in saline	• Expression of IL-12		[158]
Plasmid	Tavokinogene Telseplasmid (tavo); plasmid IL-12		• 6215 bp	• Expression of IL-12	NCT00323206 NCT01579318 NCT01440816 NCT02345330	[159]
Plasmid	EGFR antisense DNA		• Estimated ~9600 base pairs • pNGVL vector (also called pUMVC) is 9287 bp, human U6 promoter is 241 bp, and EGFRAS is 39 bp • In complex with DC-Chol liposomes • Phosphase-buffered saline	• Suppresses expression of EGFR by tumor cells • Inhibits tumor proliferation/growth	NCT00009841	[241]
Plasmid	BC-819 (also called DTA-H19)		• 4560 bp	• DT-A expressed in tumor cells that can activate H19 promoter	NCT00711997	[177, 242-243]

			• Gene for the diphtheria toxin-A chain (DT-A) under the regulation of the 814-bp 5′ flanking region of the H19 promoter sequence • Tris-EDTA buffer (10 mM Tris, 1 mM EDTA, pH 8) • Forms 80-90 nm polyplexes with PEI			
Plasmid	CYL-02		• Complex of plasmid DNA and linear polymers of polyethyleneimine (JetPEI 22 kDa from Polyplus Transfection, Illkirch, France) • N/P ratio of 8 to 10 • Estimated ~45nm • 5% w/v glucose	• Expression of DCK-UMK fusion protein, which activates the cytotoxic pro-drug gemcitabine	NCT01274455 NCT02806687	[164, 178]
Immunost-imulatory mAbs	Ipilimumab	anti-CTLA-4	• Human immunoglobulin (IgG1k) consisting of four peptide chains • $C_{6572}H_{10126}N_{1734}O_{2080}S_{40}$, 147991 Daltons • 5 mg/mL clear colorless aqueous solution. pH 7.0	• DCs present an inhibitory to signal that binds to cytotoxic T lymphocyte-associated antigen 4 (CTLA-4) to suppress cytotoxic T lymphocytes (CTLs). Ipilimumab binds to CTLA-4 to block the inhibitory signal and release the cytotoxic reaction of CTLs to attach cancer cells.	NCT01672450	[182]
	L19IL2	IL-2 conjugated to L19 mAb	• Recombinant fusion proteins, consisting of a human cytokine linked (at its N- or C-terminus) to a monoclonal antibody or to an antibody fragment	• A pharmacodelivery vehicle for the selective localization of the immunostimulatory payload at sites of disease	NCT01253096	[244]
	ADC-1013	Anti-CD40 mAbs	• A human monospecific IgG1 antibody	• Stimulation of CD40 on dendritic cells is intended to induce effector T-cells that attack the tumor.	NCT02379741	[245]
	TTI-621	Modified antibody targeting CD47	• Anti-CD47 antibody binding domains conjugated to human IgG1 Fc	• TTI-621 (SIRPαFc) is an immune checkpoint inhibitor designed to bind human CD47 and block the “do not eat” signal that suppress macrophage phagocytosis, thereby enhancing phagocytosis, and antitumor activity.	NCT02890368	[215]
	BMS 986178	anti-OX40 mAb	• A human IgG1	• Anti-OX40 mAbs selectively binds to and activates OX40	NCT03831295	[246]

				to induce proliferation of T lymphocytes that attack tumor associated antigens.		
Small Molecule	INT230-6	Cisplatin	• A formulation consisting of an amphiphilic cell penetration enhancer molecule combined with cisplatin and vinblastine. • The penetration enhancer facilitates dispersion of the two drugs throughout injected tumors and enables increased diffusion into cancer cells.	• INT230-6 thoroughly saturates and kills injected tumors. In addition, the drug induces an adaptive (T-cell mediated) immune response that attacks not only the injected tumor, but non-injected tumors and unseen micro-metastases.	NCT03058289	[247]
	Cisplatin/Epinephrine injectable gel	Cisplatin	• Contains 4 mg/mL cisplatin, 0.1 mg/mL epinephrine, and bovine collagen as a protein carrier matrix	• Intratumoral injection of cisplatin/epinephrine injectable gel achieves high concentrations of cisplatin in the tumor with very low concentrations in plasma and other tissues.	NCT00002659 NCT00022217	[248]
	Para-toluenesulfonamide (PTS)		• $C_7H_9NO_2S$, MW= 171 • Formal charge 0	• Significantly inhibit tumor growth by eliciting tumor necrosis • Induces lysosomal instability, mitochondrial damage, and inhibits ATP biosynthesis	NCT03448146	[249]
	Gemcitabine		• A Nucleoside prodrug, an analog of deoxcycytidine • Water-soluble, low-molecular weight (299.66)	• Gemcitabine causes cancer cell death by attaching to the end of the elongating DNA strand and inhibiting DNA synthesis	NCT02723838 NCT01834170	[250]
	PV-10	Rose Bengal (RB) disodium, an xanthene dye	• 10% RB in saline	• Promotes expression of hallmarks related to immunogenic cell death in colon cancer cell lines	NCT02693067 NCT02557321	[251]

References

1. Marabelle, A.; Andtbacka, R.; Harrington, K.; Melero, I.; Leidner, R.; De Baere, T.; Robert, C.; Ascierto, P. A.; Baurain, J.-F.; Imperiale, M.; Rahimian, S.; Tersago, D.; Klumper, E.; Hendriks, M.; Kumar, R.; Stern, M.; Öhrling, K.; Massacesi, C.; Tchakov, I.; Tse, A.; Douillard, J.-Y.; Tabernero, J.; Haanen, J.; Brody, J., Starting the fight in the tumor: expert recommendations for the development of human intratumoral immunotherapy (HIT-IT). *Annals of Oncology* **2018,** *29* (11), 2163-2174.
2. Milling, L.; Zhang, Y.; Irvine, D. J., Delivering safer immunotherapies for cancer. *Advanced Drug Delivery Reviews* **2017,** *114*, 79-101.
3. Marabelle, A.; Kohrt, H.; Caux, C.; Levy, R., Intratumoral Immunization: A New Paradigm for Cancer Therapy. *Clinical Cancer Research* **2014,** *20* (7), 1747-1756.
4. Marabelle, A.; Tselikas, L.; De Baere, T.; Houot, R., Intratumoral immunotherapy: using the tumor as the remedy. *Annals of Oncology* **2017,** *28* (suppl_12), xii33-xii43.
5. Checkmate Pharmaceuticals. https://checkmatepharma.com/about.
6. Jenkins, R. W.; Barbie, D. A.; Flaherty, K. T., Mechanisms of resistance to immune checkpoint inhibitors. *British Journal Of Cancer* **2018,** *118*, 9.
7. Keown, A. Merck Acquires Immune Design for $300 Million in Cash 2019. https://www.biospace.com/article/merck-acquires-immune-design-for-300-million-in-cash/.
8. Design, I. Pipeline. http://www.immunedesign.com/pipeline/.
9. Sagiv-Barfi, I.; Lu, H.; Hewitt, J.; Hsu, F. J.; Meulen, J. T.; Levy, R., Intratumoral Injection of TLR4 Agonist (G100) Leads to Tumor Regression of A20 Lymphoma and Induces Abscopal Responses. *Blood* **2015,** *126* (23), 820-820.
10. Inacio, P. Immune Design's G100 Receives EMA's Orphan Drug Designation for Follicular Non-Hodgkin's Lymphoma 2017. https://lymphomanewstoday.com/2017/10/24/g100-ema-orphan-drug-status-treatment-follicular-non-hodgkins-lymphoma/.
11. Coley, W. B., THE TREATMENT OF INOPERABLE SARCOMA WITH THE MIXED TOXINS OF ERYSIPELAS AND BACILLUS PRODIGIOSUS.: IMMEDIATE AND FINAL RESULTS IN ONE HUNDRED AND FORTY CASES. *Journal of the American Medical Association* **1898,** *XXXI* (8), 389-395.
12. Coley, W. B., The Treatment of Inoperable Sarcoma by Bacterial Toxins (the Mixed Toxins of the Streptococcus erysipelas and the Bacillus prodigiosus). *Proceedings of the Royal Society of Medicine* **1910,** *3* (Surg Sect), 1-48.
13. Fuge, O.; Vasdev, N.; Allchorne, P.; Green, J. S., Immunotherapy for bladder cancer. *Research and reports in urology* **2015,** *7*, 65-79.
14. Fda, Aldara (Imiquimod) Cream 5% Package Insert. 2004.
15. Aznar, M. A.; Tinari, N.; Rullán, A. J.; Sánchez-Paulete, A. R.; Rodriguez-Ruiz, M. E.; Melero, I., Intratumoral Delivery of Immunotherapy—Act Locally, Think Globally. *The Journal of Immunology* **2017,** *198* (1), 31-39.
16. Siegel, R. L.; Miller, K. D.; Jemal, A., Cancer statistics, 2018. *CA: A Cancer Journal for Clinicians* **2018,** *68* (1), 7-30.
17. Bae, Y. H.; Park, K., Targeted drug delivery to tumors: myths, reality and possibility. *Journal of controlled release : official journal of the Controlled Release Society* **2011,** *153* (3), 198-205.
18. Zhan, W.; Alamer, M.; Xu, X. Y., Computational modelling of drug delivery to solid tumour: Understanding the interplay between chemotherapeutics and biological system for optimised delivery systems. *Advanced Drug Delivery Reviews* **2018,** *132*, 81-103.
19. Shamsi, M.; Saghafian, M.; Dejam, M.; Sanati-Nezhad, A., Mathematical Modeling of the Function of Warburg Effect in Tumor Microenvironment. *Scientific Reports* **2018,** *8* (1), 8903.
20. Heldin, C.-H.; Rubin, K.; Pietras, K.; Östman, A., High interstitial fluid pressure — an obstacle in cancer therapy. *Nature Reviews Cancer* **2004,** *4*, 806.
21. Jain, R. K., Transport of Molecules in the Tumor Interstitium: A Review. *Cancer Research* **1987,** *47* (12), 3039-3051.
22. Jain, R. K., Transport of molecules across tumor vasculature. *Cancer and Metastasis Reviews* **1987,** *6* (4), 559-593.
23. Galmarini, C. M.; Tannock, I. F.; Patel, K.; Trédan, O., Drug Resistance and the Solid Tumor Microenvironment. *JNCI: Journal of the National Cancer Institute* **2007,** *99* (19), 1441-1454.
24. Junttila, M. R.; De Sauvage, F. J., Influence of tumour micro-environment heterogeneity on therapeutic response. *Nature* **2013,** *501*, 346.
25. Sriraman, S. K.; Aryasomayajula, B.; Torchilin, V. P., Barriers to drug delivery in solid tumors. *Tissue barriers* **2014,** *2*, e29528-e29528.
26. Matsumura, Y.; Maeda, H., A New Concept for Macromolecular Therapeutics in Cancer Chemotherapy: Mechanism of Tumoritropic Accumulation of Proteins and the Antitumor Agent Smancs. *Cancer Research* **1986,** *46* (12 Part 1), 6387-6392.
27. Gerweck, L. E.; Kozin, S. V.; Stocks, S. J., The pH partition theory predicts the accumulation and toxicity of doxorubicin in normal and low-pH-adapted cells. *British Journal Of Cancer* **1999,** *79*, 838.
28. Payen, V. L.; Porporato, P. E.; Baselet, B.; Sonveaux, P., Metabolic changes associated with tumor metastasis, part 1: tumor pH, glycolysis and the pentose phosphate pathway. *Cellular and Molecular Life Sciences* **2016,** *73* (7), 1333-1348.

29. Estrella, V.; Chen, T.; Lloyd, M.; Wojtkowiak, J.; Cornnell, H. H.; Ibrahim-Hashim, A.; Bailey, K.; Balagurunathan, Y.; Rothberg, J. M.; Sloane, B. F.; Johnson, J.; Gatenby, R. A.; Gillies, R. J., Acidity Generated by the Tumor Microenvironment Drives Local Invasion. *Cancer Research* **2013,** *73* (5), 1524-1535.
30. Kareva, I.; Hahnfeldt, P., The Emerging "Hallmarks" of Metabolic Reprogramming and Immune Evasion: Distinct or Linked? *Cancer Research* **2013,** *73* (9), 2737-2742.
31. Vinay, D. S.; Ryan, E. P.; Pawelec, G.; Talib, W. H.; Stagg, J.; Elkord, E.; Lichtor, T.; Decker, W. K.; Whelan, R. L.; Kumara, H. M. C. S.; Signori, E.; Honoki, K.; Georgakilas, A. G.; Amin, A.; Helferich, W. G.; Boosani, C. S.; Guha, G.; Ciriolo, M. R.; Chen, S.; Mohammed, S. I.; Azmi, A. S.; Keith, W. N.; Bilsland, A.; Bhakta, D.; Halicka, D.; Fujii, H.; Aquilano, K.; Ashraf, S. S.; Nowsheen, S.; Yang, X.; Choi, B. K.; Kwon, B. S., Immune evasion in cancer: Mechanistic basis and therapeutic strategies. *Seminars in Cancer Biology* **2015,** *35*, S185-S198.
32. Gabrilovich, D., Mechanisms and functional significance of tumour-induced dendritic-cell defects. *Nature Reviews Immunology* **2004,** *4* (12), 941-952.
33. Binnewies, M.; Roberts, E. W.; Kersten, K.; Chan, V.; Fearon, D. F.; Merad, M.; Coussens, L. M.; Gabrilovich, D. I.; Ostrand-Rosenberg, S.; Hedrick, C. C.; Vonderheide, R. H.; Pittet, M. J.; Jain, R. K.; Zou, W.; Howcroft, T. K.; Woodhouse, E. C.; Weinberg, R. A.; Krummel, M. F., Understanding the tumor immune microenvironment (TIME) for effective therapy. *Nature Medicine* **2018,** *24* (5), 541-550.
34. Li, K.; Qu, S.; Chen, X.; Wu, Q.; Shi, M., Promising Targets for Cancer Immunotherapy: TLRs, RLRs, and STING-Mediated Innate Immune Pathways. *Int J Mol Sci* **2017,** *18* (2), 404.
35. Berraondo, P.; Sanmamed, M. F.; Ochoa, M. C.; Etxeberria, I.; Aznar, M. A.; Pérez-Gracia, J. L.; Rodríguez-Ruiz, M. E.; Ponz-Sarvise, M.; Castañón, E.; Melero, I., Cytokines in clinical cancer immunotherapy. *British Journal of Cancer* **2019,** *120* (1), 6-15.
36. Jhawar, S. R.; Thandoni, A.; Bommareddy, P. K.; Hassan, S.; Kohlhapp, F. J.; Goyal, S.; Schenkel, J. M.; Silk, A. W.; Zloza, A., Oncolytic Viruses-Natural and Genetically Engineered Cancer Immunotherapies. *Front Oncol* **2017,** *7*, 202-202.
37. Coulson, A.; Levy, A.; Gossell-Williams, M., Monoclonal Antibodies in Cancer Therapy: Mechanisms, Successes and Limitations. *West Indian Med J* **2014,** *63* (6), 650-654.
38. Goldman, I. D., Membrane Transport of Chemotherapeutics and Drug Resistance. *Beyond the ABC Family of Exporters to the Role of Carrier-mediated Processes* **2002,** *8* (1), 4-6.
39. Yang, N. J.; Hinner, M. J., Getting across the cell membrane: an overview for small molecules, peptides, and proteins. *Methods Mol Biol* **2015,** *1266*, 29-53.
40. Groh, C. M.; Hubbard, M. E.; Jones, P. F.; Loadman, P. M.; Periasamy, N.; Sleeman, B. D.; Smye, S. W.; Twelves, C. J.; Phillips, R. M., Mathematical and computational models of drug transport in tumours. *Journal of The Royal Society Interface* **2014,** *11* (94), 20131173.
41. Minchinton, A. I.; Tannock, I. F., Drug penetration in solid tumours. *Nature Reviews Cancer* **2006,** *6* (8), 583-592.
42. Liu, C.; Krishnan, J.; Stebbing, J.; Xu, X. Y., Use of mathematical models to understand anticancer drug delivery and its effect on solid tumors. *Pharmacogenomics* **2011,** *12* (9), 1337-1348.
43. Mellor, H. R.; Callaghan, R., Resistance to Chemotherapy in Cancer: A Complex and Integrated Cellular Response. *Pharmacology* **2008,** *81* (4), 275-300.
44. Danhof, M.; De Lange, E. C. M.; Della Pasqua, O. E.; Ploeger, B. A.; Voskuyl, R. A., Mechanism-based pharmacokinetic-pharmacodynamic (PK-PD) modeling in translational drug research. *Trends in Pharmacological Sciences* **2008,** *29* (4), 186-191.
45. Fang, J.; Nakamura, H.; Maeda, H., The EPR effect: Unique features of tumor blood vessels for drug delivery, factors involved, and limitations and augmentation of the effect. *Advanced Drug Delivery Reviews* **2011,** *63* (3), 136-151.
46. Kuh, H.-J.; Jang, S. H.; Wientjes, M. G.; Au, J. L.-S., Computational Model of Intracellular Pharmacokinetics of Paclitaxel. *Journal of Pharmacology and Experimental Therapeutics* **2000,** *293* (3), 761-770.
47. Venkatasubramanian, R.; Henson, M. A.; Forbes, N. S., Integrating cell-cycle progression, drug penetration and energy metabolism to identify improved cancer therapeutic strategies. *J Theor Biol* **2008,** *253* (1), 98-117.
48. Bertuzzi, A.; Gandolfi, A., Cell Kinetics in a Tumour Cord. *J Theor Biol* **2000,** *204* (4), 587-599.
49. Eikenberry, S., A tumor cord model for doxorubicin delivery and dose optimization in solid tumors. *Theor Biol Med Model* **2009,** *6*, 16-16.
50. Piretto, E.; Delitala, M.; Ferraro, M., Combination therapies and intra-tumoral competition: Insights from mathematical modeling. *J Theor Biol* **2018,** *446*, 149-159.
51. Arabameri, A.; Asemani, D.; Hadjati, J., A structural methodology for modeling immune-tumor interactions including pro- and anti-tumor factors for clinical applications. *Mathematical Biosciences* **2018,** *304*, 48-61.
52. Sinek, J.; Frieboes, H.; Zheng, X.; Cristini, V., Two-dimensional chemotherapy simulations demonstrate fundamental transport and tumor response limitations involving nanoparticles. *Biomedical microdevices* **2004,** *6* (4), 297-309.
53. Tzafriri, A. R.; Lerner, E. I.; Flashner-Barak, M.; Hinchcliffe, M.; Ratner, E.; Parnas, H., Mathematical Modeling and Optimization of Drug Delivery from Intratumorally Injected Microspheres. *Clinical Cancer Research* **2005,** *11* (2), 826-834.
54. Goodman, T. T.; Chen, J.; Matveev, K.; Pun, S. H., Spatio-temporal modeling of nanoparticle delivery to multicellular tumor spheroids. *Biotechnology and Bioengineering* **2008,** *101* (2), 388-399.
55. Huai, Y.; Hossen, M. N.; Wilhelm, S.; Bhattacharya, R.; Mukherjee, P., Nanoparticle Interactions with the Tumor Microenvironment. *Bioconjugate Chemistry* **2019,** *30* (9), 2247-2263.

56. Baskar, R.; Lee, K. A.; Yeo, R.; Yeoh, K.-W., Cancer and radiation therapy: current advances and future directions. *International journal of medical sciences* **2012,** *9* (3), 193-199.
57. Radiation Therapy to Treat Cancer. https://www.cancer.gov/about-cancer/treatment/types/radiation-therapy (accessed May 2019). NIH National Cancer Institute.
58. Society, A. C. Radiation Therapy Basics. https://www.cancer.org/treatment/treatments-and-side-effects/treatment-types/radiation/basics.html.
59. Citrin, D. E., Recent Developments in Radiotherapy. *New England Journal of Medicine* **2017,** *377* (11), 1065-1075.
60. Devita, V. T.; Chu, E., A History of Cancer Chemotherapy. *Cancer Research* **2008,** *68* (21), 8643-8653.
61. Corrie, P. G., Cytotoxic chemotherapy: clinical aspects. *Medicine* **2011,** *39* (12), 717-722.
62. Cohen, E. E. W.; Nabell, L.; Wong, D. J. L.; Day, T. A.; Daniels, G. A.; Milhem, M. M.; Deva, S.; Jameson, M. B.; Guntinas-Lichius, O.; Almubarak, M.; Strother, R. M.; Whitman, E. D.; Chisamore, M. J.; Obiozor, C. C.; Bagulho, T.; Candia, A.; Gamelin, E.; Janssen, R.; Algazi, A. P., Phase 1b/2, open label, multicenter study of intratumoral SD-101 in combination with pembrolizumab in anti-PD-1 treatment naïve patients with recurrent or metastatic head and neck squamous cell carcinoma (HNSCC). *Journal of Clinical Oncology* **2019,** *37* (15_suppl), 6039-6039.
63. Mellman, I.; Coukos, G.; Dranoff, G., Cancer immunotherapy comes of age. *Nature* **2011,** *480*, 480.
64. Lesterhuis, W. J.; Haanen, J. B. a. G.; Punt, C. J. A., Cancer immunotherapy – revisited. *Nature Reviews Drug Discovery* **2011,** *10*, 591.
65. Topalian, Suzanne l.; Drake, Charles g.; Pardoll, Drew m., Immune Checkpoint Blockade: A Common Denominator Approach to Cancer Therapy. *Cancer Cell* **2015,** *27* (4), 450-461.
66. Mahoney, K. M.; Freeman, G. J.; Mcdermott, D. F., The Next Immune-Checkpoint Inhibitors: PD-1/PD-L1 Blockade in Melanoma. *Clinical Therapeutics* **2015,** *37* (4), 764-782.
67. Spain, L.; Diem, S.; Larkin, J., Management of toxicities of immune checkpoint inhibitors. *Cancer Treatment Reviews* **2016,** *44*, 51-60.
68. Lawler, S. E.; Speranza, M.-C.; Cho, C.-F.; Chiocca, E. A., Oncolytic Viruses in Cancer Treatment: A ReviewOncolytic Viruses in Cancer TreatmentOncolytic Viruses in Cancer Treatment. *JAMA Oncology* **2017,** *3* (6), 841-849.
69. Lee, S.; Margolin, K., Cytokines in cancer immunotherapy. *Cancers* **2011,** *3* (4), 3856-3893.
70. Monie, A.; Hung, C.-F.; Roden, R.; Wu, T. C., Cervarix: a vaccine for the prevention of HPV 16, 18-associated cervical cancer. *Biologics : targets & therapy* **2008,** *2* (1), 97-105.
71. Cheever, M. A.; Higano, C. S., PROVENGE (Sipuleucel-T) in Prostate Cancer: The First FDA-Approved Therapeutic Cancer Vaccine. *Clinical Cancer Research* **2011,** *17* (11), 3520-3526.
72. Xu, H.; Wang, F.; Li, H.; Ji, J.; Cao, Z.; Lyu, J.; Shi, X.; Zhu, Y.; Zhang, C.; Guo, F.; Fang, Z.; Yang, B.; Sun, Y., Prostatic Acid Phosphatase (PAP) Predicts Prostate Cancer Progress in a Population-Based Study: The Renewal of PAP? *Dis Markers* **2019,** *2019*, 7090545-7090545.
73. Sridhar, P.; Petrocca, F., Regional Delivery of Chimeric Antigen Receptor (CAR) T-Cells for Cancer Therapy. *Cancers* **2017,** *9* (7), 92.
74. Aleynick, M.; Svensson-Arvelund, J.; Flowers, C. R.; Marabelle, A.; Brody, J. D., Pathogen molecular pattern receptor agonists: treating cancer by mimicking infection. *Clinical Cancer Research* **2019**, clincanres.1800.2019.
75. Krieg, A. M., CpG Motifs in Bacterial DNA and Their Immune Effects. *Annual Review of Immunology* **2002,** *20* (1), 709-760.
76. Klinman, D. M., Immunotherapeutic uses of CpG oligodeoxynucleotides. *Nature Reviews Immunology* **2004,** *4* (4), 249-259.
77. Wittig, B.; Schmidt, M.; Scheithauer, W.; Schmoll, H.-J., MGN1703, an immunomodulator and toll-like receptor 9 (TLR-9) agonist: From bench to bedside. *Critical Reviews in Oncology/Hematology* **2015,** *94* (1), 31-44.
78. Cornfeld, M. J., IMO-2125, an investigational intratumoral tolllike receptor 9 agonist, modulates the tumor microenvironment to enhance anti-tumor immunity. Pharmaceuticals, I., Ed. 2016.
79. Merck, TICE BCG Package Insert. 2019.
80. Pfizer, Agatolimod Sodium. STATEMENT ON A NONPROPRIETARY NAME ADOPTED BY THE USAN COUNCIL
81. Klein, D. C. G.; Latz, E.; Espevik, T.; Stokke, B. T., Higher order structure of short immunostimulatory oligonucleotides studied by atomic force microscopy. *Ultramicroscopy* **2010,** *110* (6), 689-693.
82. Brody, J. D.; Ai, W. Z.; Czerwinski, D. K.; Torchia, J. A.; Levy, M.; Advani, R. H.; Kim, Y. H.; Hoppe, R. T.; Knox, S. J.; Shin, L. K.; Wapnir, I.; Tibshirani, R. J.; Levy, R., In Situ Vaccination With a TLR9 Agonist Induces Systemic Lymphoma Regression: A Phase I/II Study. *Journal of Clinical Oncology* **2010,** *28* (28), 4324-4332.
83. A Phase 2 Intratumoral Injection PF-3512676 Plus Local Radiation in Low-Grade B-Cell Lymphomas. https://ClinicalTrials.gov/show/NCT00880581.
84. Agrawal, S., Creating a Beneficial Tumor Microenvironment for Effective Cancer Immunotherapy. Pharmaceuticals, I., Ed. 2017.
85. Pharmaceuticals, I., Tilsotolimod. Statement on a nonproprietary name adopted by the USAN council: 2018.
86. Engel, A. L.; Holt, G. E.; Lu, H., The pharmacokinetics of Toll-like receptor agonists and the impact on the immune system. *Expert Review of Clinical Pharmacology* **2011,** *4* (2), 275-289.
87. Schmidt, M.; Hagner, N.; Marco, A.; König-Merediz, S. A.; Schroff, M.; Wittig, B., Design and Structural Requirements of the Potent and Safe TLR-9 Agonistic Immunomodulator MGN1703. *Nucleic Acid Ther* **2015,** *25* (3), 130-140.

88. Rodas, I. M. In *Intratumoral BO-112, a double-stranded RNA (dsRNA), alone and in combination with systemic anti-PD-1 in solid tumors*, ESMO 2018 Congress, 2018.
89. Pozuelo Rubio, Q. O., Villanueva Garcia Novel pharmaceutical composition comprising particles comprising a complex of a double-stranded polyribonucleotide and a polyalkyleneimine. 2017.
90. Anderson, R. C.; Fox, C. B.; Dutill, T. S.; Shaverdian, N.; Evers, T. L.; Poshusta, G. R.; Chesko, J.; Coler, R. N.; Friede, M.; Reed, S. G.; Vedvick, T. S., Physicochemical characterization and biological activity of synthetic TLR4 agonist formulations. *Colloids and Surfaces B: Biointerfaces* **2010,** *75* (1), 123-132.
91. Salazar, A. M.; Erlich, R. B.; Mark, A.; Bhardwaj, N.; Herberman, R. B., Therapeutic In Situ Autovaccination against Solid Cancers with Intratumoral Poly-ICLC: Case Report, Hypothesis, and Clinical Trial. *Cancer Immunology Research* **2014,** *2* (8), 720-724.
92. Levy, H. B. Nuclease-Resistant Hydrophilic Complex of Polyinsosinic-Polyribocytidylic Acid. 1982.
93. Middleton, M. R.; Wermke, M.; Calvo, E.; Chartash, E.; Zhou, H.; Zhao, X.; Niewel, M.; Dobrenkov, K.; Moreno, V., LBA16Phase I/II, multicenter, open-label study of intratumoral/intralesional administration of the retinoic acid–inducible gene I (RIG-I) activator MK-4621 in patients with advanced or recurrent tumors. *Annals of Oncology* **2018,** *29* (suppl_8).
94. Intratumoral/Intralesional Administration of MK-4621/JetPEI™ With or Without Pembrolizumab in Participants With Advanced/Metastatic or Recurrent Solid Tumors (MK-4621-002). https://ClinicalTrials.gov/show/NCT03739138.
95. Coler, R. N.; Bertholet, S.; Moutaftsi, M.; Guderian, J. A.; Windish, H. P.; Baldwin, S. L.; Laughlin, E. M.; Duthie, M. S.; Fox, C. B.; Carter, D.; Friede, M.; Vedvick, T. S.; Reed, S. G., Development and Characterization of Synthetic Glucopyranosyl Lipid Adjuvant System as a Vaccine Adjuvant. *PLOS ONE* **2011,** *6* (1), e16333.
96. Sun, J.; Remmele, R. L.; Sanyal, G., Analytical Characterization of an Oil-in-Water Adjuvant Emulsion. *AAPS PharmSciTech* **2017,** *18* (5), 1595-1604.
97. Carter, D.; Fox, C. B.; Day, T. A.; Guderian, J. A.; Liang, H.; Rolf, T.; Vergara, J.; Sagawa, Z. K.; Ireton, G.; Orr, M. T.; Desbien, A.; Duthie, M. S.; Coler, R. N.; Reed, S. G., A structure-function approach to optimizing TLR4 ligands for human vaccines. *Clin Transl Immunology* **2016,** *5* (11), e108-e108.
98. Misquith, A.; Fung, H. W. M.; Dowling, Q. M.; Guderian, J. A.; Vedvick, T. S.; Fox, C. B., In vitro evaluation of TLR4 agonist activity: Formulation effects. *Colloids and Surfaces B: Biointerfaces* **2014,** *113*, 312-319.
99. Nomura, T.; Koreeda, N.; Yamashita, F.; Takakura, Y.; Hashida, M., Effect of Particle Size and Charge on the Disposition of Lipid Carriers After Intratumoral Injection into Tissue-isolated Tumors. *Pharmaceutical Research* **1998,** *15* (1), 128-132.
100. Kawakami, S.; Yamashita, F.; Hashida, M., Disposition characteristics of emulsions and incorporated drugs after systemic or local injection. *Advanced Drug Delivery Reviews* **2000,** *45* (1), 77-88.
101. Theys, J.; Lambin, P., Clostridium to treat cancer: dream or reality? *Annals of Translational Medicine* **2015**.
102. Groves, M. J., Pharmaceutical Characterization of Mycobacterium bovis Bacillus Calmette-Guérin (BCG) Vaccine Used for the Treatment of Superficial Bladder Cancer. *Journal of Pharmaceutical Sciences* **1993,** *82* (6), 555-562.
103. Adams, S., Toll-like receptor agonists in cancer therapy. *Immunotherapy* **2009,** *1* (6), 949-964.
104. Lynn, G. M.; Laga, R.; Darrah, P. A.; Ishizuka, A. S.; Balaci, A. J.; Dulcey, A. E.; Pechar, M.; Pola, R.; Gerner, M. Y.; Yamamoto, A.; Buechler, C. R.; Quinn, K. M.; Smelkinson, M. G.; Vanek, O.; Cawood, R.; Hills, T.; Vasalatiy, O.; Kastenmüller, K.; Francica, J. R.; Stutts, L.; Tom, J. K.; Ryu, K. A.; Esser-Kahn, A. P.; Etrych, T.; Fisher, K. D.; Seymour, L. W.; Seder, R. A., In vivo characterization of the physicochemical properties of polymer-linked TLR agonists that enhance vaccine immunogenicity. *Nature Biotechnology* **2015,** *33* (11), 1201-1210.
105. Waldmann, T., Cytokines in Cancer Immunotherapy. *Cold Spring Harbor Perspectives in Biology* **2017,** *10*, a028472.
106. Conlon, K. C.; Miljkovic, M. D.; Waldmann, T. A., Cytokines in the Treatment of Cancer. *Journal of Interferon & Cytokine Research* **2019,** *39* (1), 6-21.
107. Hong, I.-S., Stimulatory versus suppressive effects of GM-CSF on tumor progression in multiple cancer types. *Experimental & molecular medicine* **2016,** *48* (7), e242.
108. Arenas-Ramirez, N.; Woytschak, J.; Boyman, O., Interleukin-2: biology, design and application. *Trends in Immunology* **2015,** *36* (12), 763-777.
109. Crespo, J.; Sun, H.; Welling, T. H.; Tian, Z.; Zou, W., T cell anergy, exhaustion, senescence, and stemness in the tumor microenvironment. *Current Opinion in Immunology* **2013,** *25* (2), 214-221.
110. Emerson, L.; Morales, A., Intralesional recombinant α-interferon for localized prostate cancer: a pilot study with follow-up of> 10 years. *BJU international* **2009,** *104* (8), 1068-1070.
111. Stenken, J. A.; Poschenrieder, A. J., Bioanalytical chemistry of cytokines--a review. *Anal Chim Acta* **2015,** *853*, 95-115.
112. Van Herpen, C. M.; Huijbens, R.; Looman, M.; De Vries, J.; Marres, H.; Van De Ven, J.; Hermsen, R.; Adema, G. J.; De Mulder, P. H., Pharmacokinetics and immunological aspects of a phase Ib study with intratumoral administration of recombinant human interleukin-12 in patients with head and neck squamous cell carcinoma: a decrease of T-bet in peripheral blood mononuclear cells. *Clinical cancer research* **2003,** *9* (8), 2950-2956.
113. Van Herpen, C. M.; Looman, M.; Zonneveld, M.; Scharenborg, N.; De Wilde, P. C.; Van De Locht, L.; Merkx, M. A.; Adema, G. J.; De Mulder, P. H., Intratumoral administration of recombinant human interleukin 12 in head and neck squamous cell carcinoma patients elicits a T-helper 1 profile in the locoregional lymph nodes. *Clinical Cancer Research* **2004,** *10* (8), 2626-2635.

114. Feinmesser, R.; Hardy, B.; Sadov, R.; Shwartz, A.; Chretien, P.; Feinmesser, M., Report of a clinical trial in 12 patients with head and neck cancer treated intratumorally and peritumorally with multikine. *Archives of Otolaryngology–Head & Neck Surgery* **2003,** *129* (8), 874-881.
115. Kurzrock, R., Granulocyte-macrophage colony-stimulating factor. In *Holland-Frei Cancer Medicine*, 6 ed.; Kufe, D. W.; Pollock, R. E.; Weichselbaum, R. R.; Robert C Bast, J.; Gansler, T. S.; Holland, J. F.; Emil Frei, I., Eds. BC Decker: Hamilton (ON), 2003.
116. Diederichs, K.; Boone, T.; Karplus, P. A., Novel fold and putative receptor binding site of granulocyte-macrophage colony-stimulating factor. *Science* **1991,** *254* (5039), 1779-1782.
117. Yan, W.-L.; Shen, K.-Y.; Tien, C.-Y.; Chen, Y.-A.; Liu, S.-J., Recent progress in GM-CSF-based cancer immunotherapy. *Immunotherapy* **2017,** *9* (4), 347-360.
118. Davidson, J. A.; Musk, A. W.; Wood, B. R.; Morey, S.; Ilton, M.; Yu, L. L.; Drury, P.; Shilkin, K.; Robinson, B., Intralesional cytokine therapy in cancer: a pilot study of GM-CSF infusion in mesothelioma. *Journal of immunotherapy (Hagerstown, Md.: 1997)* **1998,** *21* (5), 389-398.
119. Si, Z.; Hersey, P.; Coates, A., Clinical responses and lymphoid infiltrates in metastatic melanoma following treatment with intralesional GM-CSF. *Melanoma research* **1996,** *6* (3), 247-255.
120. Hoeller, C.; Jansen, B.; Heere-Ress, E.; Pustelnik, T.; Mossbacher, U.; Schlagbauer-Wadl, H.; Wolff, K.; Pehamberger, H., Perilesional injection of r-GM-CSF in patients with cutaneous melanoma metastases. *Journal of investigative dermatology* **2001,** *117* (2), 371-374.
121. Butz, M.; Devenish, S.; Com, *Interleukin-2 stability in changing buffer and temperature conditions Application note*. 2018.
122. Weide, B.; Derhovanessian, E.; Pflugfelder, A.; Eigentler, T. K.; Radny, P.; Zelba, H.; Pföhler, C.; Pawelec, G.; Garbe, C., High response rate after intratumoral treatment with interleukin-2: results from a phase 2 study in 51 patients with metastasized melanoma. *Cancer* **2010,** *116* (17), 4139-4146.
123. Radny, P.; Caroli, U.; Bauer, J.; Paul, T.; Schlegel, C.; Eigentler, T.; Weide, B.; Schwarz, M.; Garbe, C., Phase II trial of intralesional therapy with interleukin-2 in soft-tissue melanoma metastases. *British journal of cancer* **2003,** *89* (9), 1620.
124. Vlock, D. R.; Snyderman, C. H.; Johnson, J. T.; Myers, E. N.; Eibling, D. E.; Rubin, J. S.; Kirkwood, J. M.; Dutcher, J. P.; Adams, G. L., Phase Ib trial of the effect of peritumoral and intranodal injections of interleukin-2 in patients with advanced squamous cell carcinoma of the head and neck: an Eastern Cooperative Oncology Group trial. *Journal of immunotherapy with emphasis on tumor immunology: official journal of the Society for Biological Therapy* **1994,** *15* (2), 134-139.
125. Kaplan, B.; Moy, R. L., Effect of perilesional injections of PEG-interleukin-2 on basal cell carcinoma. *Dermatologic surgery* **2000,** *26* (11), 1037-1040.
126. Mattijssen, V.; De Mulder, P.; De Graeff, A.; Hupperets, P.; Joosten, F.; Ruiter, D.; Bier, H.; Palmer, P.; Van Den Broek, P., Intratumoral PEG-interleukin-2 therapy in patients with locoregionally recurrent head and neck squamous-cell carcinoma. *Annals of oncology* **1994,** *5* (10), 957-960.
127. Charych, D.; Khalili, S.; Dixit, V.; Kirk, P.; Chang, T.; Langowski, J.; Rubas, W.; Doberstein, S. K.; Eldon, M.; Hoch, U., Modeling the receptor pharmacology, pharmacokinetics, and pharmacodynamics of NKTR-214, a kinetically-controlled interleukin-2 (IL2) receptor agonist for cancer immunotherapy. *PloS one* **2017,** *12* (7), e0179431.
128. Joshi, B.; Leland, P.; Silber, J.; Kreitman, R.; Pastan, I.; Berger, M.; Puri, R., IL-4 receptors on human medulloblastoma tumours serve as a sensitive target for a circular permuted IL-4-Pseudomonas exotoxin fusion protein. *British journal of cancer* **2002,** *86* (2), 285.
129. Prados, M.; Kunwar, S.; Lang, F.; Ram, Z.; Westphal, M.; Barnett, G.; Sampson, J.; Croteau, D.; Puri, R., Final results of phase I/II studies of IL13-PE38QQR administered intratumorally (IT) and/or peritumorally (PT) via convection-enhanced delivery (CED) in patients undergoing tumor resection for recurrent malignant glioma. *Journal of Clinical Oncology* **2005,** *23* (16_suppl), 1506-1506.
130. Tang, A.; Harding, F., The challenges and molecular approaches surrounding interleukin-2-based therapeutics in cancer. *Cytokine: X* **2018**, 100001.
131. Danielli, R.; Patuzzo, R.; Di Giacomo, A. M.; Gallino, G.; Maurichi, A.; Di Florio, A.; Cutaia, O.; Lazzeri, A.; Fazio, C.; Miracco, C.; Giovannoni, L.; Elia, G.; Neri, D.; Maio, M.; Santinami, M., Intralesional administration of L19-IL2/L19-TNF in stage III or stage IVM1a melanoma patients: results of a phase II study. *Cancer Immunology, Immunotherapy* **2015,** *64* (8), 999-1009.
132. Mullen, J. T.; Tanabe, K. K., Viral oncolysis. *The oncologist* **2002,** *7* (2), 106-119.
133. Ganly, I.; Kirn, D.; Eckhardt, S. G.; Rodriguez, G. I.; Soutar, D. S.; Otto, R.; Robertson, A. G.; Park, O.; Gulley, M. L.; Heise, C., A phase I study of Onyx-015, an E1B attenuated adenovirus, administered intratumorally to patients with recurrent head and neck cancer. *Clinical Cancer Research* **2000,** *6* (3), 798-806.
134. Khuri, F. R.; Nemunaitis, J.; Ganly, I.; Arseneau, J.; Tannock, I. F.; Romel, L.; Gore, M.; Ironside, J.; Macdougall, R.; Heise, C., A controlled trial of intratumoral ONYX-015, a selectively-replicating adenovirus, in combination with cisplatin and 5-fluorouracil in patients with recurrent head and neck cancer. *Nature medicine* **2000,** *6* (8), 879.
135. Lang, F. F.; Conrad, C.; Gomez-Manzano, C.; Yung, W. A.; Sawaya, R.; Weinberg, J. S.; Prabhu, S. S.; Rao, G.; Fuller, G. N.; Aldape, K. D., Phase I study of DNX-2401 (Delta-24-RGD) oncolytic adenovirus: replication and immunotherapeutic effects in recurrent malignant glioma. *Journal of Clinical Oncology* **2018,** *36* (14), 1419.
136. Andtbacka, R. H. I.; Curti, B. D.; Kaufman, H.; Daniels, G. A.; Nemunaitis, J. J.; Spitler, L. E.; Hallmeyer, S.; Lutzky, J.; Schultz, S. M.; Whitman, E. D., Final data from CALM: A phase II study of Coxsackievirus A21 (CVA21) oncolytic virus immunotherapy in patients with advanced melanoma. American Society of Clinical Oncology: 2015.

137. Nakao, A.; Kasuya, H.; Sahin, T.; Nomura, N.; Kanzaki, A.; Misawa, M.; Shirota, T.; Yamada, S.; Fujii, T.; Sugimoto, H., A phase I dose-escalation clinical trial of intraoperative direct intratumoral injection of HF10 oncolytic virus in non-resectable patients with advanced pancreatic cancer. *Cancer gene therapy* **2011,** *18* (3), 167.
138. Hirooka, Y.; Kasuya, H.; Ishikawa, T.; Kawashima, H.; Ohno, E.; Villalobos, I. B.; Naoe, Y.; Ichinose, T.; Koyama, N.; Tanaka, M., A Phase I clinical trial of EUS-guided intratumoral injection of the oncolytic virus, HF10 for unresectable locally advanced pancreatic cancer. *BMC cancer* **2018,** *18* (1), 596.
139. Rampling, R.; Cruickshank, G.; Papanastassiou, V.; Nicoll, J.; Hadley, D.; Brennan, D. A.; Petty, R.; Maclean, A.; Harland, J.; Mckie, E., Toxicity evaluation of replication-competent herpes simplex virus (ICP 34.5 null mutant 1716) in patients with recurrent malignant glioma. *Gene therapy* **2000,** *7* (10), 859.
140. Geletneky, K.; Hajda, J.; Angelova, A. L.; Leuchs, B.; Capper, D.; Bartsch, A. J.; Neumann, J.-O.; Schöning, T.; Hüsing, J.; Beelte, B., Oncolytic H-1 parvovirus shows safety and signs of immunogenic activity in a first phase I/IIa glioblastoma trial. *Molecular Therapy* **2017,** *25* (12), 2620-2634.
141. Heinzerling, L.; Künzi, V.; Oberholzer, P. A.; Kündig, T.; Naim, H.; Dummer, R., Oncolytic measles virus in cutaneous T-cell lymphomas mounts antitumor immune responses in vivo and targets interferon-resistant tumor cells. *Blood* **2005,** *106* (7), 2287-2294.
142. Mahalingam, D.; Goel, S.; Aparo, S.; Patel Arora, S.; Noronha, N.; Tran, H.; Chakrabarty, R.; Selvaggi, G.; Gutierrez, A.; Coffey, M., A phase II study of pelareorep (REOLYSIN®) in combination with gemcitabine for patients with advanced pancreatic adenocarcinoma. *Cancers* **2018,** *10* (6), 160.
143. Zeh, H. J.; Downs-Canner, S.; Mccart, J. A.; Guo, Z. S.; Rao, U. N.; Ramalingam, L.; Thorne, S. H.; Jones, H. L.; Kalinski, P.; Wieckowski, E., First-in-man study of western reserve strain oncolytic vaccinia virus: safety, systemic spread, and antitumor activity. *Molecular Therapy* **2015,** *23* (1), 202-214.
144. Hidai, C.; Kitano, H., Nonviral Gene Therapy for Cancer: A Review. *Diseases* **2018,** *6* (3), 57.
145. Rehman, H.; Silk, A. W.; Kane, M. P.; Kaufman, H. L., Into the clinic: Talimogene laherparepvec (T-VEC), a first-in-class intratumoral oncolytic viral therapy. *Journal for immunotherapy of cancer* **2016,** *4*, 53-53.
146. Ranki, T.; Pesonen, S.; Hemminki, A.; Partanen, K.; Kairemo, K.; Alanko, T.; Lundin, J.; Linder, N.; Turkki, R.; Ristimäki, A.; Jäger, E.; Karbach, J.; Wahle, C.; Kankainen, M.; Backman, C.; Von Euler, M.; Haavisto, E.; Hakonen, T.; Heiskanen, R.; Jaderberg, M.; Juhila, J.; Priha, P.; Suoranta, L.; Vassilev, L.; Vuolanto, A.; Joensuu, T., Phase I study with ONCOS-102 for the treatment of solid tumors - an evaluation of clinical response and exploratory analyses of immune markers. *Journal for immunotherapy of cancer* **2016,** *4*, 17-17.
147. Heo, J.; Reid, T.; Ruo, L.; Breitbach, C. J.; Rose, S.; Bloomston, M.; Cho, M.; Lim, H. Y.; Chung, H. C.; Kim, C. W.; Burke, J.; Lencioni, R.; Hickman, T.; Moon, A.; Lee, Y. S.; Kim, M. K.; Daneshmand, M.; Dubois, K.; Longpre, L.; Ngo, M.; Rooney, C.; Bell, J. C.; Rhee, B.-G.; Patt, R.; Hwang, T.-H.; Kirn, D. H., Randomized dose-finding clinical trial of oncolytic immunotherapeutic vaccinia JX-594 in liver cancer. *Nature Medicine* **2013,** *19*, 329.
148. Dummer, R.; Eichmüller, S.; Gellrich, S.; Assaf, C.; Dreno, B.; Schiller, M.; Dereure, O.; Baudard, M.; Bagot, M.; Khammari, A.; Bleuzen, P.; Bataille, V.; Derbij, A.; Wiedemann, N.; Waterboer, T.; Lusky, M.; Acres, B.; Urosevic-Maiwald, M., Phase II Clinical Trial of Intratumoral Application of TG1042 (adenovirus-interferon-gamma) in Patients with Advanced Cutaneous T-cell Lymphomas and Multilesional Cutaneous B-cell Lymphomas. *Mol Ther* **2010,** *18* (6), 1244-1247.
149. Dreno, B.; Urosevic-Maiwald, M.; Kim, Y.; Guitart, J.; Duvic, M.; Dereure, O.; Khammari, A.; Knol, A.-C.; Derbij, A.; Lusky, M.; Didillon, I.; Santoni, A.-M.; Acres, B.; Bataille, V.; Chenard, M.-P.; Bleuzen, P.; Limacher, J.-M.; Dummer, R., TG1042 (Adenovirus-interferon-γ) in Primary Cutaneous B-cell Lymphomas: A Phase II Clinical Trial. *PLOS ONE* **2014,** *9* (2), e83670.
150. Hecht, J. R.; Farrell, J. J.; Senzer, N.; Nemunaitis, J.; Rosemurgy, A.; Chung, T.; Hanna, N.; Chang, K. J.; Javle, M.; Posner, M., EUS or percutaneously guided intratumoral TNFerade biologic with 5-fluorouracil and radiotherapy for first-line treatment of locally advanced pancreatic cancer: a phase I/II study. *Gastrointestinal endoscopy* **2012,** *75* (2), 332-338.
151. Mundt, A. J.; Vijayakumar, S.; Nemunaitis, J.; Sandler, A.; Schwartz, H.; Hanna, N.; Peabody, T.; Senzer, N.; Chu, K.; Rasmussen, C. S., A Phase I trial of TNFerade biologic in patients with soft tissue sarcoma in the extremities. *Clinical cancer research* **2004,** *10* (17), 5747-5753.
152. Chang, K. J.; Reid, T.; Senzer, N.; Swisher, S.; Pinto, H.; Hanna, N.; Chak, A.; Soetikno, R., Phase I evaluation of TNFerade biologic plus chemoradiotherapy before esophagectomy for locally advanced resectable esophageal cancer. *Gastrointestinal endoscopy* **2012,** *75* (6), 1139-1146. e2.
153. Linette, G. P.; Hamid, O.; Whitman, E. D.; Nemunaitis, J. J.; Chesney, J.; Agarwala, S. S.; Starodub, A.; Barrett, J. A.; Marsh, A.; Martell, L. A.; Cho, A.; Reed, T. D.; Youssoufian, H.; Vergara-Silva, A., A phase I open-label study of Ad-RTS-hIL-12, an adenoviral vector engineered to express hIL-12 under the control of an oral activator ligand, in subjects with unresectable stage III/IV melanoma. *Journal of Clinical Oncology* **2013,** *31* (15_suppl), 3022-3022.
154. Rosenthal, E. L.; Chung, T. K.; Parker, W. B.; Allan, P. W.; Clemons, L.; Lowman, D.; Hong, J.; Hunt, F. R.; Richman, J.; Conry, R. M.; Mannion, K.; Carroll, W. R.; Nabell, L.; Sorscher, E. J., Phase I dose-escalating trial of Escherichia coli purine nucleoside phosphorylase and fludarabine gene therapy for advanced solid tumors†. *Annals of Oncology* **2015,** *26* (7), 1481-1487.
155. Sangro, B.; Mazzolini, G.; Ruiz, M.; Ruiz, J.; Quiroga, J.; Herrero, I.; Qian, C.; Benito, A.; Larrache, J.; Olagüe, C., A phase I clinical trial of thymidine kinase-based gene therapy in advanced hepatocellular carcinoma. *Cancer gene therapy* **2010,** *17* (12), 837.

156. Sung, M. W.; Yeh, H.-C.; Thung, S. N.; Schwartz, M. E.; Mandeli, J. P.; Chen, S.-H.; Woo, S. L., Intratumoral adenovirus-mediated suicide gene transfer for hepatic metastases from colorectal adenocarcinoma: results of a phase I clinical trial. *Molecular Therapy* **2001,** *4* (3), 182-191.
157. Trask, T. W.; Trask, R. P.; Aguilar-Cordova, E.; Shine, H. D.; Wyde, P. R.; Goodman, J. C.; Hamilton, W. J.; Rojas-Martinez, A.; Chen, S.-H.; Woo, S. L., Phase I study of adenoviral delivery of the HSV-tk gene and ganciclovir administration in patients with recurrent malignant brain tumors. *Molecular therapy* **2000,** *1* (2), 195-203.
158. Mahvi, D.; Henry, M.; Albertini, M.; Weber, S.; Meredith, K.; Schalch, H.; Rakhmilevich, A.; Hank, J.; Sondel, P., Intratumoral injection of IL-12 plasmid DNA–results of a phase I/IB clinical trial. *Cancer gene therapy* **2007,** *14* (8), 717.
159. Canton, D. A.; Shirley, S.; Wright, J.; Connolly, R.; Burkart, C.; Mukhopadhyay, A.; Twitty, C.; Qattan, K. E.; Campbell, J. S.; Le, M. H.; Pierce, R. H.; Gargosky, S.; Daud, A.; Algazi, A., Melanoma treatment with intratumoral electroporation of tavokinogene telseplasmid (pIL-12, tavokinogene telseplasmid). *Immunotherapy* **2017,** *9* (16), 1309-1321.
160. Daud, A. I.; Deconti, R. C.; Andrews, S.; Urbas, P.; Riker, A. I.; Sondak, V. K.; Munster, P. N.; Sullivan, D. M.; Ugen, K. E.; Messina, J. L., Phase I trial of interleukin-12 plasmid electroporation in patients with metastatic melanoma. *Journal of clinical oncology* **2008,** *26* (36), 5896.
161. Tros De Ilarduya, C.; Sun, Y.; Düzgüneş, N., Gene delivery by lipoplexes and polyplexes. *European Journal of Pharmaceutical Sciences* **2010,** *40* (3), 159-170.
162. Lai, S. Y.; Koppikar, P.; Thomas, S. M.; Childs, E. E.; Egloff, A. M.; Seethala, R. R.; Branstetter, B. F.; Gooding, W. E.; Muthukrishnan, A.; Mountz, J. M., Intratumoral epidermal growth factor receptor antisense DNA therapy in head and neck cancer: first human application and potential antitumor mechanisms. *Journal of Clinical Oncology* **2009,** *27* (8), 1235.
163. Gofrit, O. N.; Benjamin, S.; Halachmi, S.; Leibovitch, I.; Dotan, Z.; Lamm, D. L.; Ehrlich, N.; Yutkin, V.; Ben-Am, M.; Hochberg, A., DNA Based Therapy with Diphtheria Toxin-A BC-819: A Phase 2b Marker Lesion Trial in Patients with Intermediate Risk Nonmuscle Invasive Bladder Cancer. *Journal of Urology* **2014,** *191* (6), 1697-1702.
164. Buscail, L.; Bournet, B.; Vernejoul, F.; Cambois, G.; Lulka, H.; Hanoun, N.; Dufresne, M.; Meulle, A.; Vignolle-Vidoni, A.; Ligat, L.; Saint-Laurent, N.; Pont, F.; Dejean, S.; Gayral, M.; Martins, F.; Torrisani, J.; Barbey, O.; Gross, F.; Guimbaud, R.; Otal, P.; Lopez, F.; Tiraby, G.; Cordelier, P., First-in-man phase 1 clinical trial of gene therapy for advanced pancreatic cancer: safety, biodistribution, and preliminary clinical findings. *Mol Ther* **2015,** *23* (4), 779-789.
165. Weiner, L. M.; Murray, J. C.; Shuptrine, C. W., Antibody-based immunotherapy of cancer. *Cell* **2012,** *148* (6), 1081-4.
166. Singh, P. K.; Doley, J.; Kumar, G. R.; Sahoo, A. P.; Tiwari, A. K., Oncolytic viruses & their specific targeting to tumour cells. *Indian J Med Res* **2012,** *136* (4), 571-584.
167. Laine, R. F.; Albecka, A.; Van De Linde, S.; Rees, E. J.; Crump, C. M.; Kaminski, C. F., Structural analysis of herpes simplex virus by optical super-resolution imaging. *Nature communications* **2015,** *6*, 5980.
168. Wong, H. H.; Lemoine, N.; Wang, Y., Oncolytic viruses for cancer therapy: overcoming the obstacles. *Viruses* **2010,** *2* (1), 78-106.
169. Xiao, C.; Bator-Kelly, C. M.; Rieder, E.; Chipman, P. R.; Craig, A.; Kuhn, R. J.; Wimmer, E.; Rossmann, M. G., The crystal structure of coxsackievirus A21 and its interaction with ICAM-1. *Structure* **2005,** *13* (7), 1019-1033.
170. Bellini, W. J.; Rota, J. S.; Rota, P. A., Virology of measles virus. *Journal of Infectious Diseases* **1994,** *170* (Supplement_1), S15-S23.
171. Liu, B.; Robinson, M.; Han, Z.; Branston, R.; English, C.; Reay, P.; Mcgrath, Y.; Thomas, S.; Thornton, M.; Bullock, P., ICP34. 5 deleted herpes simplex virus with enhanced oncolytic, immune stimulating, and anti-tumour properties. *Gene therapy* **2003,** *10* (4), 292.
172. Andtbacka, R. H.; Collichio, F.; Harrington, K. J.; Middleton, M. R.; Downey, G.; Öhrling, K.; Kaufman, H. L., Final analyses of OPTiM: a randomized phase III trial of talimogene laherparepvec versus granulocyte-macrophage colony-stimulating factor in unresectable stage III–IV melanoma. *Journal for immunotherapy of cancer* **2019,** *7* (1), 145.
173. Rochlitz, C., Gene therapy of cancer. *Swiss medical weekly* **2001,** *131* (0102).
174. Stewart, S. A.; Dykxhoorn, D. M.; Palliser, D.; Mizuno, H.; Yu, E. Y.; An, D. S.; Sabatini, D. M.; Chen, I. S.; Hahn, W. C.; Sharp, P. A., Lentivirus-delivered stable gene silencing by RNAi in primary cells. *Rna* **2003,** *9* (4), 493-501.
175. Kabadi, A. M.; Ousterout, D. G.; Hilton, I. B.; Gersbach, C. A., Multiplex CRISPR/Cas9-based genome engineering from a single lentiviral vector. *Nucleic acids research* **2014,** *42* (19), e147-e147.
176. Rols, M.-P., Mechanism by which electroporation mediates DNA migration and entry into cells and targeted tissues. In *Electroporation Protocols*, Springer: 2008; pp 19-33.
177. Hochberg, A.; Gallula, J. Nucleic Acid-Cationic Polymer Compositions and Methods of Making and Using the Same. 2018.
178. Gossart, J.-B.; Kédinger, V.; Guérin-Peyrou, G.; Erbacher, P.; Bolcato-Bellemin, A.-L., Application Note: Bioimaging of Gene Delivery with In Vivo-jetPEI. PerkinElmer, Inc. : 2013.
179. Darvin, P.; Toor, S. M.; Sasidharan Nair, V.; Elkord, E., Immune checkpoint inhibitors: recent progress and potential biomarkers. *Exp Mol Med* **2018,** *50* (12), 165.
180. Kohrt, H. E.; Tumeh, P. C.; Benson, D.; Bhardwaj, N.; Brody, J.; Formenti, S.; Fox, B. A.; Galon, J.; June, C. H.; Kalos, M.; Kirsch, I.; Kleen, T.; Kroemer, G.; Lanier, L.; Levy, R.; Lyerly, H. K.; Maecker, H.; Marabelle, A.; Melenhorst, J.; Miller, J.; Melero, I.; Odunsi, K.; Palucka, K.; Peoples, G.; Ribas, A.; Robins, H.; Robinson, W.; Serafini, T.; Sondel, P.; Vivier, E.; Weber, J.; Wolchok, J.; Zitvogel, L.; Disis, M. L.; Cheever, M. A.; Cancer Immunotherapy Trials, N., Immunodynamics: a cancer immunotherapy trials network review of immune monitoring in immuno-oncology clinical trials. *J Immunother Cancer* **2016,** *4*, 15.

181. Ellmark, P.; Mangsbo, S. M.; Furebring, C.; Norlen, P.; Totterman, T. H., Tumor-directed immunotherapy can generate tumor-specific T cell responses through localized co-stimulation. *Cancer Immunol Immunother* **2017,** *66* (1), 1-7.
182. Ray, A.; Williams, M. A.; Meek, S. M.; Bowen, R. C.; Grossmann, K. F.; Andtbacka, R. H.; Bowles, T. L.; Hyngstrom, J. R.; Leachman, S. A.; Grossman, D.; Bowen, G. M.; Holmen, S. L.; Vanbrocklin, M. W.; Suneja, G.; Khong, H. T., A phase I study of intratumoral ipilimumab and interleukin-2 in patients with advanced melanoma. *Oncotarget* **2016,** *7* (39), 64390-64399.
183. A Study of Intratumoral Injection of Interleukin-2 and Ipilimumab in Patients With Unresectable Stages III-IV Melanoma. https://ClinicalTrials.gov/show/NCT01672450.
184. Irenaeus, S. M. M.; Nielsen, D.; Ellmark, P.; Yachnin, J.; Deronic, A.; Nilsson, A.; Norlen, P.; Veitonmaki, N.; Wennersten, C. S.; Ullenhag, G. J., First-in-human study with intratumoral administration of a CD40 agonistic antibody, ADC-1013, in advanced solid malignancies. *Int J Cancer* **2019,** *145* (5), 1189-1199.
185. ADC-1013 First-in-Human Study. https://ClinicalTrials.gov/show/NCT02379741.
186. Reth, M., Matching cellular dimensions with molecular sizes. *Nature Immunology* **2013,** *14*, 765.
187. Broos, S.; Sandin, L. C.; Apel, J.; Totterman, T. H.; Akagi, T.; Akashi, M.; Borrebaeck, C. A.; Ellmark, P.; Lindstedt, M., Synergistic augmentation of CD40-mediated activation of antigen-presenting cells by amphiphilic poly(gamma-glutamic acid) nanoparticles. *Biomaterials* **2012,** *33* (26), 6230-9.
188. Dominguez, A. L.; Lustgarten, J., Targeting the tumor microenvironment with anti-neu/anti-CD40 conjugated nanoparticles for the induction of antitumor immune responses. *Vaccine* **2010,** *28* (5), 1383-90.
189. Fransen, M. F.; Cordfunke, R. A.; Sluijter, M.; Van Steenbergen, M. J.; Drijfhout, J. W.; Ossendorp, F.; Hennink, W. E.; Melief, C. J., Effectiveness of slow-release systems in CD40 agonistic antibody immunotherapy of cancer. *Vaccine* **2014,** *32* (15), 1654-60.
190. Sandin, L. C.; Orlova, A.; Gustafsson, E.; Ellmark, P.; Tolmachev, V.; Totterman, T. H.; Mangsbo, S. M., Locally delivered CD40 agonist antibody accumulates in secondary lymphoid organs and eradicates experimental disseminated bladder cancer. *Cancer Immunol Res* **2014,** *2* (1), 80-90.
191. Mangsbo, S. M.; Broos, S.; Fletcher, E.; Veitonmaki, N.; Furebring, C.; Dahlen, E.; Norlen, P.; Lindstedt, M.; Totterman, T. H.; Ellmark, P., The human agonistic CD40 antibody ADC-1013 eradicates bladder tumors and generates T-cell-dependent tumor immunity. *Clin Cancer Res* **2015,** *21* (5), 1115-26.
192. Danielli, R.; Patuzzo, R.; Ruffini, P. A.; Maurichi, A.; Giovannoni, L.; Elia, G.; Neri, D.; Santinami, M., Armed antibodies for cancer treatment: a promising tool in a changing era. *Cancer Immunol Immunother* **2015,** *64* (1), 113-21.
193. A Phase 1/2 Safety Study of Intratumorally Dosed INT230-6. https://ClinicalTrials.gov/show/NCT03058289.
194. Liu, D.; Auguste, D. T., Cancer targeted therapeutics: From molecules to drug delivery vehicles. *Journal of Controlled Release* **2015,** *219*, 632-643.
195. Bae, Y.; Nishiyama, N.; Fukushima, S.; Koyama, H.; Yasuhiro, M.; Kataoka, K., Preparation and biological characterization of polymeric micelle drug carriers with intracellular pH-triggered drug release property: tumor permeability, controlled subcellular drug distribution, and enhanced in vivo antitumor efficacy. *Bioconjug Chem* **2005,** *16* (1), 122-30.
196. Ernsting, M. J.; Murakami, M.; Roy, A.; Li, S. D., Factors controlling the pharmacokinetics, biodistribution and intratumoral penetration of nanoparticles. *J Control Release* **2013,** *172* (3), 782-94.
197. Kim, J. H.; Kim, Y. S.; Park, K.; Lee, S.; Nam, H. Y.; Min, K. H.; Jo, H. G.; Park, J. H.; Choi, K.; Jeong, S. Y.; Park, R. W.; Kim, I. S.; Kim, K.; Kwon, I. C., Antitumor efficacy of cisplatin-loaded glycol chitosan nanoparticles in tumor-bearing mice. *J Control Release* **2008,** *127* (1), 41-9.
198. Moreno, D.; Zalba, S.; Navarro, I.; Tros De Ilarduya, C.; Garrido, M. J., Pharmacodynamics of cisplatin-loaded PLGA nanoparticles administered to tumor-bearing mice. *Eur J Pharm Biopharm* **2010,** *74* (2), 265-74.
199. Li, X.; Li, R.; Qian, X.; Ding, Y.; Tu, Y.; Guo, R.; Hu, Y.; Jiang, X.; Guo, W.; Liu, B., Superior antitumor efficiency of cisplatin-loaded nanoparticles by intratumoral delivery with decreased tumor metabolism rate. *Eur J Pharm Biopharm* **2008,** *70* (3), 726-34.
200. Chen, F. A.; Kuriakose, M. A.; Zhou, M. X.; Delacure, M. D.; Dunn, R. L., Biodegradable polymer-mediated intratumoral delivery of cisplatin for treatment of human head and neck squamous cell carcinoma in a chimeric mouse model. *Head Neck* **2003,** *25* (7), 554-60.
201. Campbell, R. B.; Fukumura, D.; Brown, E. B.; Mazzola, L. M.; Izumi, Y.; Jain, R. K.; Torchilin, V. P.; Munn, L. L., Cationic Charge Determines the Distribution of Liposomes between the Vascular and Extravascular Compartments of Tumors. *Cancer Research* **2002,** *62* (23), 6831-6836.
202. Kim, B.; Han, G.; Toley, B. J.; Kim, C. K.; Rotello, V. M.; Forbes, N. S., Tuning payload delivery in tumour cylindroids using gold nanoparticles. *Nat Nanotechnol* **2010,** *5* (6), 465-72.
203. Diab, A.; Rahimian, S.; Haymaker, C. L.; Bernatchez, C.; Andtbacka, R. H. I.; James, M.; Johnson, D. B.; Markowitz, J.; Murthy, R.; Puzanov, I.; Shaheen, M. F.; Swann, S., A phase 2 study to evaluate the safety and efficacy of Intratumoral (IT) injection of the TLR9 agonist IMO-2125 (IMO) in combination with ipilimumab (ipi) in PD-1 inhibitor refractory melanoma. *Journal of Clinical Oncology* **2018,** *36* (15_suppl), 9515-9515.
204. A Phase I/II Study of Intratumoral Injection of SD-101. https://ClinicalTrials.gov/show/NCT02254772.
205. Frank, M. J.; Reagan, P. M.; Bartlett, N. L.; Gordon, L. I.; Friedberg, J. W.; Czerwinski, D. K.; Long, S. R.; Hoppe, R. T.; Janssen, R.; Candia, A. F.; Coffman, R. L.; Levy, R., In Situ Vaccination with a TLR9 Agonist and Local Low-Dose Radiation Induces Systemic Responses in Untreated Indolent Lymphoma. *Cancer Discovery* **2018,** *8* (10), 1258-1269.

206. Bhatia, S.; Miller, N.; Lu, H.; Ibrani, D.; Shinohara, M.; Byrd, D. R.; Parvathaneni, U.; Vandeven, N.; Kulikauskas, R.; Meulen, J. T.; Hsu, F. J.; Koelle, D. M.; Ngheim, P., Pilot trial of intratumoral (IT) G100, a toll-like receptor-4 (TLR4) agonist, in patients (pts) with Merkel cell carcinoma (MCC): Final clinical results and immunologic effects on the tumor microenvironment (TME). *Journal of Clinical Oncology* **2016,** *34* (15_suppl), 3021-3021.
207. Pollack, S.; Kim, E. Y.; Conrad, E. U.; O'malley, R. B.; Cooper, S.; Donahue, B.; Cranmer, L. D.; Lu, H.; Loggers, E. T.; Hain, T.; Davidson, D. J.; Bonham, L.; Pillarisetty, V. G.; Kane, G.; Riddell, S. R.; Jones, R. L., Using G100 (Glucopyranosyl Lipid A) to transform the sarcoma tumor immune microenvironment. *Journal of Clinical Oncology* **2016,** *34* (15_suppl), 11017-11017.
208. Flowers, C.; Isufi, I.; Herrera, A. F.; Okada, C.; Cull, E. H.; Kis, B.; Chaves, J.; Bartlett, N. L.; Bryan, L. J.; Houot, R.; Ai, W. Z.; Chau, I.; Linton, K.; Briones, J.; Merino, L. D. L. C.; Panizo, C.; Keudell, G. R. V.; Lu, H.; Hsu, F. J.; Halwani, A. S., Intratumoral G100 to induce systemic immune responses and abscopal tumor regression in patients with follicular lymphoma. *Journal of Clinical Oncology* **2017,** *35* (15_suppl), 7537-7537.
209. Phase I Study of Intralesional Bacillus Calmette-Guerin (BCG) Followed by Ipilimumab in Advanced Metastatic Melanoma. https://ClinicalTrials.gov/show/NCT01838200.
210. Roberts, N. J.; Zhang, L.; Janku, F.; Collins, A.; Bai, R.-Y.; Staedtke, V.; Rusk, A. W.; Tung, D.; Miller, M.; Roix, J.; Khanna, K. V.; Murthy, R.; Benjamin, R. S.; Helgason, T.; Szvalb, A. D.; Bird, J. E.; Roy-Chowdhuri, S.; Zhang, H. H.; Qiao, Y.; Karim, B.; Mcdaniel, J.; Elpiner, A.; Sahora, A.; Lachowicz, J.; Phillips, B.; Turner, A.; Klein, M. K.; Post, G.; Diaz, L. A.; Riggins, G. J.; Papadopoulos, N.; Kinzler, K. W.; Vogelstein, B.; Bettegowda, C.; Huso, D. L.; Varterasian, M.; Saha, S.; Zhou, S., Intratumoral injection of Clostridium novyi-NT spores induces antitumor responses. *Science Translational Medicine* **2014,** *6* (249), 249ra111-249ra111.
211. Ridolfi, L.; Ridolfi, R.; Ascari-Raccagni, A.; Fabbri, M.; Casadei, S.; Gatti, A.; Trevisan, G.; Righini, M., Intralesional granulocyte-monocyte colony-stimulating factor followed by subcutaneous interleukin-2 in metastatic melanoma: a pilot study in elderly patients. *Journal of the European Academy of Dermatology and Venereology* **2001,** *15* (3), 218-223.
212. Kramer, G.; Steiner, G. E.; Sokol, P.; Handisurya, A.; Klingler, H. C.; Maier, U.; Földy, M.; Marberger, M., Local Intratumoral Tumor Necrosis Factor-α and Systemic IFN-α2b in Patients with Locally Advanced Prostate Cancer. *Journal of Interferon & Cytokine Research* **2001,** *21* (7), 475-484.
213. Rand, R. W.; Kreitman, R. J.; Patronas, N.; Varricchio, F.; Pastan, I.; Puri, R. K., Intratumoral administration of recombinant circularly permuted interleukin-4-Pseudomonas exotoxin in patients with high-grade glioma. *Clinical Cancer Research* **2000,** *6* (6), 2157-2165.
214. Dummer, R.; Eichmüller, S.; Gellrich, S.; Assaf, C.; Dreno, B.; Schiller, M.; Dereure, O.; Baudard, M.; Bagot, M.; Khammari, A.; Bleuzen, P.; Bataille, V.; Derbij, A.; Wiedemann, N.; Waterboer, T.; Lusky, M.; Acres, B.; Urosevic-Maiwald, M., Phase II Clinical Trial of Intratumoral Application of TG1042 (Adenovirus-interferon-γ) in Patients With Advanced Cutaneous T-cell Lymphomas and Multilesional Cutaneous B-cell Lymphomas. *Molecular Therapy* **2010,** *18* (6), 1244-1247.
215. Trillium Pipeline. Inc., T. T., Ed. 2019.
216. Wenig, B. L.; Werner, J. A.; Castro, D. J.; Sridhar, K. S.; Garewal, H. S.; Kehrl, W.; Pluzanska, A.; Arndt, O.; Costantino, P. D.; Mills, G. M.; Dunphy Ii, F. R.; Orenberg, E. K.; Leavitt, R. D., The Role of Intratumoral Therapy With Cisplatin/Epinephrine Injectable Gel in the Management of Advanced Squamous Cell Carcinoma of the Head and Neck. *Archives of Otolaryngology–Head & Neck Surgery* **2002,** *128* (8).
217. Li, S. Y.; Li, Q.; Guan, W. J.; Huang, J.; Yang, H. P.; Wu, G. M.; Jin, F. G.; Hu, C. P.; Chen, L. A.; Xu, G. L.; Liu, S. Z.; Wu, C. G.; Han, B. H.; Xiang, Y.; Zhao, J. P.; Wang, J.; Zhou, X.; Li, H. P.; Zhong, N. S., Effects of para-toluenesulfonamide intratumoral injection on non-small cell lung carcinoma with severe central airway obstruction: A multi-center, non-randomized, single-arm, open-label trial. *Lung Cancer* **2016,** *98*, 43-50.
218. Guan, W. J.; Li, S. Y.; Zhong, N. S., Effects of para-toluenesulfonamide intratumoral injection on pulmonary adenoid cystic carcinoma complicating with severe central airway obstruction: a 5-year follow-up study. *J Thorac Dis* **2018,** *10* (4), 2448-2455.
219. Mohamadnejad, M.; Zamani, F.; Setareh, M.; Nikfam, S.; Malekzadeh, R., Mo1495 EUS-Guided Intratumoral Gemcitabine Injection in Locally Advanced Non-Metastatic Pancreatic Cancer. *Gastrointestinal Endoscopy* **2015,** *81* (5, Supplement), AB440-AB441.
220. Ross, M. I., Intralesional therapy with PV-10 (Rose Bengal) for in-transit melanoma. *J Surg Oncol* **2014,** *109* (4), 314-9.
221. Thompson, J. F.; Hersey, P.; Wachter, E., Chemoablation of metastatic melanoma using intralesional Rose Bengal. *Melanoma Res* **2008,** *18* (6), 405-11.
222. Agarwala, S. S., Intralesional therapy for advanced melanoma: promise and limitation. *Curr Opin Oncol* **2015,** *27* (2), 151-6.
223. Provectus Biopharmaceuticals, I., PV-10-based Cancer Combination Therapy Clinical Trial Design Wins Australasian Gastro-Intestinal Trials Group's New Concepts Award. 2019.
224. Read, T. A.; Smith, A.; Thomas, J.; David, M.; Foote, M.; Wagels, M.; Barbour, A.; Smithers, B. M., Intralesional PV-10 for the treatment of in-transit melanoma metastases—Results of a prospective, non-randomized, single center study. *Journal of Surgical Oncology* **2018,** *117* (4), 579-587.
225. Marshall, J. D.; Fearon, K. L.; Higgins, D.; Hessel, E. M.; Kanzler, H.; Abbate, C.; Yee, P.; Gregorio, J.; Cruz, T. D.; Lizcano, J. O.; Zolotorev, A.; Mcclure, H. M.; Brasky, K. M.; Murthy, K. K.; Coffman, R. L.; Nest, G. V., Superior

Activity of the Type C Class of ISS In Vitro and In Vivo Across Multiple Species. *DNA and Cell Biology* **2005,** *24* (2), 63-72.
226. Thermofisher, DNA and RNA Molecular Weights and Conversions.
227. Aznar, M. A.; Planelles, L.; Perez-Olivares, M.; Molina, C.; Garasa, S.; Etxeberría, I.; Perez, G.; Rodriguez, I.; Bolaños, E.; Lopez-Casas, P.; Rodriguez-Ruiz, M. E.; Perez-Gracia, J. L.; Marquez-Rodas, I.; Teijeira, A.; Quintero, M.; Melero, I., Immunotherapeutic effects of intratumoral nanoplexed poly I:C. *Journal for ImmunoTherapy of Cancer* **2019,** *7* (1), 116.
228. Coler, R. N.; Day, T. A.; Ellis, R.; Piazza, F. M.; Beckmann, A. M.; Vergara, J.; Rolf, T.; Lu, L.; Alter, G.; Hokey, D.; Jayashankar, L.; Walker, R.; Snowden, M. A.; Evans, T.; Ginsberg, A.; Reed, S. G.; Ashman, J.; Sagawa, Z. K.; Tait, D.; Ishmukhamedov, S.; Blatner, G.; Sutton, S.; Shepherd, B.; Johnson, C.; The, T.-S. T., The TLR-4 agonist adjuvant, GLA-SE, improves magnitude and quality of immune responses elicited by the ID93 tuberculosis vaccine: first-in-human trial. *npj Vaccines* **2018,** *3* (1), 34.
229. Terheyden, P.; Weishaupt, C.; Heinzerling, L.; Klinkhardt, U.; Krauss, J.; Mohr, P.; Kiecker, F.; Becker, J. C.; Dähling; Döner, F.; Heidenreich, R.; Scheel, B.; Schönborn-Kellenberger, O.; Seibel, T.; Gnad-Vogt, U., 1305TiPPhase I dose-escalation and expansion study of intratumoral CV8102, a RNA-based TLR- and RIG-1 agonist in patients with advanced solid tumors. *Annals of Oncology* **2018,** *29* (suppl_8).
230. ssRNA-based immunomodulator CV8102. https://www.cancer.gov/publications/dictionaries/cancer-drug/def/792862 (accessed Oct. 2019). National Cancer Institute.
231. Pettenati, C.; Ingersoll, M. A., Mechanisms of BCG immunotherapy and its outlook for bladder cancer. *Nature Reviews Urology* **2018,** *15* (10), 615-625.
232. Staedtke, V.; Roberts, N. J.; Bai, R.-Y.; Zhou, S., Clostridium novyi-NT in cancer therapy. *Genes & diseases* **2016,** *3* (2), 144-152.
233. NCI Drug Dictionary: Daromun. https://www.cancer.gov/publications/dictionaries/cancer-drug/def/794649 (accessed June 2019). National Cancer Institute.
234. Lee, C. S.; Bishop, E. S.; Zhang, R.; Yu, X.; Farina, E. M.; Yan, S.; Zhao, C.; Zeng, Z.; Shu, Y.; Wu, X.; Lei, J.; Li, Y.; Zhang, W.; Yang, C.; Wu, K.; Wu, Y.; Ho, S.; Athiviraham, A.; Lee, M. J.; Wolf, J. M.; Reid, R. R.; He, T.-C., Adenovirus-mediated gene delivery: Potential applications for gene and cell-based therapies in the new era of personalized medicine. *Genes & Diseases* **2017,** *4* (2), 43-63.
235. Eissa, I. R.; Naoe, Y.; Bustos-Villalobos, I.; Ichinose, T.; Tanaka, M.; Zhiwen, W.; Mukoyama, N.; Morimoto, T.; Miyajima, N.; Hitoki, H.; Sumigama, S.; Aleksic, B.; Kodera, Y.; Kasuya, H., Genomic Signature of the Natural Oncolytic Herpes Simplex Virus HF10 and Its Therapeutic Role in Preclinical and Clinical Trials. *Front Oncol* **2017,** *7*, 149-149.
236. Harrow, S.; Papanastassiou, V.; Harland, J.; Mabbs, R.; Petty, R.; Fraser, M.; Hadley, D.; Patterson, J.; Brown, S. M.; Rampling, R., HSV1716 injection into the brain adjacent to tumour following surgical resection of high-grade glioma: safety data and long-term survival. *Gene Therapy* **2004,** *11* (22), 1648-1658.
237. Gong, J.; Mita, M. M., Activated ras signaling pathways and reovirus oncolysis: an update on the mechanism of preferential reovirus replication in cancer cells. *Front Oncol* **2014,** *4*, 167-167.
238. Koski, A.; Kangasniemi, L.; Escutenaire, S.; Pesonen, S.; Cerullo, V.; Diaconu, I.; Nokisalmi, P.; Raki, M.; Rajecki, M.; Guse, K.; Ranki, T.; Oksanen, M.; Holm, S.-L.; Haavisto, E.; Karioja-Kallio, A.; Laasonen, L.; Partanen, K.; Ugolini, M.; Helminen, A.; Karli, E.; Hannuksela, P.; Pesonen, S.; Joensuu, T.; Kanerva, A.; Hemminki, A., Treatment of Cancer Patients With a Serotype 5/3 Chimeric Oncolytic Adenovirus Expressing GMCSF. *Molecular Therapy* **2010,** *18* (10), 1874-1884.
239. Vaccinia Virus. http://www.aabb.org/tm/eid/Documents/160s.pdf (accessed Sept. 2019). AABB Center for Cellular Therapies.
240. Cyrklaff, M.; Risco, C.; Fernández, J. J.; Jiménez, M. V.; Estéban, M.; Baumeister, W.; Carrascosa, J. L., Cryo-electron tomography of vaccinia virus. *Proceedings of the National Academy of Sciences of the United States of America* **2005,** *102* (8), 2772-2777.
241. NCI Drug Dictionary: EGFR antisense DNA. https://www.cancer.gov/publications/dictionaries/cancer-drug/def/egfr-antisense-dna (accessed July 2019). National Cancer Institute.
242. Lavie, O.; Edelman, D.; Levy, T.; Fishman, A.; Hubert, A.; Segev, Y.; Raveh, E.; Gilon, M.; Hochberg, A., A phase 1/2a, dose-escalation, safety, pharmacokinetic, and preliminary efficacy study of intraperitoneal administration of BC-819 (H19-DTA) in subjects with recurrent ovarian/peritoneal cancer. *Archives of Gynecology and Obstetrics* **2017,** *295* (3), 751-761.
243. Hanna, N.; Ohana, P.; Konikoff, F. M.; Leichtmann, G.; Hubert, A.; Appelbaum, L.; Kopelman, Y.; Czerniak, A.; Hochberg, A., Phase 1/2a, dose-escalation, safety, pharmacokinetic and preliminary efficacy study of intratumoral administration of BC-819 in patients with unresectable pancreatic cancer. *Cancer Gene Therapy* **2012,** *19* (6), 374-381.
244. Darleukin. http://www.philogen.com/en/products/darleukin_9.html (accessed Sept 2019). Philogen.
245. ADC-1013: Clinical drug candidate. https://alligatorbioscience.se/en/research-and-development/pipeline/adc-1013/ (accessed Sept 2019). Alligator Bioscience.
246. Wang, R.; Feng, Y.; Hilt, E.; Yuan, X.; Gao, C.; Shao, X.; Sun, Y.; D'silva, M.; Yang, K.; Penhallow, B.; Bogdanoski, G.; Anand, R.; Pak, I.; Greenawalt, D.; Klippel, A.; Manjarrez-Orduno, N.; Neely, R.; Quigley, M.; Hedrick, M.; Aanur, P.; Cao, Z., Abstract LB-127: From bench to bedside: Exploring OX40 receptor modulation in a phase 1/2a study of the OX40 costimulatory agonist BMS-986178 ± nivolumab (NIVO) or ipilimumab (IPI) in patients with advanced solid tumors. *Cancer Research* **2018,** *78* (13 Supplement), LB-127-LB-127.

247. Lead Product: INT230-6. https://intensitytherapeutics.com/products/lead-product-int230-6/ (accessed July 2019). Intensity Therapeutics.
248. Malhotra, H.; Plosker, G. L., Cisplatin/Epinephrine Injectable Gel. *Drugs & Aging* **2001,** *18* (10), 787-793.
249. Liu, Z.; Liang, C.; Zhang, Z.; Pan, J.; Xia, H.; Zhong, N.; Li, L., Para-toluenesulfonamide induces tongue squamous cell carcinoma cell death through disturbing lysosomal stability. *Anti-Cancer Drugs* **2015,** *26* (10), 1026-1033.
250. Plunkett, W.; Huang, P.; Xu, Y. Z.; Heinemann, V.; Grunewald, R.; Gandhi, V., Gemcitabine: metabolism, mechanisms of action, and self-potentiation. *Seminars in oncology* **1995,** *22* (4 Suppl 11), 3-10.
251. Qin, J.; Kunda, N.; Qiao, G.; Calata, J. F.; Pardiwala, K.; Prabhakar, B. S.; Maker, A. V., Colon cancer cell treatment with rose bengal generates a protective immune response via immunogenic cell death. *Cell Death Dis* **2017,** *8* (2), e2584-e2584.

Chapter 2:

Immunostimulant Complexed with Polylysine for Sustained Delivery and Immune Cell Activation

1. Introduction

Immunotherapy is a powerful form of cancer treatment that harnesses the body's own immune system to fight cancer. Therapies range from checkpoint inhibitors to decrease immune suppression, adoptive T cell transfer using autologous cells engineered to express chimeric antigen receptors against tumor antigen, monoclonal antibodies that can mark tumor cells for killing, and immunostimulants like toll-like receptor agonists, cytokines, or bacteria.[1] Immunostimulants, or compounds that activate innate immune responses, are particularly useful for surmounting the suppressive tumor microenvironment. The tumor microenvironment employs a variety of immune evasion and suppression techniques, including suppressive cell subtypes, cytokines, T-cell exhaustion, and even downregulation of tumor antigen expression.[2-5] The use of immunostimulants in the presence of tumor antigens causes a number of reactions including upregulation of co-stimulatory molecules, increased antigen presentation, and secretion of proinflammatory cytokines which can induce tumor specific T-cells.[6-8] Immunostimulants, however, can induce off-target side effects by causing improper activation of the immune system in healthy tissue, thus beckoning improved delivery systems.

Toll-like-receptor agonists are a class of immunostimulants capable of inducing strong T cell activation after binding to their respective toll-like receptors (TLRs). TLRs recognize bacterial and viral pathogen associated molecular patterns (PAMPs), which then trigger pro-inflammatory, innate immune responses. Only two TLR agonists are currently FDA approved. The TLR4 agonist monophosphoryl lipid A (MPL) is incorporated into the adjuvant system for Ceravarix™, a cervical cancer vaccine.[9] In Aldara™, a cream for superficial basal cell carcinoma, the main active ingredient is a TLR7/8 agonist called imiquimod.[10] Currently there are many immunotherapy clinical trials utilizing TLR agonists either alone or in combination with other immunotherapy strategies like checkpoint inhibitors.[11]

Many research efforts and clinical trials have explored the use of polyI:C (polyinosinic:polycyticylic acid) and CpG, two TLR agonists with the ability to induce strong pro-inflammatory responses after binding to their respective TLRs. PolyI:C is a TLR3 agonist consisting of

double-stranded (ds) RNA that resembles viral RNA and has shown both antiviral and anticancer activity.[12-13] Furthermore, TLR3 agonists have demonstrated the ability to directly inhibit tumors *in vitro* by decreasing proliferation and inducing apoptotic cell death.[12] CpG is a short, single-stranded unmethylated synthetic oligonucleotide resembling bacterial DNA that agonizes TLR9.[14] Both TLR3 and TLR9 are located within endosomes, therefore the immunostimulants must be endocytosed to reach their target. While both polyI:C and CpG are promising candidates for use in cancer immunotherapy, one major challenge is determining how to properly deliver these potential therapies to tumor tissue.

Traditional systemic delivery offers the potential to target multiple tumor sites, however, full body exposure of immunostimulants can cause improper activation of the immune system in healthy tissue, causing inflammation and generating autoimmune reactions.[15] Intratumoral (IT) delivery offers a possible solution with an aim of generating anti-tumor immune responses capable of reaching distal tumor sites concurrently with shrinkage of treated tumors. This process, called the abscopal effect, can occur when tumor-activated immune cells drain to lymph nodes and circulate to distal cancer loci.[16] In this work, we aim to create a formulation of polyI:C or CpG that will be retained at the site of injection to avoid systemic toxicity and facilitate intracellular delivery.

Poly-L-lysine (PLL) is a highly positively charged polycation that has been extensively utilized as a delivery tool in intracellular genetic material (DNA or RNA) delivery research.[17-20] In fact, a candidate drug called Hiltonol, consisting of polyI:C combined with PLL stabilized by carboxymethylcellulose, has been seen some success as a vaccine adjuvant and as an immunostimulant in cancer therapy.[21] Where DNA alone would be small and have electrostatic repulsion from cell membranes, formulation of DNA into polycationic complexes compacts DNA into a particle and allows for attraction to cell membranes followed by endocytosis and lysosomal release once inside the acidic conditions of lysosomes. While similar polyplexes have been broadly explored in their capacity to deliver genetic material intracellularly, less work has been conducted on the formulation and transport of polyplexes and intracellular delivery of TLR agonists. The current study was focused on exploring the relationship between PLL molecular weight and complexation, TLR activation, and transport in a simple, simulated tumor microenvironment. Various

characterization methods were employed including particle sizing, and zeta potential but also experiments to assess the accessibility of the TLR agonist within the polyplex. To evaluate injection site retention, polyplexes were tested in an assay to emulate transport in human tissue. Finally, HEK blue TLR cells were used to assess the ability of the complexed TLR agonist to activate its respective TLR *in vitro*. Overall, this work illuminates the possibility of an additional purpose for polycationic polyplexes in cancer immunotherapy and emphasizes the importance of optimizing physiochemical properties of IT delivery systems.

2. Methods

2.1 Polyplex formation

Poly-L-lysine (K9) was purchased from Biomatik (Cambridge, Ontario, Canada). Poly-L-lysine hydrobromide of lengths K20 through K250 were purchased from Alamanda Polymers (Huntsville, AL). Poly-L-lysines will be referred to generally as PLL or specifically as poly(number of lysines). CpG ODN 1826 and LMW polyI:C were purchased from Invivogen (San Diego, CA). The average molecular weight (MW) of the individual polyplex components is provided in **table 1.** PLL polyplexes with CpG ODN 1826 or LMW polyI:C were prepared in 4% mannitol by adding equal volumes of pre-diluted PLL and pre-diluted CpG or polyI:C followed by repeated pipetting for 30 seconds (**figure 1**). The polyplexes were then stored at room temperature for a minimum of 20 minutes before measurements or cell culture use. Polyplexes were prepared at varying mass ratios of 0.5, 1, 2, 3, 5, 10 that represent mass of PLL divided by the polyplex partner, CpG or polyI:C. Mass ratio was utilized rather than a N:P ratio due to heterogeneity of the components. **Supplementary table 1** contains a translation of mass ratio to molar ratio which for PLL+CpG polyplexes is exact and for PLL+polyI:C polyplexes is based on the median average MW of polyI:C. For PLL+CpG polyplexes N/P ratio can be calculated and is available in **supplementary table 2**.

2.2 Agarose gel electrophoresis

Agarose was purchased from Sigma Aldrich (St. Louis, MO). Tris-acetate-EDTA (TAE) buffer was purchased from Invitrogen (Carlsbad, CA). PLL + CpG or polyI:C polyplexes were prepared as described holding the CpG or polyI:C concentration constant while varying the PLL concentration. Then, 4 µL 6x DNA Loading dye (Takara Bio Inc., Japan) was added to 10 µL of the polyplex and subsequently 12 µL was loaded onto a 3% agarose gel, and electrophoresed for 25 minutes at 100 V. CpG and polyI:C alone were run as controls and a 1 kb bench top DNA ladder (Promega, Madison, WI) was used. The gel was stained using SYBR Gold (Invitrogen, Carlsbad, CA) in TAE buffer for 25 minutes, shaking at room temperature then imaged on AlphaImager (Protein Simple, San Jose, CA).

2.3 Particle sizing

The effective radius (nm) of PLL + CpG or polyI:C polyplexes was determined by dynamic light scattering (DynaPro, Wyatt Technology, Santa Barbara, CA). Samples for particle sizing were prepared in 4% mannitol (Sigma Aldrich, St. Louis, MO). Measurements were conducted after a minimum of 20 minutes of incubation at room temperature.

2.4 Zeta potential

Zeta potential measurements were measured by Zeta PALS (Brookhaven Instruments, Holtsville, NY). All samples for zeta potential measurements were prepared in 4% mannitol and diluted into 1 mM KCl for analysis.

2.5 Scanning electron microscopy (SEM)

SEM images were captured using Hitachi SU8230 field emission scanning electron microscope at the University of Kansas Microscopy and Analytical Imaging Laboratory. Polyplexes or individual components were added to carbon coated grids and touched on a Kimwipe to remove excess liquid, then immediately dipped into liquid nitrogen prior to imaging.

2.6 Assessment of DNA/RNA accessibility by SYBR gold staining

The degree of accessibility of the DNA or RNA following complexation with PLL was assessed by the staining of SYBR Gold to accessible DNA or RNA. Polyplexes were made as described above and after 20 minutes polyplexes were added to a 96-well plate in triplicate followed by SYBR gold stain and mixed well. After approximately 5 minutes the fluorescence was measured using a Synergy H4 microplate reader (BioTek, Winooski, VT). The excitation filter was set to 495 nm and emission filter to 537 nm.

2.7 Hyaluronic acid gel retention

To test the polyplexes ability to retain at an injection site, we devised a model *in vitro* system to evaluate transport in human tissue made of highly viscous hyaluronic acid (HA) to which we could inject labeled polyplexes in the center and watch it spread over time. 0.8-1.5 MDa HA was added to PBS buffer at 20 mg/mL then placed on end-over-end rotator overnight to dissolve. The HA gel was then weighed out into a 96 well black plate at 0.28 g/well. The plate was centrifuged to remove bubbles then placed at 4 ˚C until use. Polyplexes were prepared as described but for this test they were first made up in 90% of the total volume, let incubate for 20 minutes, then 10% of the total volume of 20x SYBR Gold stain was added for an additional 5 minutes. A 3D printed device was designed to allow uniform injection into the wells at half the depth of the gel. 7 μL of sample was injected through the device into the center of the well using reverse pipetting. Fluorescent images were obtained at varying time points on a MaestroFlex Imager (Cambridge Research and Instrumentation, Woburn, MA). A control placed in each image was used to normalize the intensity across all images. To further normalize the data, a percent reduction was calculated based on the intensity at time 0 between pixels 15-25 as depicted in **figure 8A**.

2.8 In Vitro HEK blue reporter cell assay

HEK-Blue TLR9, TLR3, and Null cell lines (Invivogen, California) were grown in Dulbecco's Modified Eagle's Medium (DMEM; Corning, NY) supplemented with 10% FBS, 1% penicillin-streptomycin, and the selective antibiotics according to the manufacturer's protocol. HEK-Blue TLR cells allow for the study

of TLR activation by observing the stimulation of SEAP, a protein associated with downstream activation of TLRs. At 50-80% confluency, cells were harvested and resuspended in HEK detection media (Invivogen, California) and 180 uL was seeded into 96-well plates at ~8x10^5 cells/well. 20 uL of treatment were added to respective wells and the plate was incubated at 37 °C, 5% CO_2 for at least 6 hours or until color change. Absorbance readings were measured at 640 nm. Null cells were used as a control. Concentration of polyplex for the study was determined based on a titration of polyI:C or CpG (**Figure# slide15**). PolyI:C was held constant at 200 μg/mL and CpG was at 100 μg/mL.

3. Results

3.1 Polyplex formation

Agarose gel electrophoresis studies were used to visually test the ability of the different molecular weights of PLL to complex with the polyanionic TLR agonists. Free polyI:C or CpG migrated freely through the agarose gel whereas PLL did not. When polyI:C or CpG are complexed with PLL, the material retained in the loading well. The agarose gels in **figures 2 and 3** show the differences in the interactions between PLL and polyI:C or CpG. PLL mass was increased, increasing the mass ratio, while the polyanion counterpart was held constant. The immobilization of polyanion was seen in every PLL polyplex and occurred at a lower ratio for the higher MW PLL's. For all studied polyplexes, full immobilization was seen by a mass ratio of 1.5.

3.2 Polyplex characterization

Zeta potential measurements (**figure 4**) agreed with the agarose gels. A net positive charge emerged at the same mass ratio where the TLR polyanion agonist was immobilized on the gels. At higher ratios, the zeta potential started to plateau, indicating PLL had saturated the surface of the polyplexes.

Particle size is also an important consideration, since size has been shown to impact cell uptake, trafficking, and ultimately immune activation.[22-27] For all CpG-containing polyplexes the radius was between 20 and

100 nm **(figure 4)**. Polyplexes with polyI:C were unable to be measured by DLS or zeta potential due to heterogeneity. To corroborate particle sizing data, SEM images were collected and the results correlate with the particle sizes determined by DLS measurements **(figure 5)**. Control solutions of PLL or TLR agonist lacked visible particles. In the CpG polyplex samples, many dark spherical particles were seen within the expected size range. PolyI:C polyplexes did not result in spherical particles, which validates the unsuccessful DLS measurements.

3.3 SYBR gold accessibility

To investigate how PLL encapsulates or polyplexes with the polyanions, we utilized a DNA/RNA stain to measure accessibility of the polyanion. In this experiment the polyanion concentration is held constant. Free polyanion was more accessible whereas complexed polyanion was more encapsulated and inaccessible. To compare between different MW PLL's, **figure 6** graphs show the fluorescence intensity normalized to the intensity of the respective control, either polyI:C or CpG. Any value under 1 implies some amount of immunostimulant encapsulation by the PLL. In general, the fluorescence decreased as the ratio increased suggesting increased encapsulation. Gel electrophoresis data previously indicated that the immunostimulant was fully immobilized by a ratio of 1.5, yet the K9 polyplexes appeared to have some accessible immunostimulant at all ratios than the higher MW PLLs. The strength of the interaction appeared weaker for lower molecular weights of PLL and at lower ratios of PLL to the polyanions.

3.4 Hyaluronic acid gel retention

To simulate tumor retention of polyplexes in correlation with the ratio of polycation to polyanion, we injected sample into a viscous HA gel and diffusion of the TLR agonist polyanions was monitored over time. HA is a major component within the tumor and high molecular weight HA has been used to model subcutaneous (SC) space injection simulators.[28-29] For typical SC injection site simulations, 10 mg/mL HA has been used. To model a denser tumor environment, the HA concentration was increased to 20 mg/mL. The negative charge of HA emulates extracellular matrix and we hypothesized positively-charged

polyplexes would remain at the injection site in the center of the well longer than polyI:C or CpG alone. The controls, polyI:C and CpG alone diffused quickly, even within two hours (**figures 7&9**). For both sets of data, the lower MW PLL polyplexes diffused much more than higher MW PLLs. Furthermore, in some of the higher MW PLL sample wells, a "donut" shaped spot was formed likely due to immediate aggregation following leaving the pipette (**figure 7)**. Due to MW differences, the ratios cannot be directly compared between polyI:C and CpG polyplexes however we can say that at the same mass ratios, the CpG polyplexes have a greater potential of retention than the polyI:C polyplexes with the same PLL. Since the polyplexes were labeled using SYBR Gold stain, each polyplex stained slightly differently depending on the accessibility of the polyI:C or CpG. To make the retention comparable between samples, a percent reduction was calculated. **Figure 8B&C** show percent reductions at 2 and 5 hours, where the greatest differences were observed. **Figures 10 and 11** have the percent reduction for every time point next to the respective spatial plots. For both polyI:C and CpG polyplexes, the percent reduction was increasingly influenced by ratio as the MW of PLL was increased. In all but the K9 polyplexes where ratio seemed to be independent, the percent reduction decreased with increase in ratio. CpG polyplexes had less dispersion from the center than polyI:C polyplexes at all PLL sizes above K9.

3.5 In vitro HEK blue reporter cell assay

PolyI:C and CpG are TLR agonists of TLR3 and TLR9, respectively. In our approach, their activation is crucial in the stimulation of the desired immune response. To examine the effect of complexation on TLR activation, we utilized HEK blue hTLR reporter cells. The polyplexes and controls were tested in the null cell line and reporter cell lines for their respective TLRs. Samples were run in the null cell line as an additional control. Polyanion concentrations were determined by selecting a concentration that achieved a reasonable response factor as shown from a concentration curve completed in the respective cell lines (**supplementary figure 1**). Polyplexes were made as previously described by holding the polyanion concentration constant and increasing the mass ratio of PLL. TLR activation in HEK blue cells could be detected by absorbance using the HEK blue detection media. **Figure 12-13** graphs show the absorbance of

the samples minus signal produced by PLL control normalized to the polyanion control. **Figure 14** combines the activation data to relate PLL length and ratio. Therefore any value above 1, reflects that the sample activated the TLR better than the polyanion alone. K20 and K30 polyplexes were only tested with CpG since polyI:C polyplexes were not yielding promising results. None of the polyI:C polyplexes were able to activate TLR3 as well as the polyI:C alone. On the other hand, some of the lower ratio CpG polyplexes activated TLR9 as well as the CpG control. In both data sets, K9 polyplexes provided better TLR activation than higher MW PLLs. CpG polyplexes appeared to have a greater dependency on ratio than polyI:C polyplexes where an increase in ratio led to decrease in activation- an expected result considering the decreased accessibility of the immunostimulant. For CpG polyplexes, the activation showed a dependency on PLL length except at R0.5, or at a lower concentration of PLL. Interestingly, there appeared to be a range of PLL length at which the activation of TLR is more dependent on the ratio. For polyI:C this is around K50 and for CpG, any tested PLL length over K9. In addition to the TLR activation, cellular metabolism was also measured in the respective HEK cells using a resazurin assay. It is well known that higher MW PLL's can cause toxicity in cells therefore we aspired to find a range in which there was limited cellular damage and acceptable TLR activation.[30] **Figure 12-13** shows metabolism of cells incubated with polyplexes adjacent to the corresponding PLL to show that the metabolism is directly a result of the PLL's effect on the cells. **Figure 15** combines the metabolism data to compare the PLL length and the ratio. Bear in mind the concentration of PLL in the CpG polyplexes is half of the concentration in the equivalent polyI:C polyplexes. The metabolism was highly dependent on both PLL length and concentration (ratio). At K9, the metabolism was not affected by ratio/concentration but with increase in PLL length, the metabolism decreased with ratio increase. The CpG polyplex's metabolism profile showed a dependence on concentration more so than PLL length (ratio=concentration and clear pattern) whereas the polyI:C polyplexes were only dependent on concentration up to K50. At ratios above R0.5, polyI:C polyplexes yielded metabolism dependent on PLL length- with values being close together regardless of ratio. The metabolism data matched the TLR activation trends especially in the CpG polyplexes' dependency on ratio.

4. Discussion

The use of the immunostimulants, polyI:C and CpG, to overcome the suppressive tumor microenvironment has shown great promise. The IT route of delivery circumvents trafficking and penetration into the tumor, but transport of therapy out of the tumor tissue and into systemic circulation is still an issue. IT clinical trials have demonstrated the necessity to optimize the retention of potent immunostimulants to decrease systemic toxicity.[31-32] Many approaches have suggested enhanced efficacy and safety when the TLR agonist is structurally modified or formulated into an emulsion or complex.[21, 33-37] Polycationic delivery vehicles have frequently been utilized for intracellular delivery of negatively charged genetic material by packing it into a net positively charged complex.[38-39] Here, we evaluated polyplexes of the polycation PLL with polyanionic TLR against. Specifically, we examined the relationship between PLL molecular weight and complex formation, TLR activation, and retention in a simulated tumor microenvironment.

All molecular weights of PLL tested were found to fully complex with both polyI:C and CpG as indicated by agarose gel electrophoresis. Interestingly, it appeared that the PLL MW did not have a significant impact on the ratio at which the immunostimulant became fully complexed but this could be elucidated by testing a smaller range of lower ratios. While immobilization is important, the biophysical characteristics of the particles like size and charge play a major role in determining transport and cell uptake following injection. While results vary depending on route of administration, a general understanding for transport after injection is that for uncharged particles <4 nm drain to systemic, particles between 10-100 nm drain to lymphatics, and particles >100 nm tend to form depot or retain at the injection site or are trafficked after being taken up by antigen-presenting cells (APCs).[40-42] One study evaluated therapy clearance from tumor space after intratumoral injection of small or large emulsions, and neutral or cationic liposomes.[22] They found that larger (120-250 nm) particles and cationic particles have increased tumor retention in comparison to smaller or neutral particles. Interestingly, they also concluded that the rate of transfer from the poorly-perfused area to well-perfused area is the determining factor for IT transport and

not the rate of transfer from interstitial space to the vascular side. Further, the efficacy of TLR agonists, polyI:C and CpG, require intracellular delivery to reach endosomes, which is typically optimal for positively charged particles 20-500 nm in diameter where the mechanism of uptake can differ based on the size.[30, 40-41, 43-45]

DLS and SEM measurements showed that PLL+CpG polyplexes formed spherical particles between 50-200 nm in diameter. For CpG polyplexes, the K9 group had a slightly greater diameter than the higher MW PLLs which could be a result of a different complex arrangement, or a weaker electrostatic interaction of the polyplex at lower MW PLL's. On the other hand, the PLL+polyI:C polyplexes did not form particles measurable by DLS or EM methods. The discrepancy between the two immunostimulants may be explained by structural differences between dsRNA (polyI:C) and ssDNA (CpG). Previous research has indicated that dsRNA resists condensation, or complexation in comparison to ds or ssDNA due to spatial and distribution of electrostatic potential differences.[46-47] For Lynn et. al., the formation of a particle by their TLR-7/8 agonist candidate was found to be critical for duration of innate cytokine production and reduced systemic toxicity.[48] Specifically, they found that while increased therapy retention was necessary, it was not sufficient for enhancing the immune response; only particles were properly taken up by APCs leading to increase in innate activation.

Model injection site retention experiments confirmed that PLL polyplexes remain at the injection site longer than immunostimulant alone. While agarose gel electrophoresis for both polyI:C and CpG polyplexes indicated immobilization at similar ratios, the diffusion profiles in concentrated HA were different, suggesting retention may have some dependency on the formation of spherical particles only seen with CpG polyplexes. We saw increased retention by the polyplexes that formed particles which agrees with the previously described research that showed particle formation does increase *in vivo* retention and persistence in lymph nodes in comparison to non-particulate material.[48] For both polyplexes, K9 was insufficient for retention even at higher ratios where there appeared to be complete immobilization. Since the fluorescence label was on the immunostimulant, the differences in retention could be explained by a weaker interaction strength between polyI:C and PLL compared to CpG polyplexes as well as K9

polyplexes versus higher MW PLL. Higher MW PLL and larger ratios increase retention overall, however CpG polyplexes appear to have superior retention abilities.

In addition to biophysical transport considerations, efficient activation of the TLRs after complexation with polycation is significant for determination of therapeutic efficacy. Only a few of the lower ratio and lower MW CpG polyplexes were able to activate the target TLR as well as CpG alone. For all polyplexes, the lowest ratio had the highest TLR activation, and at higher ratios, the increase in MW PLL led to decreased activation. Taken together with resazurin data, it is likely that the decrease in activation at higher ratios and MWs of PLL was due to toxicity caused by the PLL except in the case of K9 whose efficacy was not dependent on ratio (concentration). Some evidence suggests that a PLL MW larger than 3000 Da is required to complex with DNA effectively.[20, 49] Higher MW polycations have enhanced intracellular delivery potential, however, there is also an increase in cellular toxicity.[38, 50-51] Futhermore, while larger ratios may be more efficient at intracellular delivery, the lower ratio polyplexes are more potent at activating TLR which could be attributed to decrease in immunostimulant availability at higher ratios.[30, 38] Availability of the immunostimulant evaluated by SYBR Gold staining indeed showed that lower ratios have more available immunostimulant and that polyI:C seems to be less accessible in a comparable polyplex of CpG. More accessible immunostimulant with K9 polyplexes could potentially be explained by a weaker polyplex interaction strength which may also account for the lack of dependency on ratio in the TLR activation experiments. Thus, there must be a balance between the ratio of PLL to immunostimulant and the MW of PLL such that there is and sufficient complexation for intracellular delivery, but a weak enough interaction to allow immunostimulant to reach its target once endocytosed, increased retention and minimal cell toxicity. The lowest MW PLL, K9 was insufficient for increasing retention and the highest MW PLLs induced cytotoxicity. Our results indicate that the ideal PLL length appeared to lie above K9, up to K50.

5. Conclusion

Immunostimulants for immunotherapeutic treatment of tumors are powerful weapons, however, delivery methods need to be optimized for minimizing systemic toxicity and maximizing retention at the injection site. For negatively charged immunostimulants like many TLR agonists, formulation with a polycation has resulted in increased intracellular delivery. Here, we present results that demonstrate the potential for polycations in polyplexes to aid in injection site retention for minimized systemic exposure of immunostimulants. TLR activation was largely driven by the MW of PLL followed by the accessibility of the immunostimulant within the polyplex. Retention was also driven by these factors but in an opposite manner. Taken together, we believe that there is an optimal window of polycation MW and ratio that favors TLR activation and retention without causing toxicity. For CpG polyplexes, K9 through K50 was ideal for limiting cytotoxicity but higher MW was best for retention. Furthermore, this work supports with the hypothesis that particle formation is critical for immune activation and retention. These findings illustrate the potential use of polycations for carrier vehicles that not only aid in intracellular delivery but also contribute to injection site retention. The characterization results in this work suggest that PLL+CpG polyplexes may be a good candidate for increased intracellular delivery and decreased transport away from the tumor. Future studies could optimize the molecular weight and composition of the polycation such that the polyplex interaction strength allows for efficient TLR activation, the biophysical characteristics strengthen the retention and intracellular delivery, and cellular toxicity is minimized.

6. Figures and Tables

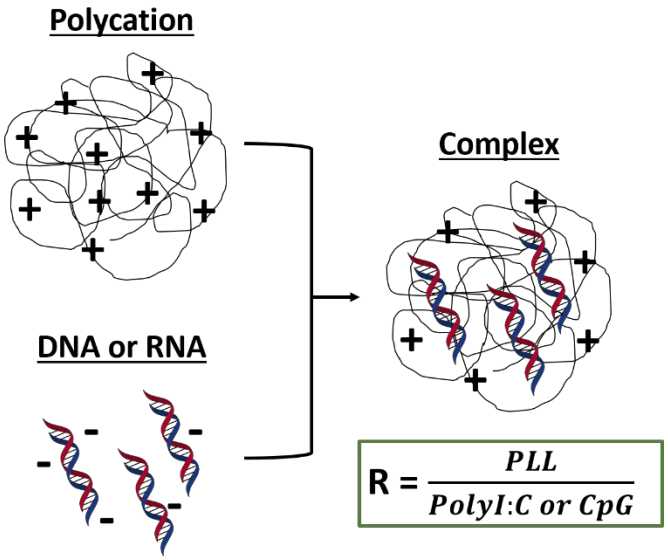

Figure 1. Polyplex formation schematic. R is a mass ratio of PLL over the immunostimulant.

Polycation	Average MW
K9	1171
K20	4200
K30	6300
K50	10000
K100	21000
K250	52000
Polyanion	**MW**
polyI:C	7,600-36,000 Median of Avg: 21,800
CpG	6364

Table 1. Molecular weights of polyplex components.

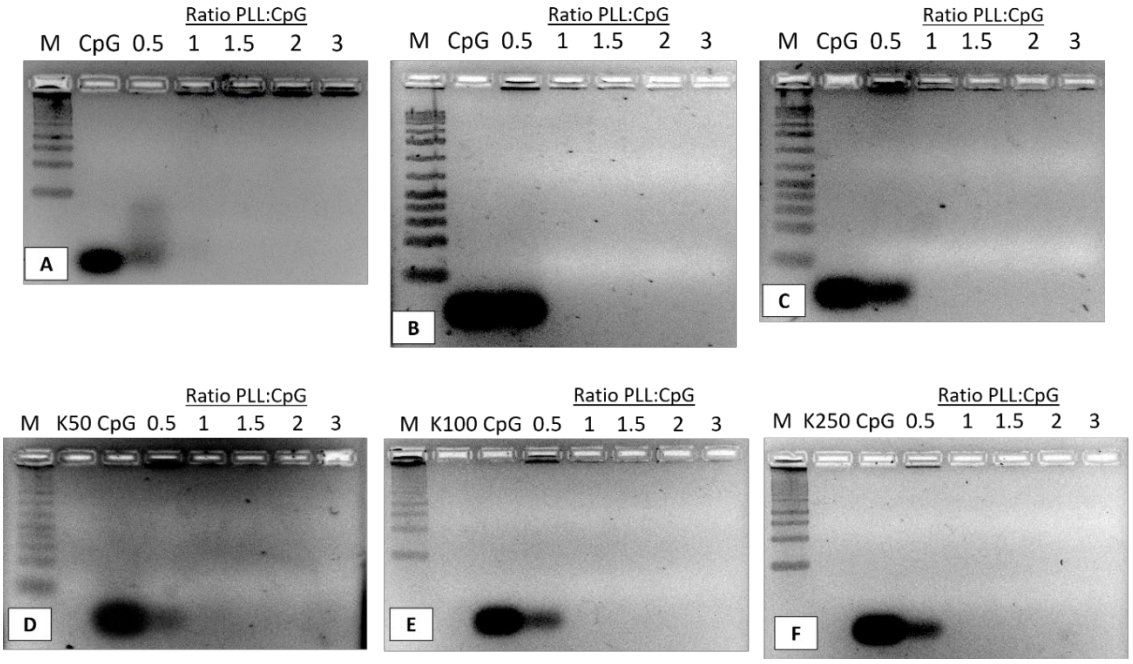

Figure 2. Agarose gels of PLL+CpG polyplexes. (A) K9+CpG, (B) K20+CpG, (C) K30+CpG, (D) K50+CpG, (E) K100+CpG, (F) K250+CpG

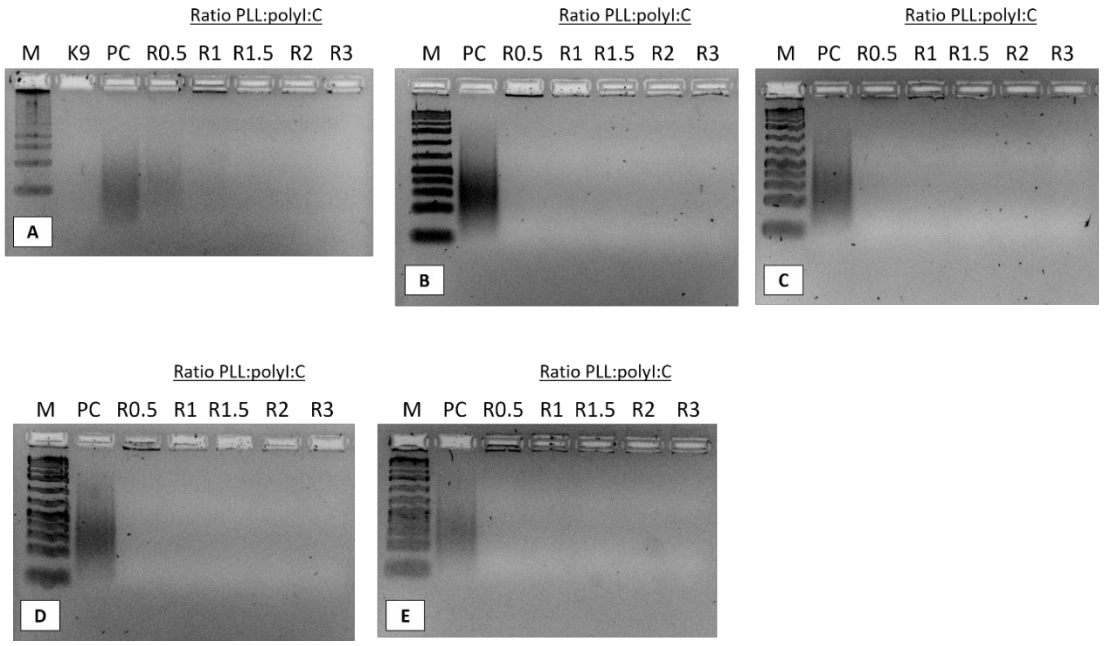

Figure 3. Agarose gels of PLL+polyI:C polyplexes. (A) K9+polyI:C, (B) K20+polyI:C, (C) K30+polyI:C, (D) K50+polyI:C, (E) K100+polyI:C

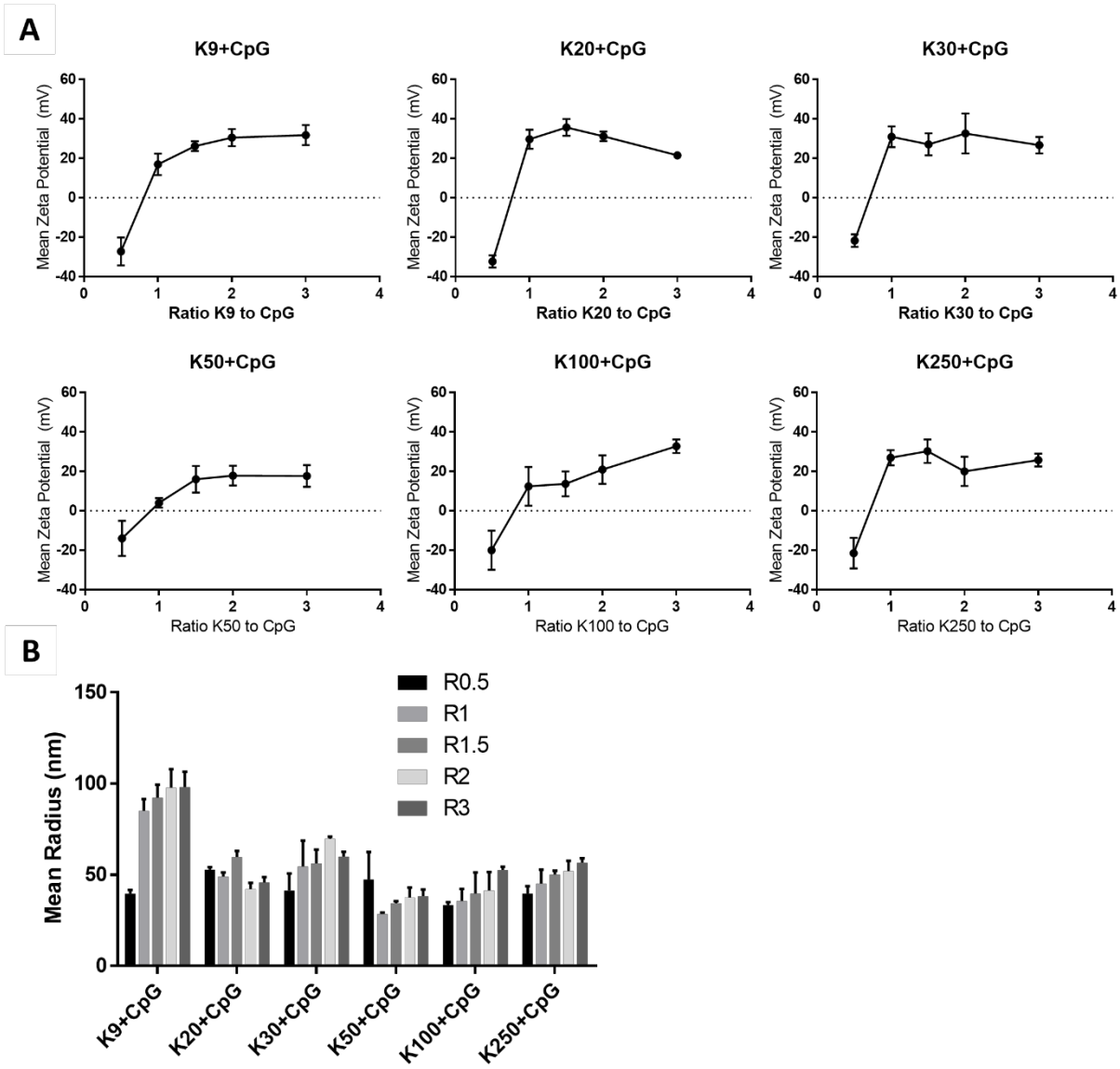

Figure 4. (A) Zeta potential and (B) dynamic light scattering (DLS) measurements of PLL+CpG polyplexes.

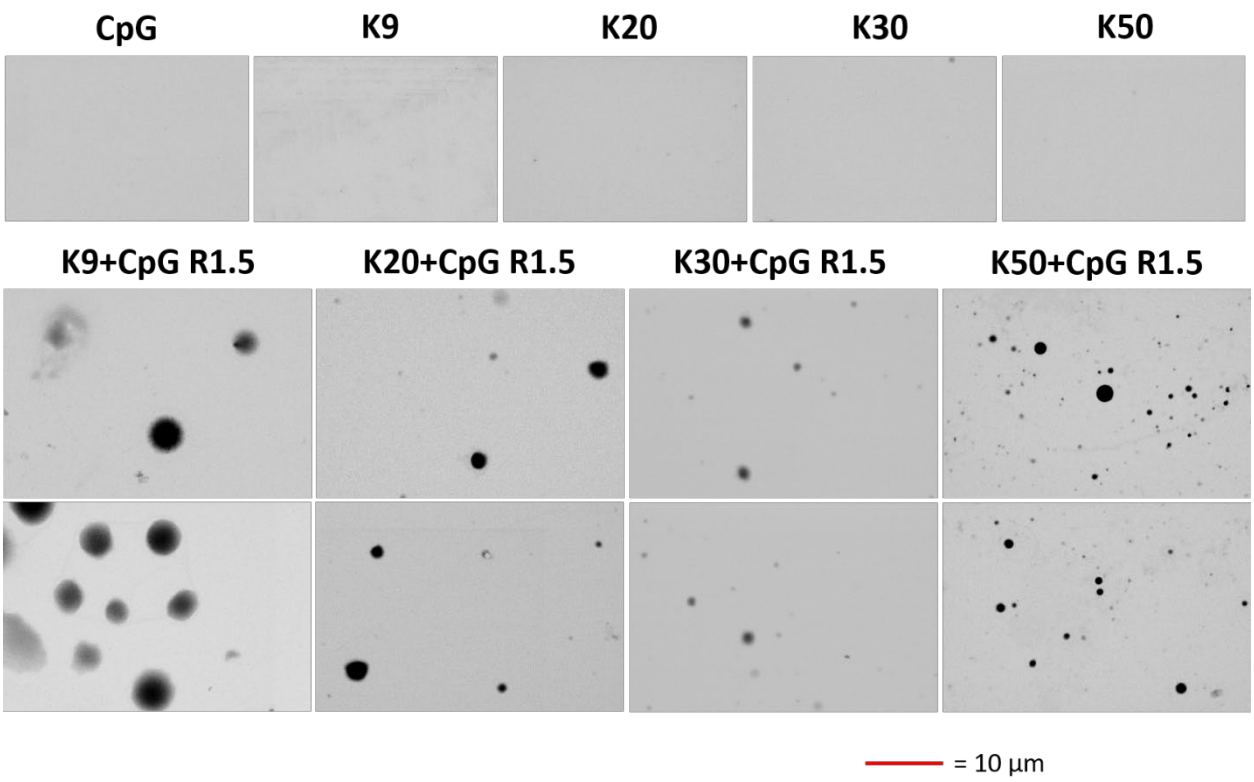

Figure 5. Representative SEM images of individual components and PLL+CpG R1.5 polyplexes

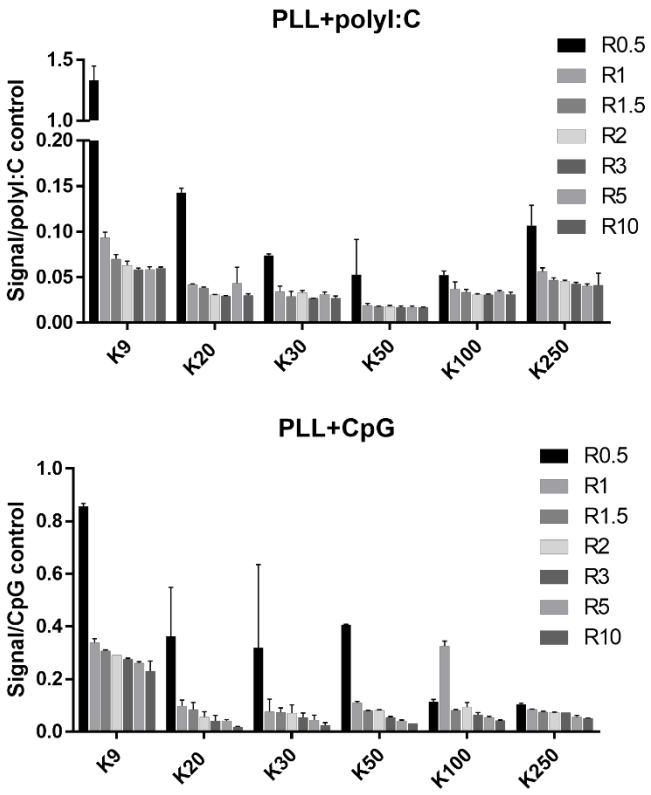

Figure 6. Effect of PLL molecular weight and mass ratio on accessibility of polyI:C or CpG using SYBR Gold assay.

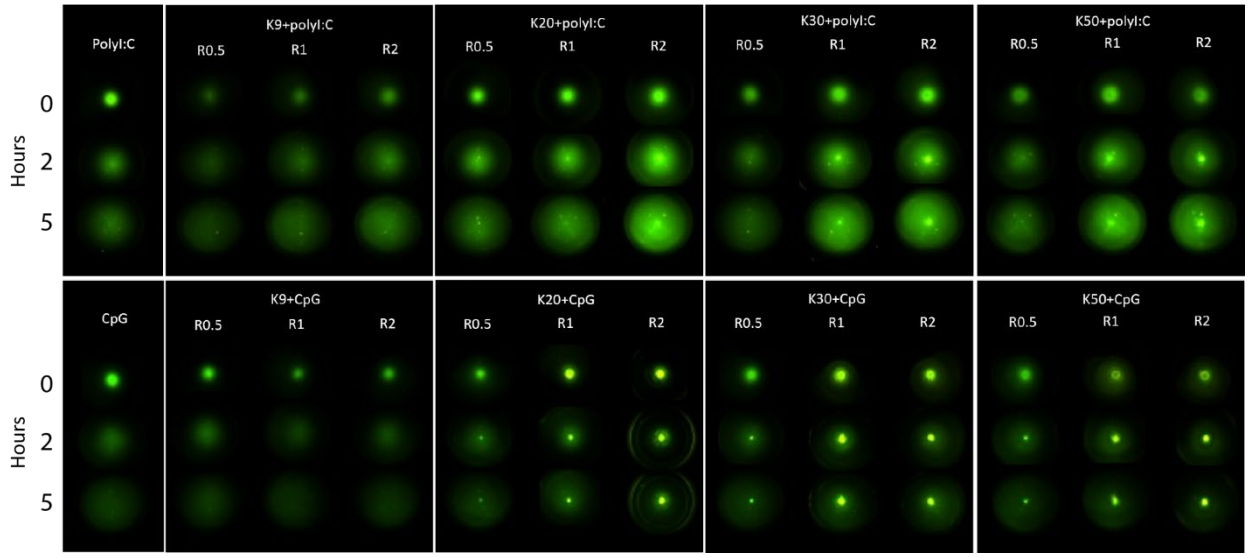

Figure 7. Fluorescent images of polyplex samples or immunostimulant alone after injection into HA gel at 0, 2, and 5 hours.

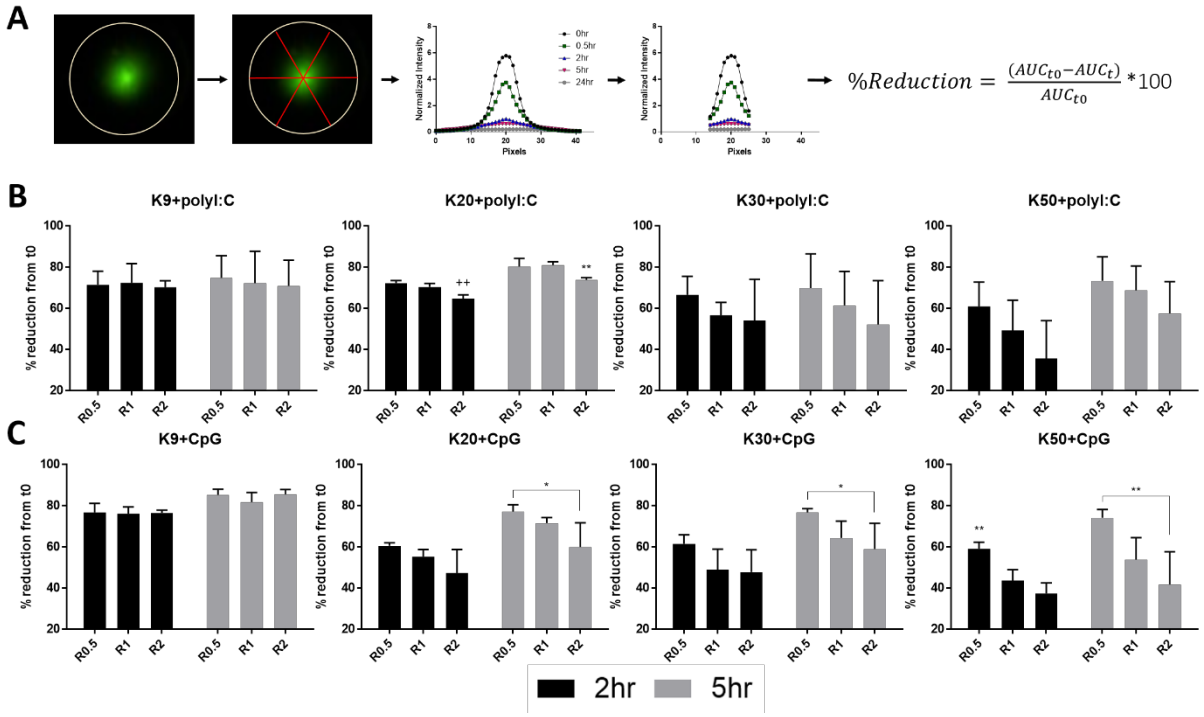

Figure 8. (A) Fluorescence intensity across the well was averaged from three measurements, normalized to a standard in each image, and then plotted. To calculate percent reduction, AUC of the middle of the well was used. Percent reduction at 2 (black) and 5 (grey) hours for (B) PLL+polyI:C polyplexes and (C) PLL+CpG polyplexes.

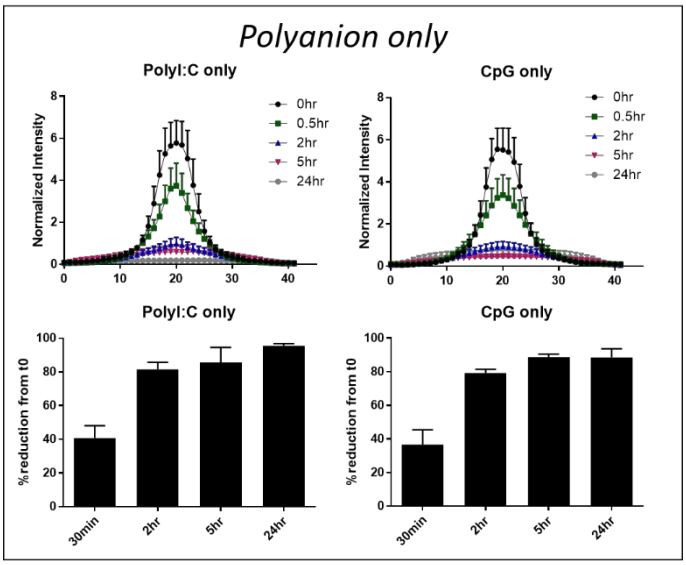

Figure 9. Normalized spatial plots and percent reduction graphs for polyanion alone controls.

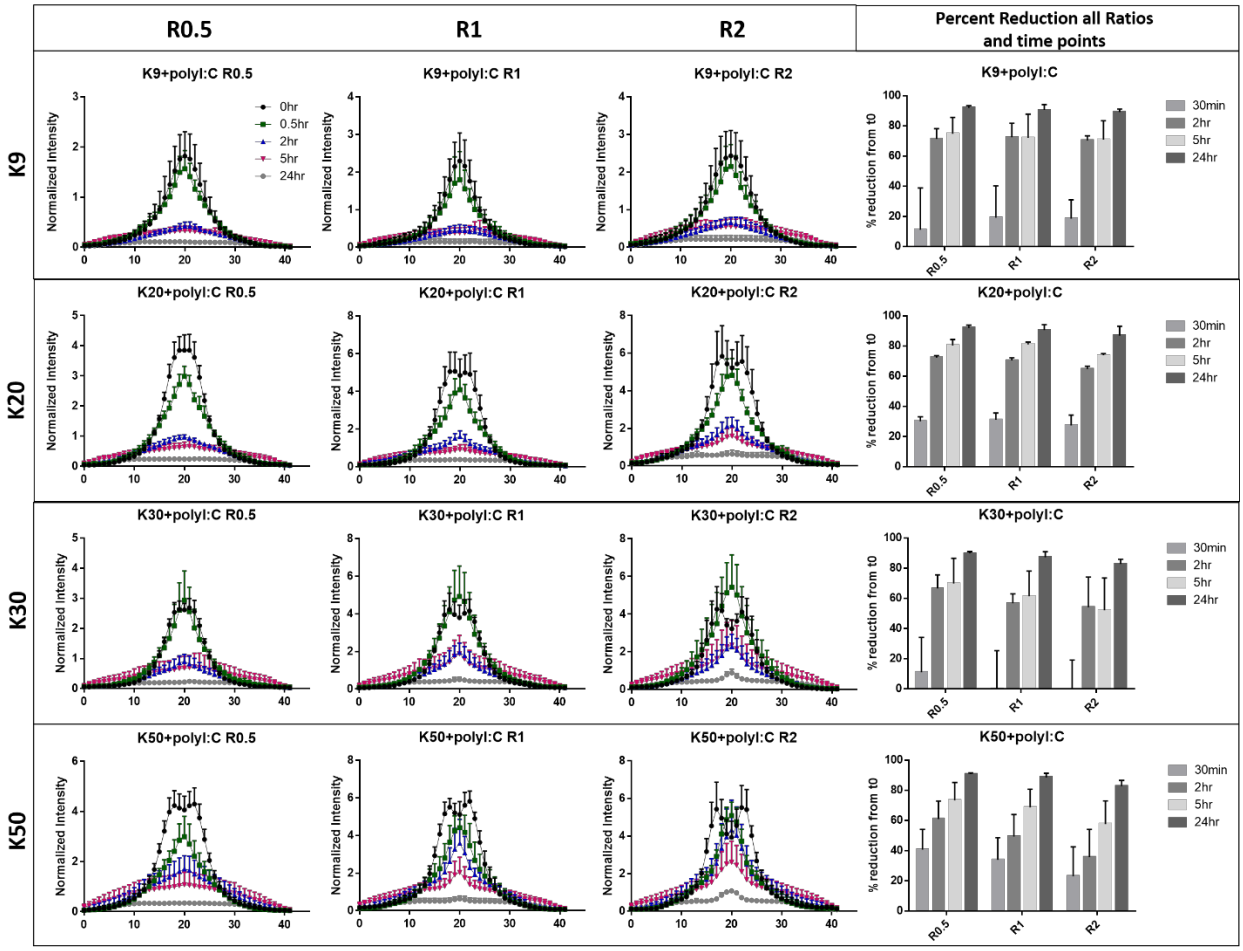

Figure 10. Normalized spatial plots and percent reduction graphs for PLL+polyI:C polyplexes.

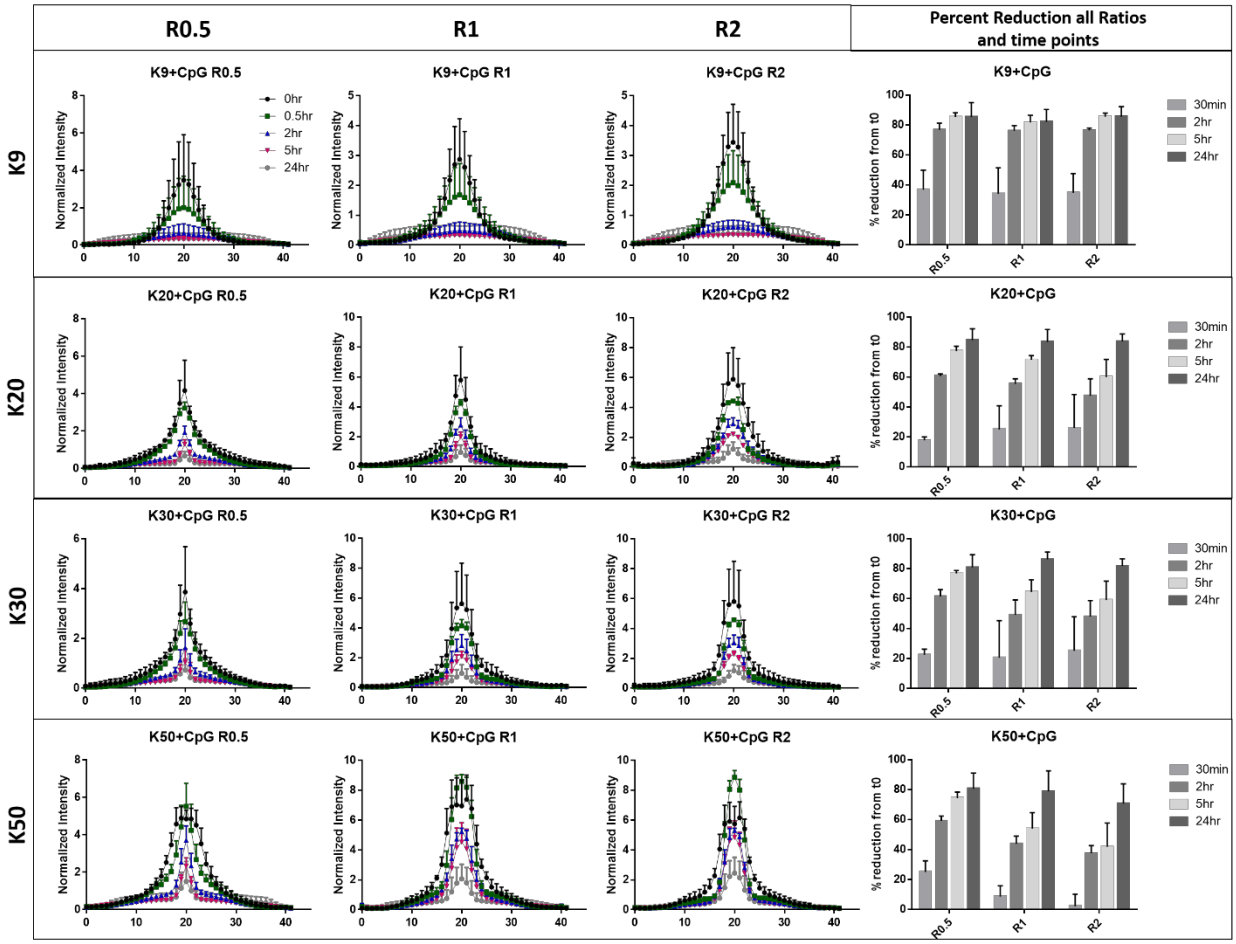

Figure 11. Normalized spatial plots and percent reduction graphs for PLL+CpG polyplexes.

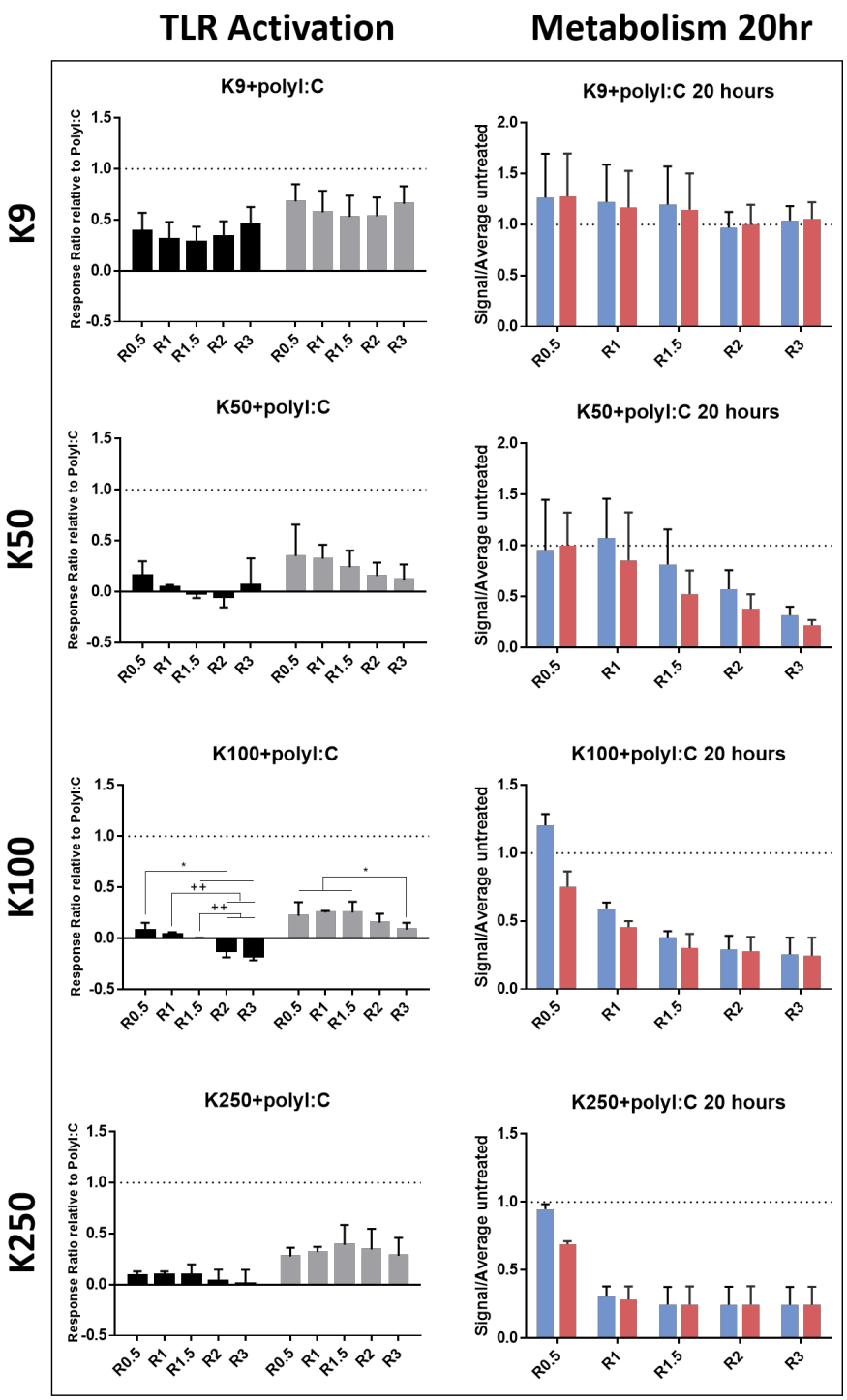

Figure 12. TLR3 activation 8 hr (black) and 20 hr (grey) and cellular metabolism of polyplex (blue) and of the equivalent PLL (red) in HEK blue TLR3 reporter cells after incubation with PLL+polyI:C polyplexes.

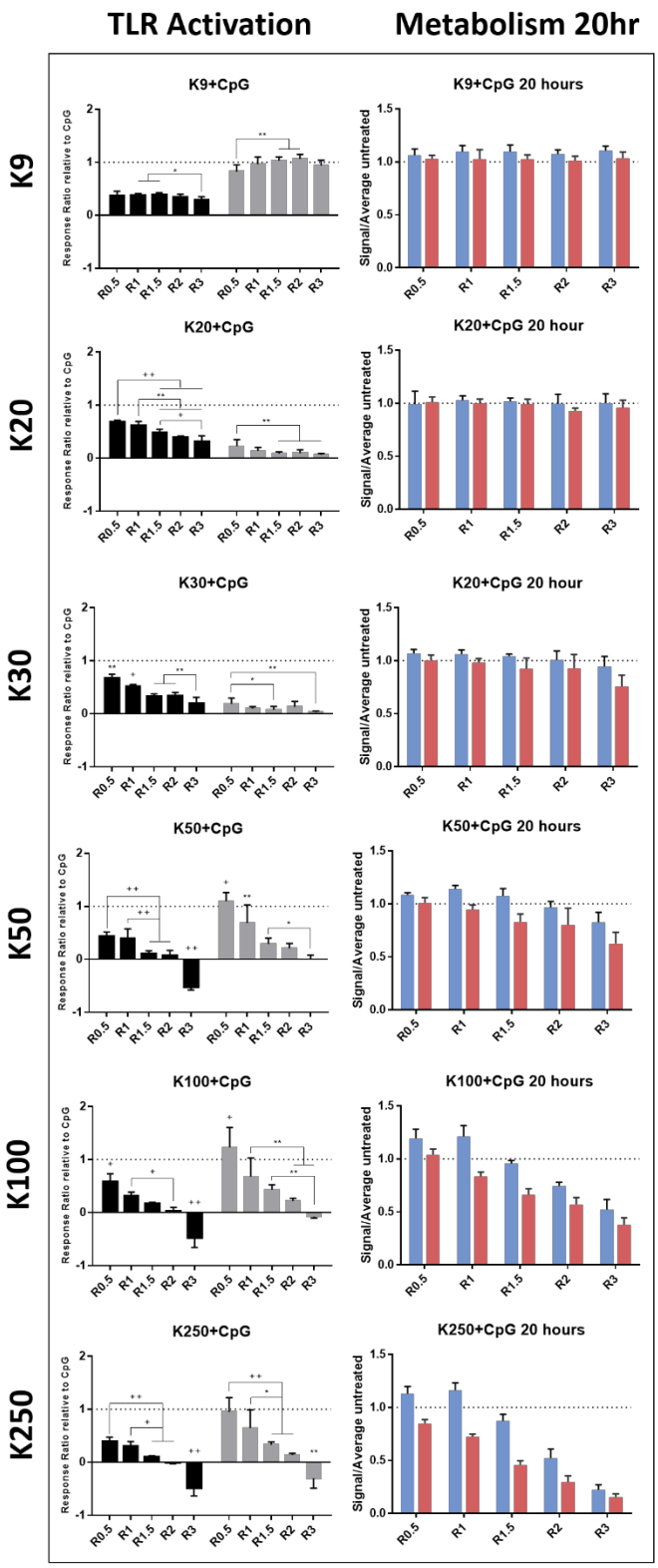

Figure 13. TLR9 activation 8 hr (black) and 20 hr (grey) and cellular metabolism of polyplex (blue) and of the equivalent PLL (red) in HEK blue TLR9 reporter cells after incubation with PLL+CpG polyplexes.

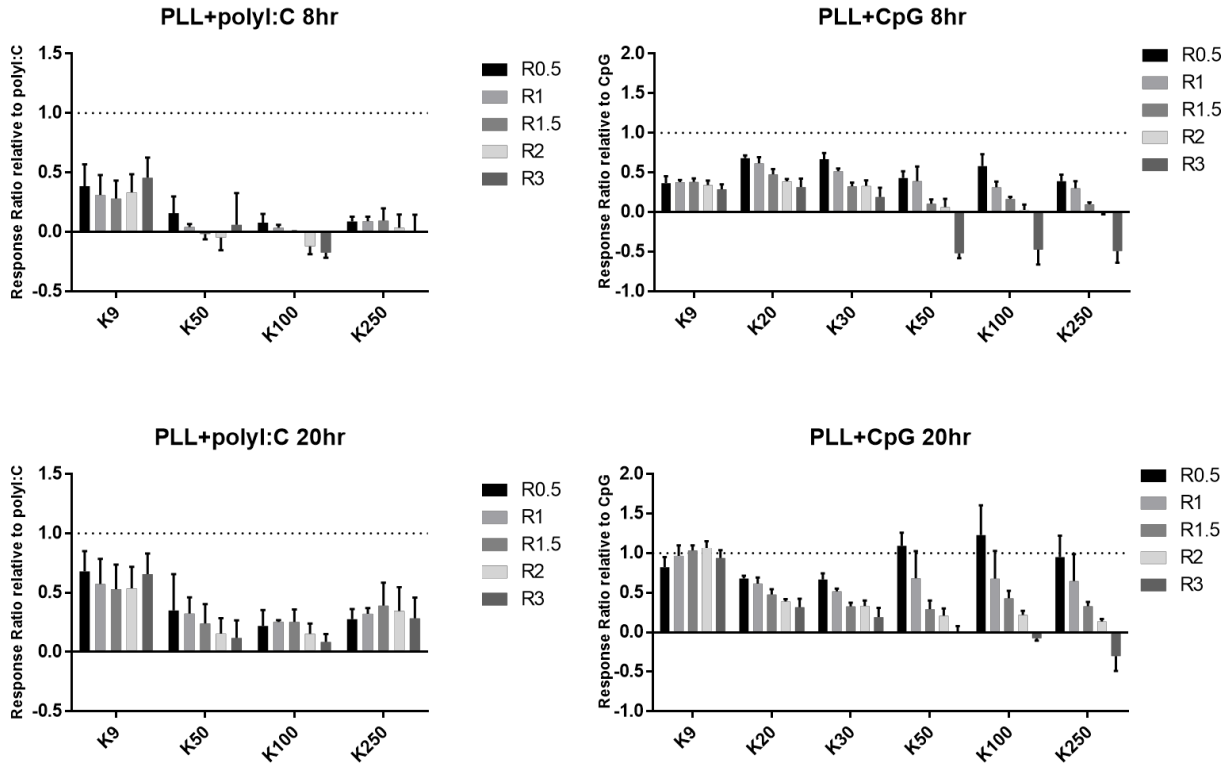

Figure 14. Effect of PLL molecular weight and mass ratio on TLR activation.

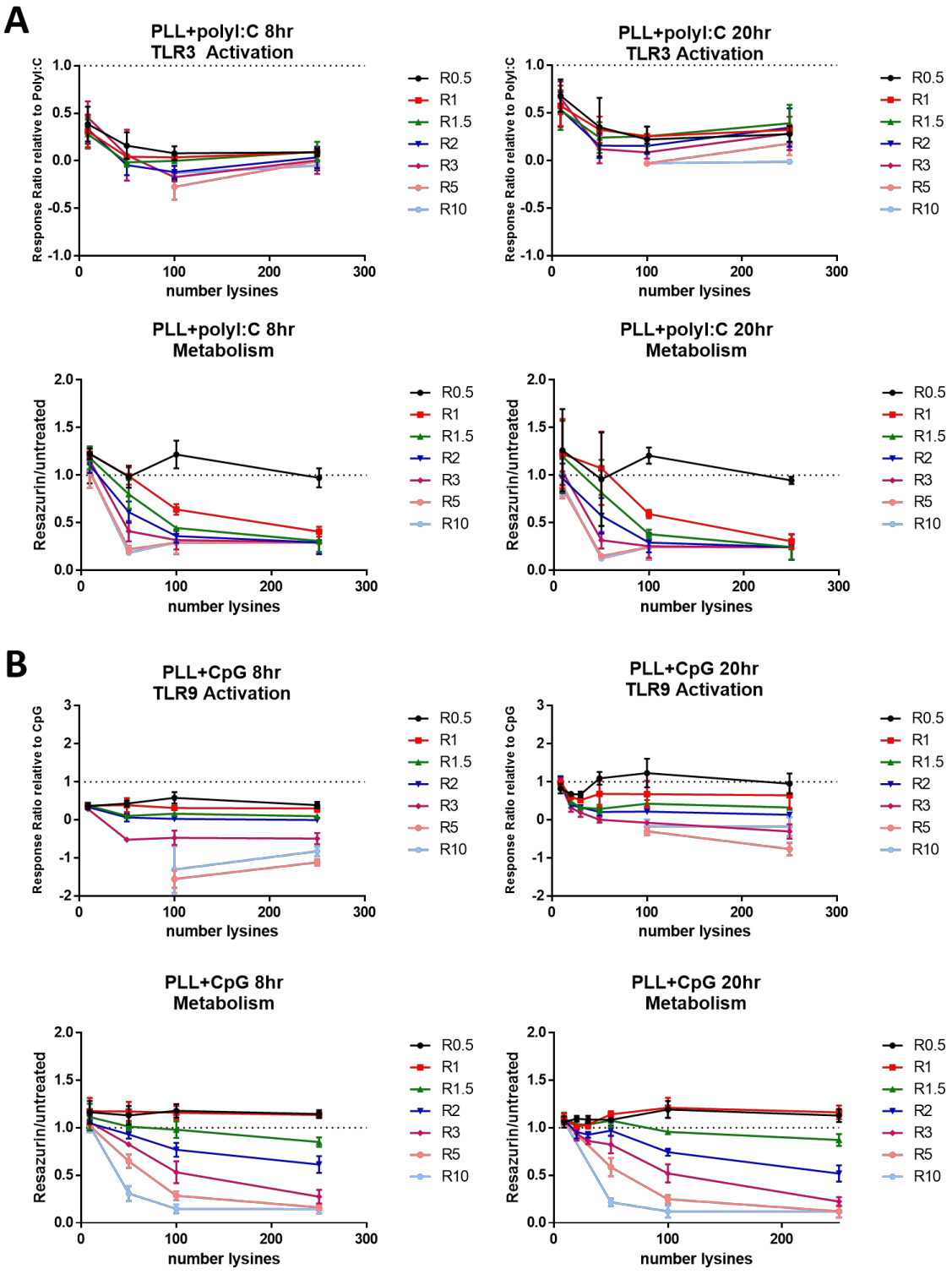

Figure 15. Effect of PLL molecular weight and mass ratio on TLR activation HEK blue cell metabolism for (A) PLL+polyI:C and (B) PLL+CpG polyplexes.

7. Supplemental Materials

PLL+polyI:C Molar Ratio Translation
based on median average MW polyI:C

Mass Ratio	K9	K20	K30	K50	K100	K250
0.5	9.4	2.6	1.7	1.1	0.5	0.2
1	18.8	5.2	3.5	2.2	1.0	0.4
1.5	28.2	7.9	5.2	3.3	1.6	0.6
2	37.6	10.5	7.0	4.4	2.1	0.8
3	56.3	15.7	10.5	6.6	3.1	1.3
5	93.9	26.2	17.5	11.0	5.2	2.1
10	187.8	52.4	34.9	22.0	10.5	4.2

PLL+CpG Molar Ratio Translation

Mass Ratio	K9	K20	K30	K50	K100	K250
0.5	2.7	0.8	0.5	0.3	0.2	0.1
1	5.4	1.5	1.0	0.6	0.3	0.1
1.5	8.1	2.3	1.5	1.0	0.5	0.2
2	10.9	3.0	2.0	1.3	0.6	0.2
3	16.3	4.5	3.0	1.9	0.9	0.4
5	27.2	7.6	5.1	3.2	1.5	0.6
10	54.3	15.2	10.1	6.4	3.0	1.2

Supplementary table 1. Mass ratio translation to molar ratio.

PLL+CpG N/P Ratio Translation

Mass Ratio	K9	K20	K30	K50	K100	K250
0.5	0.2	0.5	0.8	1.3	2.6	6.6
1	0.5	1.1	1.6	2.6	5.3	13.2
1.5	0.7	1.6	2.4	3.9	7.9	19.7
2	0.9	2.1	3.2	5.3	10.5	26.3
3	1.4	3.2	4.7	7.9	15.8	39.5
5	2.4	5.3	7.9	13.2	26.3	65.8
10	4.7	10.5	15.8	26.3	52.6	131.6

Supplementary Table 2. Mass ratio translation to N/P ratio for PLL+CpG polyplexes

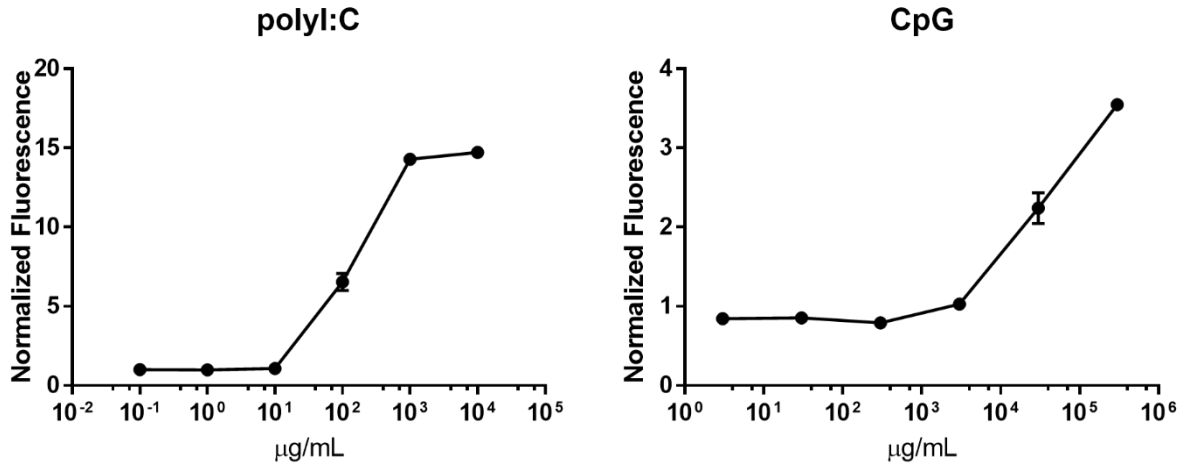

Supplementary Figure 1. Concentration curve of polyI:C and CpG in their respective HEK blue reporter cell lines.

References

1. Immunotherapy to Treat Cancer. https://www.cancer.gov/about-cancer/treatment/types/immunotherapy (accessed May 2019). National Cancer Institute.
2. Vinay, D. S.; Ryan, E. P.; Pawelec, G.; Talib, W. H.; Stagg, J.; Elkord, E.; Lichtor, T.; Decker, W. K.; Whelan, R. L.; Kumara, H. M. C. S.; Signori, E.; Honoki, K.; Georgakilas, A. G.; Amin, A.; Helferich, W. G.; Boosani, C. S.; Guha, G.; Ciriolo, M. R.; Chen, S.; Mohammed, S. I.; Azmi, A. S.; Keith, W. N.; Bilsland, A.; Bhakta, D.; Halicka, D.; Fujii, H.; Aquilano, K.; Ashraf, S. S.; Nowsheen, S.; Yang, X.; Choi, B. K.; Kwon, B. S., Immune evasion in cancer: Mechanistic basis and therapeutic strategies. *Seminars in Cancer Biology* **2015,** *35*, S185-S198.
3. Binnewies, M.; Roberts, E. W.; Kersten, K.; Chan, V.; Fearon, D. F.; Merad, M.; Coussens, L. M.; Gabrilovich, D. I.; Ostrand-Rosenberg, S.; Hedrick, C. C.; Vonderheide, R. H.; Pittet, M. J.; Jain, R. K.; Zou, W.; Howcroft, T. K.; Woodhouse, E. C.; Weinberg, R. A.; Krummel, M. F., Understanding the tumor immune microenvironment (TIME) for effective therapy. *Nature Medicine* **2018,** *24* (5), 541-550.
4. Junttila, M. R.; De Sauvage, F. J., Influence of tumour micro-environment heterogeneity on therapeutic response. *Nature* **2013,** *501*, 346.
5. Sriraman, S. K.; Aryasomayajula, B.; Torchilin, V. P., Barriers to drug delivery in solid tumors. *Tissue barriers* **2014,** *2*, e29528-e29528.
6. Velcheti, V.; Schalper, K., Basic Overview of Current Immunotherapy Approaches in Cancer. *American Society of Clinical Oncology Educational Book* **2016,** (36), 298-308.
7. Nierkens, S.; Den Brok, M. H.; Roelofsen, T.; Wagenaars, J. a. L.; Figdor, C. G.; Ruers, T. J.; Adema, G. J., Route of Administration of the TLR9 Agonist CpG Critically Determines the Efficacy of Cancer Immunotherapy in Mice. *PLOS ONE* **2009,** *4* (12), e8368.
8. Temizoz, B.; Kuroda, E.; Ishii, K. J., Vaccine adjuvants as potential cancer immunotherapeutics. *International Immunology* **2016,** *28* (7), 329-338.
9. Ceravarix. https://www.fda.gov/vaccines-blood-biologics/vaccines/cervarix. FDA.
10. Smith, M.; García-Martínez, E.; Pitter, M. R.; Fucikova, J.; Spisek, R.; Zitvogel, L.; Kroemer, G.; Galluzzi, L., Trial Watch: Toll-like receptor agonists in cancer immunotherapy. *OncoImmunology* **2018,** *7* (12), e1526250.
11. Aznar, M. A.; Tinari, N.; Rullán, A. J.; Sánchez-Paulete, A. R.; Rodriguez-Ruiz, M. E.; Melero, I., Intratumoral Delivery of Immunotherapy—Act Locally, Think Globally. *The Journal of Immunology* **2017,** *198* (1), 31-39.
12. Bianchi, F.; Pretto, S.; Tagliabue, E.; Balsari, A.; Sfondrini, L., Exploiting poly(I:C) to induce cancer cell apoptosis. *Cancer Biology & Therapy* **2017,** *18* (10), 747-756.
13. Kumar, A.; Zhang, J.; Yu, F.-S. X., Toll-like receptor 3 agonist poly(I:C)-induced antiviral response in human corneal epithelial cells. *Immunology* **2006,** *117* (1), 11-21.
14. Krieg, A. M., CpG Motifs in Bacterial DNA and Their Immune Effects. *Annual Review of Immunology* **2002,** *20* (1), 709-760.
15. Yang, L.; Yu, H.; Dong, S.; Zhong, Y.; Hu, S., Recognizing and managing on toxicities in cancer immunotherapy. *Tumor Biology* **2017,** *39* (3), 1010428317694542.
16. Ngwa, W.; Irabor, O. C.; Schoenfeld, J. D.; Hesser, J.; Demaria, S.; Formenti, S. C., Using immunotherapy to boost the abscopal effect. *Nature Reviews Cancer* **2018,** *18*, 313.
17. Wiethoff, C. M.; Middaugh, C. R., Barriers to Nonviral Gene Delivery. *Journal of Pharmaceutical Sciences* **2003,** *92* (2), 203-217.
18. Baoum, A. A.; Berkland, C., Calcium Condensation of DNA Complexed with Cell-Penetrating Peptides Offers Efficient, Noncytotoxic Gene Delivery. *Journal of Pharmaceutical Sciences* **2011,** *100* (5), 1637-1642.
19. Midoux, P.; Monsigny, M., Efficient Gene Transfer by Histidylated Polylysine/pDNA Complexes. *Bioconjugate Chemistry* **1999,** *10* (3), 406-411.
20. Fu, J.; Cai, J.; Ling, G.; Li, A.; Zhao, J.; Guo, X.; Zhang, P., Cationic polymers for enhancing CpG oligodeoxynucleotides-mediated cancer immunotherapy. *European Polymer Journal* **2019,** *113*, 115-132.
21. Oncovir, I., Oncovir. 2019.
22. Nomura, T.; Koreeda, N.; Yamashita, F.; Takakura, Y.; Hashida, M., Effect of particle size and charge on the disposition of lipid carriers after intratumoral injection into tissue-isolated tumors. *Pharmaceutical research* **1998,** *15* (1), 128-32.
23. Durymanov, M. O.; Rosenkranz, A. A.; Sobolev, A. S., Current Approaches for Improving Intratumoral Accumulation and Distribution of Nanomedicines. *Theranostics* **2015,** *5* (9), 1007-1020.
24. Tang, L.; Yang, X.; Yin, Q.; Cai, K.; Wang, H.; Chaudhury, I.; Yao, C.; Zhou, Q.; Kwon, M.; Hartman, J. A.; Dobrucki, I. T.; Dobrucki, L. W.; Borst, L. B.; Lezmi, S.; Helferich, W. G.; Ferguson, A. L.; Fan, T. M.; Cheng, J., Investigating the optimal size of anticancer nanomedicine. *Proceedings of the National Academy of Sciences* **2014,** *111* (43), 15344-15349.
25. Bao, A.; Phillips, W. T.; Goins, B.; Zheng, X.; Sabour, S.; Natarajan, M.; Ross Woolley, F.; Zavaleta, C.; Otto, R. A., Potential use of drug carried-liposomes for cancer therapy via direct intratumoral injection. *International Journal of Pharmaceutics* **2006,** *316* (1), 162-169.
26. Shang, L.; Nienhaus, K.; Nienhaus, G. U., Engineered nanoparticles interacting with cells: size matters. *J Nanobiotechnology* **2014,** *12*, 5-5.
27. Lee, H.; Fonge, H.; Hoang, B.; Reilly, R. M.; Allen, C., The Effects of Particle Size and Molecular Targeting on the Intratumoral and Subcellular Distribution of Polymeric Nanoparticles. *Molecular Pharmaceutics* **2010,** *7* (4), 1195-1208.

28. Kinnunen, H. M.; Sharma, V.; Contreras-Rojas, L. R.; Yu, Y.; Alleman, C.; Sreedhara, A.; Fischer, S.; Khawli, L.; Yohe, S. T.; Bumbaca, D.; Patapoff, T. W.; Daugherty, A. L.; Mrsny, R. J., A novel in vitro method to model the fate of subcutaneously administered biopharmaceuticals and associated formulation components. *Journal of Controlled Release* **2015,** *214*, 94-102.
29. Kinnunen, H. M.; Mrsny, R. J., Improving the outcomes of biopharmaceutical delivery via the subcutaneous route by understanding the chemical, physical and physiological properties of the subcutaneous injection site. *Journal of Controlled Release* **2014,** *182*, 22-32.
30. Chen, J.; Wang, K.; Wu, J.; Tian, H.; Chen, X., Polycations for Gene Delivery: Dilemmas and Solutions. *Bioconjugate Chemistry* **2019,** *30* (2), 338-349.
31. Marabelle, A.; Andtbacka, R.; Harrington, K.; Melero, I.; Leidner, R.; De Baere, T.; Robert, C.; Ascierto, P. A.; Baurain, J. F.; Imperiale, M.; Rahimian, S.; Tersago, D.; Klumper, E.; Hendriks, M.; Kumar, R.; Stern, M.; Öhrling, K.; Massacesi, C.; Tchakov, I.; Tse, A.; Douillard, J. Y.; Tabernero, J.; Haanen, J.; Brody, J., Starting the fight in the tumor: expert recommendations for the development of human intratumoral immunotherapy (HIT-IT). *Annals of Oncology* **2018,** *29* (11), 2163-2174.
32. Milling, L.; Zhang, Y.; Irvine, D. J., Delivering safer immunotherapies for cancer. *Advanced drug delivery reviews* **2017,** *114*, 79-101.
33. Albershardt, T. C.; Parsons, A. J.; Berglund, P.; Ter Meulen, J., Intratumoral injections of G100 (synthetic TLR4 agonist) increase trafficking of lentiviral vector-induced antigen-specific CD8 T cells to the tumor microenvironment. *J Immunother Cancer* **2015,** *3* (Suppl 2), P290-P290.
34. Schmidt, M.; Hagner, N.; Marco, A.; König-Merediz, S. A.; Schroff, M.; Wittig, B., Design and Structural Requirements of the Potent and Safe TLR-9 Agonistic Immunomodulator MGN1703. *Nucleic Acid Ther* **2015,** *25* (3), 130-140.
35. Cornfield, M. J. In *IMO-2125, an investigational intratumoral tolllike receptor 9 agonist, modulates the tumor microenvironment to enhance anti-tumor immunity*, Society for Immunotherapy of Cancer, National Harbor, MD, November 9, 2016; Pharmaceuticals, I., Ed. National Harbor, MD, 2016.
36. Pharmaceuticals, C., Technology.
37. Bioncotech, BO-112: a Potent Immunotherapy.
38. Alhakamy, N. A.; Berkland, C. J., Polyarginine Molecular Weight Determines Transfection Efficiency of Calcium Condensed Complexes. *Molecular Pharmaceutics* **2013,** *10* (5), 1940-1948.
39. Hall, A.; Lächelt, U.; Bartek, J.; Wagner, E.; Moghimi, S. M., Polyplex Evolution: Understanding Biology, Optimizing Performance. *Molecular Therapy* **2017,** *25* (7), 1476-1490.
40. Foged, C.; Brodin, B.; Frokjaer, S.; Sundblad, A., Particle size and surface charge affect particle uptake by human dendritic cells in an in vitro model. *International Journal of Pharmaceutics* **2005,** *298* (2), 315-322.
41. Jia, J.; Zhang, Y.; Xin, Y.; Jiang, C.; Yan, B.; Zhai, S., Interactions Between Nanoparticles and Dendritic Cells: From the Perspective of Cancer Immunotherapy. *Front Oncol* **2018,** *8*, 404-404.
42. Bookstaver, M. L.; Tsai, S. J.; Bromberg, J. S.; Jewell, C. M., Improving Vaccine and Immunotherapy Design Using Biomaterials. *Trends Immunol* **2018,** *39* (2), 135-150.
43. Carmona-Ribeiro, A. M., Cationic Nanostructures for Vaccines, Immune Response Activation. Guy Huynh Thien Duc, IntechOpen, 2014.
44. Canton, I.; Battaglia, G., Endocytosis at the nanoscale. *Chemical Society Reviews* **2012,** *41* (7), 2718-2739.
45. Iversen, T.-G.; Skotland, T.; Sandvig, K., Endocytosis and intracellular transport of nanoparticles: Present knowledge and need for future studies. *Nano Today* **2011,** *6* (2), 176-185.
46. Tolokh, I. S.; Pabit, S. A.; Katz, A. M.; Chen, Y.; Drozdetski, A.; Baker, N.; Pollack, L.; Onufriev, A. V., Why double-stranded RNA resists condensation. *Nucleic Acids Res* **2014,** *42* (16), 10823-10831.
47. Li, L.; Pabit, S. A.; Meisburger, S. P.; Pollack, L., Double-stranded RNA resists condensation. *Phys Rev Lett* **2011,** *106* (10), 108101-108101.
48. Lynn, G. M.; Laga, R.; Darrah, P. A.; Ishizuka, A. S.; Balaci, A. J.; Dulcey, A. E.; Pechar, M.; Pola, R.; Gerner, M. Y.; Yamamoto, A.; Buechler, C. R.; Quinn, K. M.; Smelkinson, M. G.; Vanek, O.; Cawood, R.; Hills, T.; Vasalatiy, O.; Kastenmüller, K.; Francica, J. R.; Stutts, L.; Tom, J. K.; Ryu, K. A.; Esser-Kahn, A. P.; Etrych, T.; Fisher, K. D.; Seymour, L. W.; Seder, R. A., In vivo characterization of the physicochemical properties of polymer-linked TLR agonists that enhance vaccine immunogenicity. *Nature Biotechnology* **2015,** *33* (11), 1201-1210.
49. Kwoh, D. Y.; Coffin, C. C.; Lollo, C. P.; Jovenal, J.; Banaszczyk, M. G.; Mullen, P.; Phillips, A.; Amini, A.; Fabrycki, J.; Bartholomew, R. M.; Brostoff, S. W.; Carlo, D. J., Stabilization of poly-l-lysine/DNA polyplexes for in vivo gene delivery to the liver. *Biochimica et Biophysica Acta (BBA) - Gene Structure and Expression* **1999,** *1444* (2), 171-190.
50. Koo, H.-B.; Kang, H.-S., Analysis of the Relationship between the Molecular Weight and Transfection Efficiency/Cytotoxicity of Poly-L-arginine on a Mammalian Cell Line. *Bulletin of the Korean Chemical Society* **2009,** *30*, 927-930.
51. Kim, H. H.; Choi, H. S.; Yang, J. M.; Shin, S., Characterization of gene delivery in vitro and in vivo by the arginine peptide system. *International Journal of Pharmaceutics* **2007,** *335* (1), 70-78.

Chapter 3:
Glatiramer Acetate Enhances Retention and Innate Activation of Immunostimulants for Cancer Immunotherapy

1. Introduction

The concept of cancer immunotherapy was proposed a century ago when Dr. William Coley first attempted to harness the body's immune system to fight off cancer.[1-2] While this approach seemed promising, manipulation of the immune response can be dangerous and therefore must be deliberately controlled. Scientists made significant progress in developing cancer immunotherapies as alternatives to traditional treatments such as chemotherapy and radiation. Currently approved cancer immunotherapies range from checkpoint inhibitor monoclonal antibodies (mAbs) that decrease tumor immune suppression, viral therapies that activate immune cells, and mAbs that label certain cell types for death.[3] Unfortunately, current therapies often fail to evoke an immune response capable of overcoming the immunosuppressive tumor microenvironment while also exhibiting acceptable safety profiles.[4-7] Additionally, checkpoint inhibitors are predominantly effective in tumors that are considered 'hot', tumors characterized by high infiltration of immune cells that express the target immune-dampening markers.[8-9] In order to properly activate T cells for tumor killing, there must be expression of co-stimulatory molecules, secretion of proinflammatory cytokines, and presentation of antigens, all of which are suppressed in the tumor microenvironment.[10-12]

One method to overcome the suppressive tumor microenvironment is the use of immunostimulants, which are typically compounds that activate a proinflammatory, innate immune response. The use of immunostimulants in the presence of antigen causes a number of reactions including upregulation of co-stimulatory molecules, increased antigen presentation, and secretion of proinflammatory cytokines, which can lead to the formation of tumor specific T-cells.[10, 13-14] One class of immunostimulants, toll-like-receptor agonists, are capable of inducing a strong T cell response after binding to their respective toll-like receptors (TLRs). TLRs recognize bacterial and viral pathogen associated molecular patterns (PAMPs), which trigger specific signaling pathways. Two TLR agonists are currently FDA approved. Ceravarix™ is a cervical cancer vaccine that contains monophosphoryl lipid A (MPL), a TLR4 agonist in the adjuvant system.[15] The

other, Aldara™, is a cream for superficial basal cell carcinoma, the main active ingredient is a TLR7/8 agonist called imiquimod.[16]

Two vastly explored TLR agonists in cancer immunotherapy are polyinosinic:polycytidylic acid (polyI:C) and CpG, which are TLR3 and TLR9 agonists, respectively. Both compounds exhibit strong induction of interferons, leading to a proinflammatory environment after binding to TLRs, thus generating memory and tumor-specific T cells.[17-19] Several clinical trials utilize TLR agonists alone or in combination with other anti-cancer therapies such as radiation or checkpoint inhibitors. PolyI:C is a double-stranded (ds) RNA mimic that has shown both antiviral and anticancer activity.[20-21] Additionally, TLR3 agonists have demonstrated the ability to directly inhibit tumors *in vitro* by decreasing cell proliferation and inducing apoptotic cell death.[20] To date, polyI:C therapy has not been successful in cancer patients because of dose-limiting side effects.[22] The side effects are reduced when polyI:C is mixed with poly-L-lysine in an experimental drug called Hiltonol.[23] Another TLR agonist, CpG, is a short, single-stranded synthetic oligonucleotide that contains multiple, unmethylated cytosine-phosphate-guanine motifs, which mimic bacterial DNA. Since its discovery in 1994, CpG has been extensively evaluated in clinical trials for cancer.[24] Unfortunately, no therapeutics containing CpG are currently approved. One company, Checkmate Pharmaceuticals, utilizes a modified version of CpG class-A that self assembles into G tetrads that stack to form G-quadruplexes.[25] Despite the fact that PolyI:C and CpG are promising candidates for use in cancer immunotherapy, one vital challenge is determining how to properly deliver these agents to tumor tissue.

While systemic delivery can target multiple tumor sites, full body exposure of immunostimulants can cause improper activation of the immune system in healthy tissue, generating harmful immune and autoimmune reactions.[6] One possible solution to this dilemma has been termed human intratumoral immunotherapy (HIT-IT) with the aim of propagating anti-tumor responses at sites distal to the injection concurrently with shrinkage of treated tumors. This process, called the abscopal effect, can occur when tumor-activated immune cells drain to the lymph nodes and circulate to other parts of the body.[26] Immune cells recruited to the site of stimulation and activated by the immunostimulant could ultimately present tumor antigen and activate tumor-specific T cells. From a drug delivery perspective, the immunostimulants

should to be retained at the tumor injection site and yet available for endocytosis by immune cells to reach endosomal TLR3 and TLR9. Since free polyI:C and CpG are both negatively charged, intracellular delivery is hindered by electrostatic repulsion due to the negatively charged cell membrane. In contrast, a net positively charged nanoparticle may allow for tumor retention, attraction to cell membranes, and increased intracellular delivery of the TLR agonists.[27] Polyplex nanoparticles, which are complexes between polycations and polyanions, have been widely explored for gene delivery therapies since they can be modulated with specific size, charge, and loading capacity.[28-31]

Previously, our lab has shown how glatiramer acetate (GA), a highly positively charged polypeptide, is effective in delivering plasmid DNA to cells.[32] GA, otherwise known as Copaxone®, is an FDA-approved drug for relapsing-remitting multiple sclerosis. Specifically, GA is comprised of four amino acids in a random sequence with the following amino acid ratios: L-glutamic acid (0.14), L-alanine (0.43), L-tyrosine (0.09), and L-lysine (0.34) (**Figure 1**). It has an average molecular weight between 5,000 and 9,000 Da, but can range anywhere from 2,500 to 20,000 Da.[33] Although the mechanism of action is unclear, GA has limited systemic exposure and pronounced reactions at the site of injection. Previous works to characterize the mechanism of GA led to an understanding that GA persists at the site of injection and forms aggregates *in situ*.[33] These aggregates appeared as spherical particles that could be seen associating with local connective tissue.[33] Unlike other polycations utilized in polyplexes, studies have shown that GA persists at the injection site and potentially aids in activating an immune response.[33]

In the current work, we aim to exploit the characteristics of positively-charged GA in order to deliver the negatively-charged immunostimulants as a polyplex nanoparticle. Moreover, due to the persistence of GA at the injection site, we hypothesized GA may recruit immune cells to the site of injection. Here, we study complexation between GA and either polyI:C or CpG and the relation to *in vitro* and *in vivo* efficacy. Various methods were employed to characterize the polyplexes including particle sizing, zeta potential, and experiments that elucidated the stability of the polyplexes. To evaluate retention, polyplexes were tested in an *in vitro* system to emulate transport in human tissue. *In vitro* assays were used to assess

the activity of the complexed TLR agonist. Finally, *in vivo* efficacy and immune responses were determined in a mouse tumor model of head and neck squamous cell carcinoma (HNSCC).

2. Methods

2.1 Polyplex formation

20 mg/mL solutions of Copaxone® 1 mL pre-filled syringes from Teva Neuroscience, Inc. (Kansas City, MO) were donated by the University of Kansas Medical Center. Copaxone, or Glatiramer acetate will hereafter be referred to as GA. CpG ODN 1826 and LMW PolyI:C were purchased from Invivogen (San Diego, CA). GA polyplexes with CpG ODN 1826 or LMW PolyI:C were prepared by adding equal volumes of GA and CpG or PolyI:C diluted to the desired concentration followed by repeated pipetting for 30 seconds. The polyplexes were then stored at room temperature for a minimum of 20 minutes before being analyzed to use in cell culture. Polyplexes were prepared at varying mass ratios of 1, 2, 3, 4, 5, 10, 20 that represent mass of GA divided by the complex partner, CpG or PolyI:C (**Figure 2**). Mass ratio was utilized rather than a polymer nitrogen to anion phosphate (N:P) ratio due to heterogeneity of the components. Polyplexes were made up in 4% mannitol except for the pH comparison in agarose gel and zeta potential measurements which used PBS and 1mM KCl.

2.2 Agarose gel electrophoresis

Agarose was purchased from Sigma Aldrich (St. Louis, MO). Tris-acetate-EDTA (TAE) buffer was purchased from Invitrogen (Carlsbad, CA). CpG or PolyI:C polyplexes were prepared as described holding the CpG or PolyI:C concentration constant while varying the GA concentration. Then, 4 µL 6x DNA loading dye (Takara Bio Inc., Japan) was added to the polyplex (10 µL) before the solution was loaded onto a 3% agarose gel, and electrophoresed for 25 minutes at 100 V. CpG and PolyI:C alone were utillized as controls. A 1 kb DNA ladder (Promega, Madison, WI) was used as a general reference. The gel was stained

by shaking with SYBR Gold (Invitrogen, Carlsbad, CA) in TAE buffer for 25 minutes at room temperature. Then, the gel was imaged on AlphaImager (Protein Simple, San Jose, CA).

2.3 Particle sizing and zeta potential

The effective radius (nm) of CpG or PolyI:C polyplexes was determined by dynamic light scattering (DynaPro, Wyatt Technology, Santa Barbara, CA). Samples for particle sizing were prepared in 4% mannitol (Sigma Aldrich, St. Louis, MO). Measurements were conducted after a 20 minute incubation time at room temperature. Zeta potential measurements were measured by Zeta PALS (Brookhaven Instruments, Holtsville, NY). All samples for zeta potential measurements were prepared in 4% mannitol and diluted into 1 mM KCl for analysis.

2.4 Rhodamine labeled GA

Copaxone® in pre-filled syringes was first dialyzed against DI water to remove the mannitol buffer. It was then reacted with 2 equivalents of Rhodamine B *N*-hydroxysuccinimide (NHS) ester in CPB buffer (10mM citrate, 20mM phosphate, 40mM borate) pH 7.5 with 20 % dimethyl sulfoxide (DMSO). The reaction was protected from light and allowed to react at room temperature for 4 hours with gentle agitation. To separate labeled drug from excess dye, the reaction mixture was placed into 2 kDa MWCO dialysis cassettes and dialyzed against 5% dimethylformamide (DMF) in water at pH 2, followed by 0.5 M LiCl solution, and finally DI water. Dialysis was performed sequentially in each buffer for 24 hours with one buffer change in between for total of 72 hours. The resulting reaction solution was characterized by HPLC and lyophilized. 7000 Da was used as the approximate molecular weight (MW) of Copaxone®. The conjugation of dye labeled onto GA was determined by constructing a calibration curve based on the fluorescence of Rhodamine B NHS ester at various concentrations and comparing the fluorescence of the labeled product to the calibration curve. The fluorescence experiments were performed using Synergy™ H4 Microplate Reader (BioTek, Winooski, VT) with 540/25 nm excitation filter and 620/40 nm emission filter.

2.5 Fluorescence polarization

Fluorescence polarization measurements were taken on Synergy H4 microplate reader (BioTek, Winooski, VT). Rhodamine labeled GA was complexed with varying amounts of CpG or PolyI:C as previously described. Standard curves for Rhod-GA, CpG, and PolyI:C were prepared. Then, 200 µL of the polyplexes, or standards were added to a 96 well, black microplate (Corning, Corning, NY). Using fluorescence polarization settings on the plate reader, the excitation filter was set to 485 nm/ 20 nm and emission filter to 620 nm/ 40 nm. To calculate the polarization, first the parallel and perpendicular values for the standards (CpG or PolyI:C alone) are subtracted from their respective polyplexes. Then polarization was calculated using the following equation: $P = \frac{I\parallel - I\perp}{I\parallel + I\perp}$.

2.6 Transmission electron microscopy (TEM)

TEM images were captured using FEI Tecnai F20 XT Field Emission Transmission Electron Microscope at the University of Kansas Microscopy and Analytical Imaging Laboratory. Polyplexes or individual components were added to carbon coated grids and touched on a Kimwipe to remove excess liquid, then immediately dipped into liquid nitrogen prior to imaging.

2.7 Assessment of DNA/RNA accessibility by SYBR gold assay

The degree of accessibility of the DNA or RNA following complexation with GA was assessed by the staining of SYBR Gold to accessible DNA or RNA. Polyplexes were made as described above and after 20 minutes polyplexes were added to a 96-well plate in triplicate followed by SYBR gold stain and mixed well. After approximately 5 minutes the fluorescence was measured using a Synergy H4 microplate reader (BioTek, Winooski, VT). The excitation filter was set to 495 nm and emission filter to 537 nm.

2.8 The effect of dextran sulfate on the stability of the polyplexes

The effect of dextran sulfate on the stability of the polyplexes was assessed by observing the change in fluorescence of SYBR Gold upon increasing amounts of dextran sulfate. 90 uL of each polyplex was added to a 96-well plate followed by 10 uL of various concentrations of dextran sulfate and mixed well. After 20-30 minutes of RT incubation, 11 uL of 10x SYBR Gold was added and 5 minutes later the plate was analyzed as described previously.

2.9 Hyaluronic acid gel retention

To test the polyplexes ability to retain at an injection site, we devised a model system to emulate transport in human tissue made of highly viscous hyaluronic acid (HA) to which we could inject labeled polyplexes in the center and observe the dispersion over time. 0.8-1.5 MDa HA was added to PBS buffer at 20 mg/mL then placed on end-over-end rotator overnight to dissolve. The HA gel was then weighed out into a 96 well black plate at 0.28 g/well. The plate was centrifuged to remove bubbles then placed at 4 ˚C until use. Polyplexes were prepared as described but for this test they were first made up in 90% of the total volume, let incubate for 20 minutes, then 10% of the total volume of 20x SYBR Gold stain was added for an additional 5 minutes. A 3D printed device was designed to allow uniform injection into the wells at half the depth of the gel. 7 µL of sample was injected through the device into the center of the well using reverse pipetting. Fluorescent images were obtained at varying time points on a MaestroFlex Imager (Cambridge Research and Instrumentation, Woburn, MA). Wells were analyzed using ImageJ software. Fluorescence intensity was measured across the well at 3 different angles (rotated 60˚ each) and averaged to create a spatial intensity plot (**figure 8A)**. The values were then normalized to a standard that was constant in every image. Area under the curve from pixels 15-25 was used to calculate the percent intensity reduction from time 0.

2.10 Jaws II cells

Jaws II cells (ATCC Manassas, VA) were cultured in RPMI, 10% FBS (Atlanta Biologicals), 1% penicillin-streptomycin (P/S, MP Biomedicals), and 5 ng/mL GM-CSF (Tonbo Biosciences). Jaws II cells were plated at $2.5x10^5$ cells/well, at 270 µL/well in a 96 well plate and allowed to adhere for an hour before adding treatments. Then, 30 µL of 10x polyplex or GA, polyI:C, or CpG was added to each well. Additionally to assess cell stability in the presence of various buffers, 30 µL of either 4% mannitol, 5% glucose, nuclease-free water (NFW), or saline was added to the well and images were taken on an inverted microscope (Accu-Scope, Hicksville, NY). Additionally, a resazurin assay was utilized to assess cell metabolism.

2.11 Bone marrow derived dendritic cells (BMDCs)

Five-week-old C57BL/6J mice were purchased from Jackson Laboratories and housed under specified, pathogen-free conditions at The University of Kansas. All protocols involving mice were approved by the Institutional Animal Care and Use Committee at The University of Kansas. Mice were sacrificed and their femurs were collected. The ends of the femur were clipped, and the bone marrow was flushed out using a 21-gauge needle attached to a 5 mL syringe containing RPMI supplemented with 1% penicillin-streptomycin. Cells were collected and centrifuged for 7 minutes at 1,350 rpm at 4℃. The supernatant was removed, replaced with red cell lysis buffer, and incubated at room temperature for 10 minutes. Lysis was stopped with 6x volume of cold complete medium (RPMI, 10% FBS, 1% penicillin-streptomycin). The cell solution was passed through a 70 µm nylon cell strainer and centrifuged for 5 minutes at 1,700 rpm and 4℃. The supernatant was removed and replaced with complete medium, and cells were plated at approximately $2x10^6$ cells per T-75 culture flask in 12 mL complete medium spiked with 20 ng/mL GM-CSF. On day 3, the medium was removed to discard any floating cells, and 12 mL of media with fresh GM-CSF was added to the cells. On day 8, the media with cells were collected and the bottom of the flask was thoroughly rinsed to collect any loosely adherent cells. BMDCs were then plated at $2.5x10^5$ cells/well and treated as previously described for the Jaws II culture conditions. Cell viability was inferred from metabolic

activity measured by the resazurin assay. Wells were washed and 100 µL of RPMI and 20 µL of 0.01% resazurin were added to the wells. Plates were incubated at 37°C for one or two hours, and the fluorescence was measured at ex/em 560/590 nm using a Synergy H4 microplate reader (BioTek, Winooski, VT). Data within each stimulation group was normalized to the untreated media control at their respective time points.

TNF-α ELISA. TNF-α expression by the dendritic cells was measured by ELISA (R&D systems, Minneapolis, MN) as per manufacturer instructions.

2.12 In vitro HEK blue reporter cell assay

HEK-Blue TLR9, TLR3, and Null cell lines (Invivogen, California) were grown in Dulbecco's Modified Eagle's Medium (DMEM; Corning, NY) supplemented with 10% FBS, 1% penicillin-streptomycin, and the selective antibiotics according to the manufacturer's protocol. HEK-Blue TLR cells allow for the study of TLR activation by observing the stimulation of secreted embryonic alkaline phosphatase (SEAP), a protein associated with downstream activation of TLRs. At 50-80% confluency, cells were harvested and resuspended in HEK detection media (Invivogen, California) and 180 uL was seeded into 96-well plates at ~$8x10^5$ cells/well. 20 uL of polyplexes or controls were added to respective wells and the plate was incubated at 37 °C, 5% CO_2 for at least 6 hours or until color change. Absorbance readings were measured at 640 nm. Null cells were used as the control. Working polyanion concentrations were determined by selecting a concentration that achieved a reasonable response factor as shown from a concentration curve completed in the respective cell lines (**supplementary figure 1**). PolyI:C was held constant at 200 µg/mL and CpG was at 100 µg/mL. Cells and sample were incubated with the HEK blue detection media for TLR activation measurements or in regular media for metabolism evaluation in resazurin assays.

2.13 AT84 cells

AT84 cells were derived from a spontaneous squamous cell carcinoma in the oral mucosa of a C3H mouse (Hier/Karp 1995, Paolini/Venuti 2013) and were gifted by Aldo Venuti (Regina Elena National

Cancer Institute, Rome, Italy). Cells tested negative for interspecies contamination (species: mouse(+), rat(-), human(-), Chinese hamster(-), African green monkey(-); Idexx BioResearch), negative for rodent pathogens (Idexx BioResearch, 21 pathogen IMPACT I PCR profile), and negative for Mycoplasm contamination prior to animal studies (Lonza, Basel, Switzerland, MycoAlert test kit). Idexx CellCheck STR (short tandem repeat) profile: MCA-4-2: 20.3, 21.3; MCA-5-5: 15; MCA-6-4: 18, 19; MCA-6-7: 12; MCA-9-2: 15; MCA-12-1: 16; MCA-15-3: 25.3, 26.3; MCA-18-3: 16; MCA-X-1: 26, 27. Cells were cultured in RPMI-1640 media (Gibco, Thermo Fisher Scientific, Waltham, MA) supplemented with 10% FBS (Corning Corning, NY), and 100 U/mL penicillin / 100 µg/mL streptomycin (HyClone, Thermo Fisher Scientific, Waltham, MA) in a humidified incubator at 37°C and 5% CO_2.

All rodent studies were done at the University of Kansas Animal Care Unit, which is in compliance with the "Guide for the Care and Use of Laboratory Animals" and is accredited by the Association for the Assessment and Accreditation of Laboratory Animal Care International (AAALAC). The studies were done according to a protocol approved by the University of Kansas IACUC committee.

2.14 Immuno-competent tumor model for efficacy

CpG polyplexes displayed better TLR activation and retention potential over polyI:C polyplexes so CpG polyplexes were selected to move forward in tumor studies. Wildtype C3H mice (Charles River Strain 025, 6-8 weeks old, 20-25g) were used for *in vivo* tumor studies. Both male and female mice were used in the studies. Since no differences were found between the sexes, results combined both sexes into one group. Mice were anesthetized using 5% isoflurane in O_2 for 5 minutes. One million AT84 cells in 50 µl PBS were injected subcutaneous (s.c.) into the floor of the mouth via an extra-oral route of C3H mice to obtain orthotopic allograft tumors (Hier/Karp 1995, Paolini/Venuti 2013). Treatment began when tumors reached ~100 mm^3, generally days 10-12 days after cell injection. Under isoflurane anesthesia, mice were treated intratumorally with 75 µg (based on immunostimulant) in 50 µL sterile 4% mannitol every three days for 5 total treatments. Serum was collected via retroorbital bleeding 2 hours after the first and fifth injections.

Serum cytokines were measured using a U-PLEX kit (Meso scale Diagnostics, LLC, Rockville, MD) as per the manufacturer instructions. Animal survival was evaluated, however, in this model, death was usually caused by a tumor size large enough to impede regular mobility. Tumor size was monitored twice per week and calculated: tumor volume (mm^3) = 0.52 × $(width)^2$ × length, where length is the longer of two perpendicular dimensions. Statistical comparisons were done using GraphPad Prism software. On day 36 when all vehicle-treated tumors reached the maximum allowable size (1800 mm^3), all animals were sacrificed, and tumors extracted. Tumor was bisected, and one half was frozen in OTC media (Fisher Scientific) for cryosectioning and staining. The other half was cut into small pieces (< 5 mm) and stored in RNA Later solution (Ambion, Inc. Austin, TX). For cryosectioning slices, the sections were fixed in 10% formalin, blocked with 5% goat serum in PBS, and stained with primary antibodies. Primary antibodies were diluted to 5 µg/mL in blocking buffer (5% goat serum in PBS) and incubated overnight at 4 °C. Antibodies used were Alexa Fluor ® 488 anti-CD8a, Alexa Fluor® 594 anti-CD11b, and Alexa Fluor® 647 anti-CD11c (BioLegend). After antibody staining, sections were stained with Hoechst 33342 and mounted in SouthernBiotech™ Fluoromount-G™ Slide Mounting Medium (SouthernBioTech, Birmingham, AL) and stored in the dark at 4 °C. Images were acquired using an Olympus IX-81 inverted epifluorescence microscope at 10x magnification. The acquired images were compiled on Slidebook 6.0.

3. Results

3.1 Polyplex formation

Agarose gel electrophoresis studies were used to visually test the ability of the GA to polyplex with the polyanions (polyI:C and CpG). Specifically, free, negatively charged polyI:C or CpG migrated through the agarose gel whereas positively charged GA did not. When polyI:C or CpG are complexed with GA, the material is retained in the loading well. In the higher pH buffer (**Figure 3A and C**), more GA (a higher mass ratio) was required to fully immobilize the polyanion. The GA immobilized polyI:C at lower mass ratios than CpG but this can be attributed to molecular weight differences of the polyanions. Differences in

complexation as a function of pH were observed with both polyI:C and CpG. In particular, polyI:C was fully immobilized at R5 at pH 7 and R2 at pH 5. A similar trend was seen with CpG polyplexes where immobilization occured at R10 and R4 for pH 7 and pH 5, respectively. In more acidic conditions, the nitrogens on GA become more protonated, requiring less GA to immobilize the polyanionic TLR agonists.

3.2 Polyplex characterization

Zeta potential measurements (**Figure 4A-B**) agreed with electrophoresis studies, showing a transition to net positive charge at the same mass ratio where the polyanion was immobilized on agarose gels. At pH 7, both polyI:C and CpG polyplexes required a higher GA ratio to achieve a net positive charge than at pH 5. At the lowest ratio, the pH did not significantly impact the zeta potential. At higher ratios, the charge started to plateau, indicating an excess of GA. At lower ratios, the negative zeta potential could be a result of free polyanion in solution or rather the polyanion exposed on the surface of the polyplex whereas at higher ratios the polyanions are encapsulated within the polyplex. These results exhibited the ability to control the surface charge with pH and ratio. For all polyplexes the radius was between 20 and 70 nm, or a diameter range of 40-140 nm **(Figure 4C-D)**. For polyI:C and CpG, the polyplexes were net positively charged when the ratio is R2 and R5, respectively in 4% mannitol buffer (pH 5), which is the diluent used for GA in the product Copaxone®. To corroborate particle sizing data, TEM images were collected and the results correlated with the particle sizes determined by DLS measurements **(Figure 5)**. With controls alone, spherical particles were not observed, but in the polyplex samples, spherical particles were detected within the expected size range.

3.3 Immunostimulant accessibility characterization

Fluorescence polarization is typically utilized to quantify the associations between a protein and a ligand, however, this technique can also be used to analyze binding of fluorescent molecules and a protein. Here, fluorescence polarization was utilized to monitor complexation of fluorescently labeled-GA to

polyI:C or CpG. In the assay, samples were first subjected to polarized light. If the fluorescent molecule is free in solution, it will emit de-polarized light. Conversely, when it is bound and its mobility is decreased, the emitted light remains polarized, resulting in an increase in polarization. Rhodamine-labeled GA and the polyanion were mixed at various ratios holding the Rhodamine-GA constant and changing the concentration of polyI:C or CpG. The data collected complimented the agarose gel and zeta potential data. Specifically, the increase in polarization plateaued at the same mass ratio in which the net charge was positive and gel electrophoresis indicated immobilization (**Figure 6**).

The accessibility of polyI:C or CpG within the polyplexes was assessed by staining with SYBR Gold (**Figure 7A-B**). Free polyanion is more accessible for stain whereas complexed polyanion is more encapsulated and inaccessible. As expected, fluorescence decreased as the mass ratio increased indicating that the polyanion was becoming more encapsulated in the polyplex. Interestingly, the polyI:C control sample did not have the highest level of fluorescence compared to the polyplexes which was expected (and seen with the CpG group). One possible explanation is that GA may be rearranging or displaying the polyI:C on the surface rather than encapsulating it at the smaller mass ratios. To assess the interaction strength of the polyplexes, dextran sulfate was titrated into polyplex samples. Fluorescence measurements were obtained after incubation with increasing amounts of dextran sulfate for each polyplex tested and the signal was normalized to the signal at 0 dextran sulfate for the same polyplex (**Figure 7C-D**). For higher mass ratios, fluorescence increased with increasing dextran sulfate. At lower ratios, no trend was evident suggesting free polyanion dominated the fluorescence emitted. Additionally, polyI:C polyplexes had a larger fold increase in fluorescence with increasing dextran sulfate than CpG polyplexes suggesting a weaker interaction strength.

3.4 Hyaluronic acid gel retention

To simulate tumor tissue transport, polyplexes were injected into a model system to emulate transport in human tissue. HA is one of the main components within the extracellular network and high molecular weight HA has been used to simulate subcutaneous (SC) space injection.[34-35] For SC injection simulation,

10 mg/mL HA was previously reported[35], thus to model a denser tumor environment, the concentration was increased to 20 mg/mL. **Figure 8C** are representative examples some of the samples in this experiment over 0, 2, and 5 hour time points- where the greatest differences were observed. Normalized spatial plots are provided in **figure 8D**. Free polyI:C and CpG diffused quickly. Interestingly, the polyI:C polyplexes also appeared to diffuse quickly, even at higher ratios of polycation in comparison to CpG polyplexes. While the ratios cannot be directly compared between polyI:C and CpG polyplexes due to MW differences, the zeta potential and agarose gel profiles are similar. For the higher ratio CpG polyplexes, a peak in the center could still be observed at 24 hours and a clear, non-diffused spot was still seen but not imaged out to 72 hours. Since the polyplexes were labeled using SYBR Gold stain, each polyplex stained differently depending on the accessibility of the polyI:C or CpG. To make the samples directly comparable, data were normalized to the fluorescence intensity at time zero (**Figure 8A-B**). PolyI:C polyplexes diffused faster and were less dependent on ratio at the time points measured, but never diffused as quickly as the polyI:C control. CpG polyplex retention at the injection site was dependent on the ratio with polyplexes made using more GA persisting longer.

3.5 Dendritic cell metabolism

In an effort to determine an optimal buffer for polyplex formulation, cellular metabolism data and microscopy images of Jaws II dendritic cells were acquired after incubation with various buffers including nuclease free water, glucose, mannitol, PBS, and NaCl (**supplementary figure 2**). Glucose was the only buffer that showed detrimental effect on the cells. Next, to evaluate cytotoxicity in dendritic cells, cellular metabolism was measured after individual component or polyplex incubation with either Jaws II cells or BMDCs at two concentrations (**supplementary figure 3**). For the controls, GA, polyI:C, and CpG, no significant toxicity was observed however the metabolism was increased in BMDCs as compared to Jaws II DCs, particularly for CpG. Polyplexes showed a similar trend where BMDCs were more effected. CpG polyplexes impact on cellular metabolism was not effected by ratio whereas polyI:C polyplexes showed decreased metabolism with increased ratio. Further, for select samples, TNFα

secretion was measured from cell culture supernatant (**supplementary figure 4**). CpG polyplexes had a significant impact on BMDCs when polyI:C polyplexes did not and the opposite trend was true for incubation with Jaws II DCs. This could be a result of levels of toll-like receptors in the different cell types.[36]

3.6 In vitro HEK blue reporter cell assay

PolyI:C and CpG are TLR agonists of TLR3 and TLR9, respectively. HEK blue hTLR reporter cells were used to examine the effect of complexation on TLR activation. TLR activation was normalized to the respective polyanion control. An increased mass ratio of GA:CpG resulted in decreased TLR activation (**Figure 9**). Interestingly, some of the CpG polyplexes were up to twice as effective at activating TLR9 as the CpG alone. The trend was less pronounced for polyI:C polyplexes, but still showed the lowest TLR activation at the highest ratio. Generally, the polyI:C polyplexes activated TLR3 similar to free polyI:C with the exception of a GA:polyI:C ratio of 20. TLR activation did not seem to be affected by the differences in cellular metabolism (**Figure 10**). There was a slight decrease in metabolism as the ratio increased which was more pronounced at 20 hours but overall there were few significant differences compared to the untreated control.

3.7 Tumor studies in mice

CpG polyplexes were evaluated in a mouse tumor model of head and neck squamous cell carcinoma. Mice were inoculated with $1x10^6$ AT84 cells into the floor of the mouth. IT injections were administered every 3 days for a total of five injection and began when tumors reached ~100 mm^3 (**Figure 11A**). Treatment groups included CpG, CpG polyplexes at two mass ratios (R4 and R6), GA low and GA high corresponding to the GA dose delivered for R4 and R6, and the 4% mannitol vehicle control. The injection volume was consistent and CpG concentration was constant in all CpG containing treatments. The polyplexes as well as CpG alone had 100% survival whereas the controls, mannitol, and both GA

concentrations had 50% or less survival (**Figure 11C**). The separation was also clear in the tumor burden data with the control groups having tumors almost twice as large as those treated with polyplexes or CpG alone at the end of the study (**Figure 11B**). At the completion of the study, tumors were resected, cryosectioned, and stained for markers of immune cells. Tumor slice staining revealed differences in CD11b, a marker for many types of immune cells (monocytes, granulocytes, macrophages, dendritic cells, NK cells, and some T and B cells), and CD11c, a marker for dendritic cells (**Figure 13-14**). Polyplexes and CpG groups induced the infiltration of CD11b and CD11c immune cells into the tumor compared to the controls. While not statistically significant, R6 appeared to have some increased CD8a (cytotoxic T lymphocyte) infiltration. Further, GA-Hi appeared to have some enhancement of CD11b and CD11c but was not statistically different than the control. Images of the staining indicated that the infiltrating immune cells remained mostly in the periphery of the tumor (**Figure 13**).

3.8 Serum cytokines

To evaluate the systemic effect of the IT treatments, cytokine levels from serum taken two hours after the first and fifth injections were determined (**Figure 15**). CpG treatment induced the greatest level of cytokines across the panel in all but IL-2 after the fifth injection where R4 and R6 were higher. CpG, R4, and R6 produced significantly greater cytokine levels compared to both mannitol and GA groups for the majority of cytokines. CpG was always significantly higher. R6 treatment showed increased cytokine production compared to R4 in all cytokines.

4. Discussion

Intratumoral injection of immunostimulants has the potential to induce immunity to local and distal tumor tissue and to work synergistically with checkpoint inhibitors. Immunostimulant transport out of the tumor and into systemic circulation requires attention. High incidences of AEs in recent clinical trials have highlighted the necessity to optimize delivery of immunostimulants to decrease systemic toxicity.[37-38] In order to achieve HIT-IT of immunostimulants without systemic toxicity, retention and activity of the

therapy at the site of injection is a critical parameter.[39-40] Immunostimulants such as PAMPs may traffic into systemic circulation after IT injection, however, studies have shown dramatic benefits to depots, slow release, and particulate formulations of PAMPs to increase tumor retention and local activity.[30, 37, 39-41] Furthermore, many approaches aimed at increased immune activation have seen slightly enhanced safety and efficacy profiles when using structurally modified immunostimulants or emulsion or complex formulations.[23, 25, 42-45] Specifically, packaging of immunostimulants into condensed particles has been found to have a positive effect on retention and innate immune activation over the unformulated active ingredient.[30, 39]

The packaging of DNA or RNA by polycations into a net positively charged particle has been frequently used for intracellular delivery[46-49], but this work introduces a new perspective that these polyplexes can also aid in tumor retention. Common polycations used for delivery have a history of toxicity problems, especially at higher molecular weights[30-31, 50-53], therefore utilization of a polycation that already has an approved safety profile is attractive. An already FDA approved and polycationic drug, glatiramer acetate (GA), is a potential delivery tool when formulated with TLR agonists, polyI:C or CpG. Based on the characteristics of GA[33], the resulting cationic polyplex particles was hypothesized to promote cellular uptake and promote injection site retention.

Major factors contributing to tissue transport and immune activation are hydrodynamic radius and charge.[39, 54] Depending on the route of administration, particles 10-70 nm tend to drain to lymph nodes and >70 nm tend to form depots at the injection site.[54-60] Furthermore, positively charged particles below 500 nm have been seen to be optimal for APC uptake.[31, 54-55, 61] Previous studies of IT injection reported cationic liposomes and particles 120 – 250 nm were retained at the injection site whereas neutral and smaller liposomes drained from the tumor.[62-63] DLS measurements of the GA polyplexes yielded particle diameters of 40 nm – 140 nm, suggesting these could retain at injection site, or localize to draining lymph nodes, and attract the attention of APCs. Similar to previous reports, the particle size did not vary significantly with changing of the mass ratio.[64] Further, the polyplexes can be tuned to achieve a net positive charge, which is important for increased cell uptake as it can enhance the attractive force towards the negatively charged

cell surface. Positive charge has been shown to be specifically significant for injection site retention[33] including tumor[62-63] retention via electrostatic interactions.

GA polyplexes enhanced TLR activation compared to free immunostimulant suggesting particle formation promoted cell uptake. Others have shown particle formation is critical for enhanced APC uptake.[39, 56, 65] While most pronounced with the CpG polyplexes, TLR activation decreased as the ratio increased. Others found a similar correlation of TLR agonist accessibility within a polyplex and the corresponding receptor activation.[66] Immunostimulant accessibility studies revealed an increasing polycation:CpG ratio rendered the immunostimulant less accessible suggesting an intermediate ratio may promote release and TLR engagement. While increased ratio may result in promotion of endocytosis into cells due to increased positive charge attracting the polyplex to the cell surface, the tighter binding causes a decrease in TLR agonist availability. Optimization of a polyplex for immunostimulant delivery would involve finding a "sweet spot", or a ratio that favors efficient internalization but also an interaction strength that allows release or availability of the agonist within the cell.

Notably, the CpG polyplexes produced similar trends between accessibility and TLR activation whereas TLR activation induced by polyI:C polyplexes did not reflect its accessibility trends. This suggests that polyI:C may have a weaker association with GA than CpG. In fact, TLR agonist accessibility evaluated after challenge with a competing charged molecule revealed that fully immobilized polyI:C polyplexes were quicker to release the immunostimulant over CpG polyplexes at the same ratios indicating a weaker polyplex interaction strength. Therefore, a possible explanation for the TLR activation trend of polyI:C polyplexes could be disassociation of the polyplexes in cell culture media resulting in activation similar to polyI:C alone. Previous studies have indicated that dsRNA resists condensation compared to DNA which could explain the differences in interaction strength and TLR agonist accessibility.[67-68] Overall, this data tells us that the polyplex interaction strength and TLR agonist accessibility are both important for TLR activation but are not necessarily directly related.

Model tissue retention studies provided evidence that net positively charged polyplexes could remain at the injection site longer than immunostimulant alone. Because of HA's negative charge, we

hypothesized that our net positively charged polyplexes would retain in the center of the well longer than polyI:C or CpG alone. These studies indicated that polyI:C polyplexes may have a weaker interaction strength than CpG polyplexes at the same mass ratio, a conclusion also drawn from the accessibility studies. Both polyI:C and CpG polyplexes showed increased retention with increase in ratio but CpG polyplexes displayed more pronounced retention capabilities. Taken together, while GA is able to condense both polyI:C and CpG into net positively charged particles, CpG polyplexes appeared to have a greater benefit to TLR activation and retention over polyI:C polyplexes.

CpG polyplexes were studied in an immunocompetent tumor model of HNSCC. Polyplexes and CpG showed highly significant and similar efficacy over mannitol and GA controls. Interestingly, the CpG alone exhibited the smallest tumor size. Evaluation of tumor infiltrating immune cells showed that polyplexes and CpG were able to induce immune cell migration into tumor in comparison to controls. Interestingly, the immune cells were mainly located around the periphery with minimal staining towards the center. This could likely be a result of lack of vasculature penetrating the tumor tissue. One theory to explain the differences in efficacy and immune infiltration seen with CpG alone over polyplexes could be that the availability of the CpG within the polyplex is effectively limiting the dose *in vivo*. However, while there may be slightly decreased efficacy, the increase in safety could mean the difference in being able to apply the immunostimulant in immunotherapy. Further work to understand the required potency and how complexation effects it would be needed.

While CpG alone did appear to have the greatest effect on tumor burden, the survival and tumor burden information do not account for potential systemic exposure and safety concerns. The free, unformulated CpG produced significantly greater systemic cytokines related to toxicity. Specifically, cytokine release syndrome (CRS), whose symptoms are frequently seen in clinical trials of immunotherapies, is associated with elevated levels of IL-6, IL-10, TNFα, and IFNγ.[37, 69] The elevated serum cytokines seen in treatment with CpG alone suggested that the polyplexes were retained at the injection site better than CpG alone. Previous studies examined CRS associated cytokines after CAR-T cell infusion immunotherapy. Patients exhibiting high grade CRS produced IL-6 that remained elevated whereas

IFNγ and IL-10 produced a more transient increase.[70-71] In this work, IFNγ and IL-2 levels in R4 and R6 increased between injection one and five whereas CpG did to a lesser degree. Along the same lines, for IL-12 and GM-CSF, R4 and R6 increase and CpG decreases between injection one and five. Overall, levels of IL-10, IFNγ, and IL-2 increase from injection one to injection five whereas IL-23 and IL-17 decrease. These trends may be useful in understanding the kinetics of cytokine induction after immunostimulant therapy but more time points would be needed to establish plausible kinetics.

5. Conclusion

Immunostimulants are potent tools in immunotherapeutic treatment of tumors, however, even in IT administration, systemic toxicity issues are of concern. Our studies found that FDA approved GA can complex with TLR agonist immunostimulants polyI:C and CpG. These polyplexes mitigated systemic markers of toxicity in comparison to free TLR agonists, demonstrating increased retention. TLR activation and diffusion in model tumor tissue were highly dependent on the TLR agonist accessibility and particle properties, which can be tuned by altering the ratio of GA to the TLR agonist polyanion. While GA formed a polyplex particle with both polyI:C and CpG, CpG polyplexes exhibited higher retention at the simulated injection site and enhanced TLR activation capabilities. These results demonstrate the importance of particle characteristics in terms of efficacy and retention ability. Particle formation and immobilization of immunostimulant are not the only requirements for subsequent TLR activation or retention; interaction strength of the polyplex plays a significant role. This work displayed a novel method of delivering immunostimulants but also highlighted the design factors that affect the function of polyplexes.

6. Figures

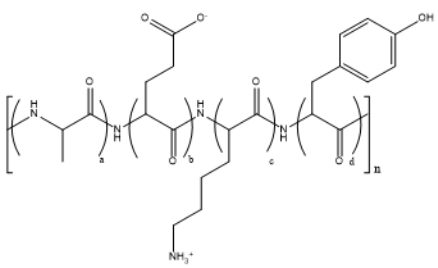

Symbol	Residue	Molar Ratio
a	L-alanine (A)	0.427
b	L-glutamic acid (E)	0.141
c	L-lysine (K)	0.338
d	L-tyrosine (T)	0.095

Figure 1. Glatiramer acetate chemical structure and the four naturally occurring amino acids at a fixed molar ratio.

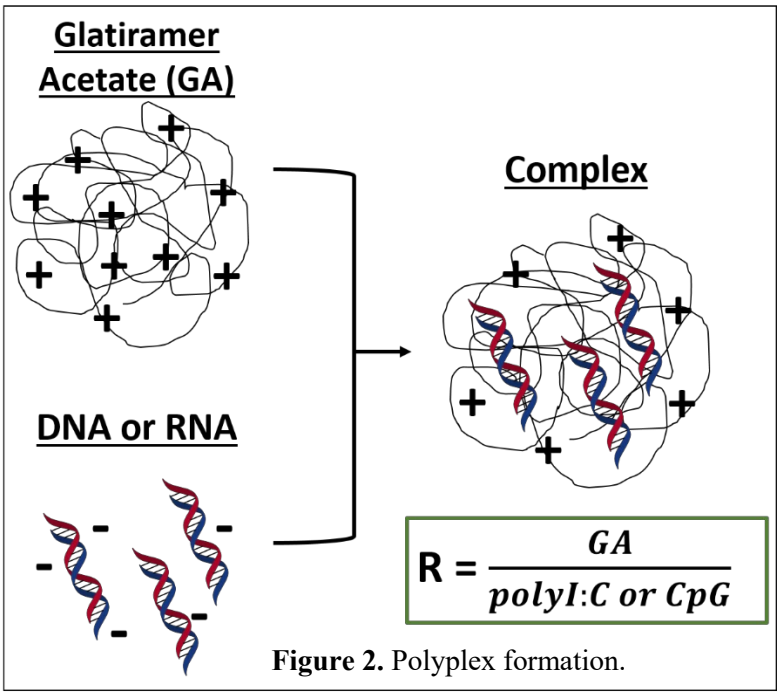

Figure 2. Polyplex formation.

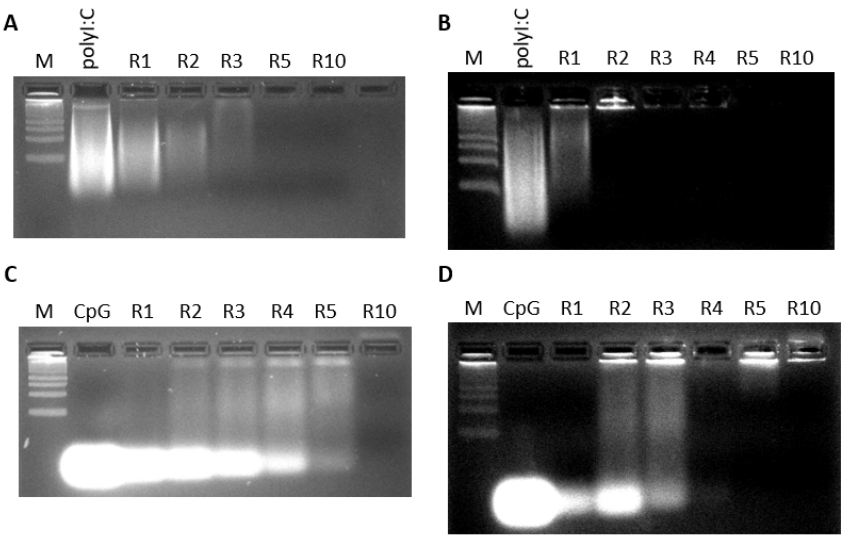

Figure 3. Agarose gel electrophoresis of varying mass ratios of (A) GA complexed with polyI:C in 1mM KCl pH ~5, (B) GA complexed with polyI:C in PBS diluted in KCl, pH~7, (C) GA complexed with CpG in 1mM KCl pH ~5, (B) GA complexed with CpG in PBS diluted in KCl, pH~7. Complexation is characterized by the DNA or RNA no longer being able to migrate through the gel due to complexation with GA. ("M" refers to the marker).

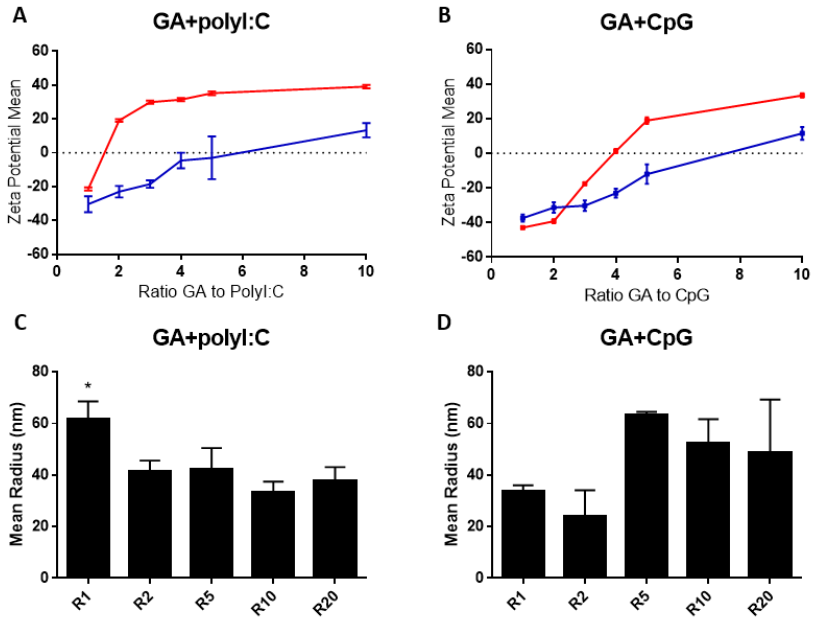

Figure 4. Zeta potential measurements of (A) GA+polyI:C and (B) GA+CpG polyplexes at pH 7 (blue) and pH 5 (red). Dynamic light scattering measurements of (C) GA+polyI:C and (D) GA+CpG polyplexes in 4% mannitol pH ~5.

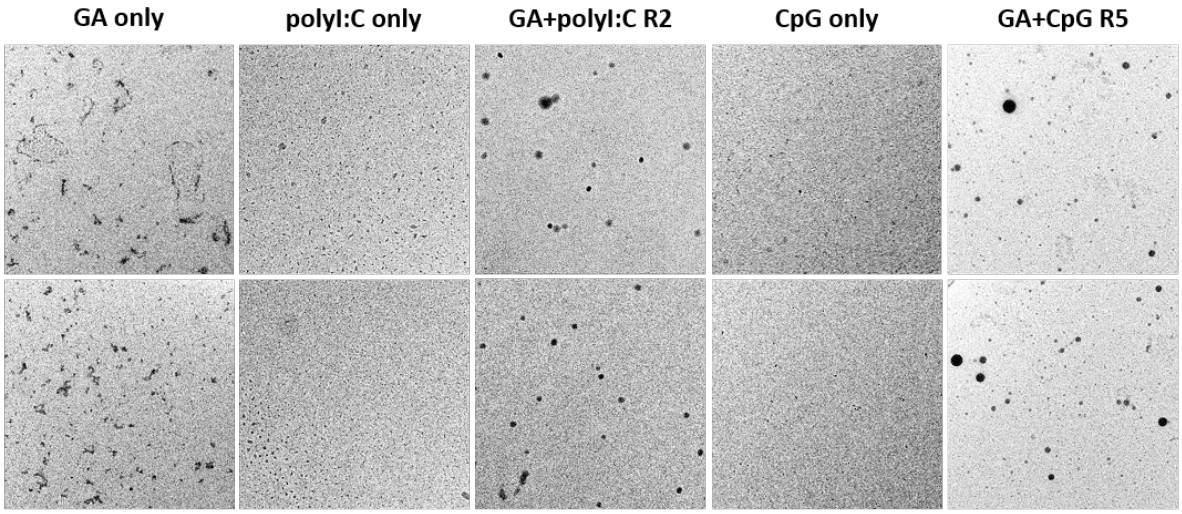

Figure 5. Transmission electron microscopy (TEM) of GA, polyI:C, GA+polyI:C R2 complex, CpG, and GA+CpG R5 polyplex. Frozen in liquid nitrogen prior to imaging — = 500 nm

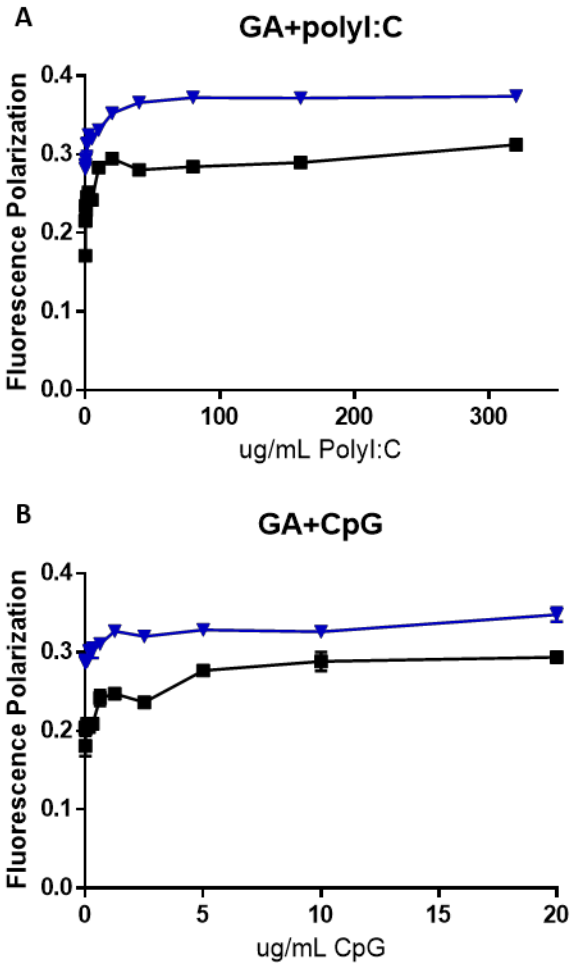

Figure 6. Fluorescence polarization measurements for (A) Rhodamine-GA+polyI:C and (B) Rhodamine-GA+CpG. Fluorescence excitation was 540 nm and emission was 620 nm. Polarization was calculated after subtracting signal produced by a standard of polyI:C or CpG at the same concentration.

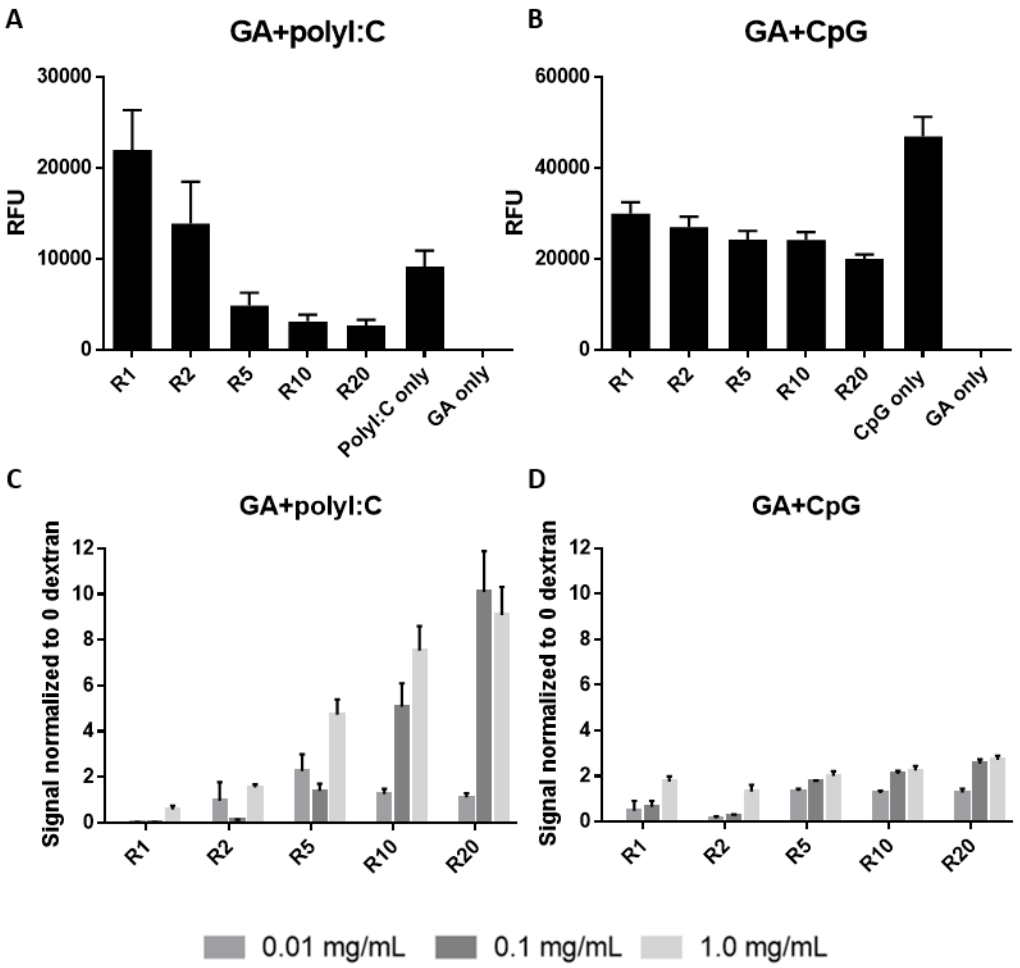

Figure 7. (A-B)DNA/RNA accessibility within the GA polyplex as determined by SYBR Gold staining. (C-D) SYBR Gold fluorescence of stained polyplexes after incubation with increasing concentrations of dextran sulfate. Fluorescence signal is normalized to the signal of the same polyplex at 0 mg/mL dextran sulfate.

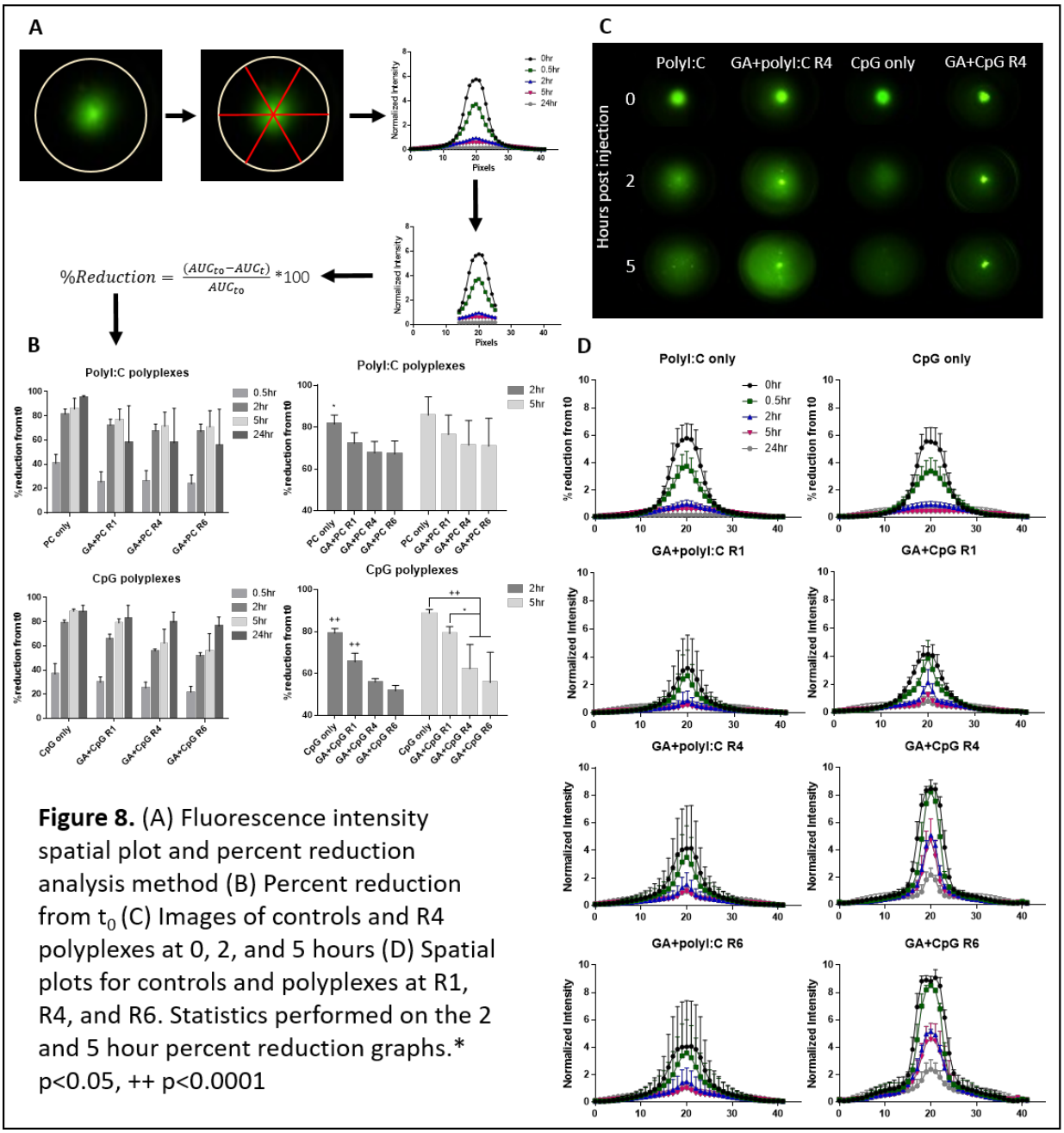

Figure 8. (A) Fluorescence intensity spatial plot and percent reduction analysis method (B) Percent reduction from t_0 (C) Images of controls and R4 polyplexes at 0, 2, and 5 hours (D) Spatial plots for controls and polyplexes at R1, R4, and R6. Statistics performed on the 2 and 5 hour percent reduction graphs.* $p<0.05$, ++ $p<0.0001$

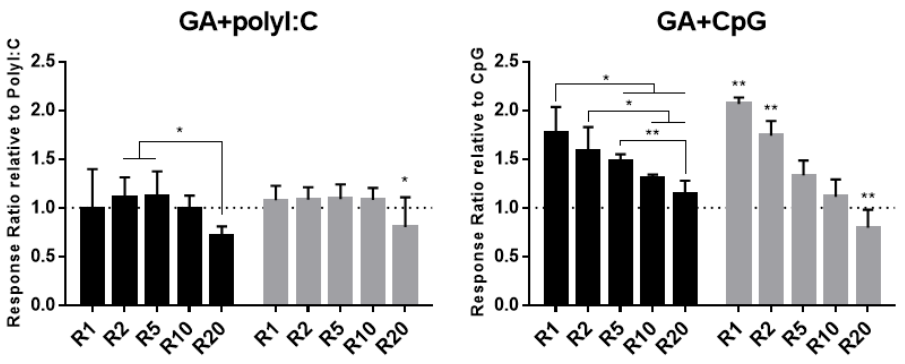

Figure 9. GA+PolyI:C or GA+CpG complexes incubated with HEK Blue hTLR3 or TLR9 respectively for 8 hours (black bars) and 20 hours (grey bars). Absorbance was read at 640 nm. Experiment was run three times with analytical duplicates or triplicates. Absorbance of sample wells were normalized to absorbance of the control (either PolyI:C or CpG). * p<0.05, ** p<0.01, + p<0.001, ++ p<0.0001. Bars with a single statistical symbol above means it is statistically different than every other sample.

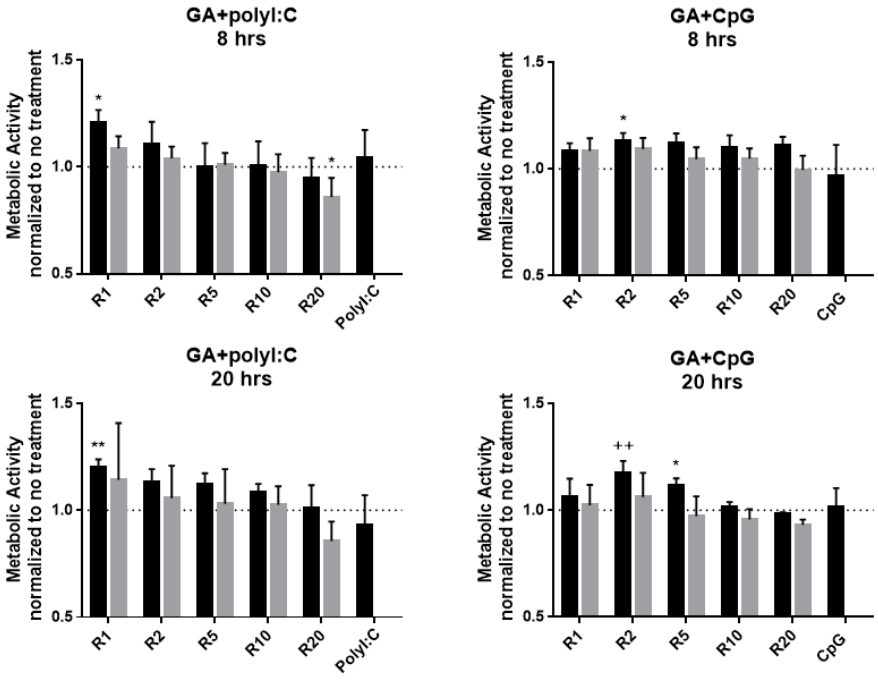

Figure 10. Resazurin assay with GA+PolyI:C or GA+CpG complexes incubated with HEK Blue hTLR3 or TLR9 respectively for 8 hours and 20 hours. Black bars are the complexes, grey bars are GA at the corresponding concentration. Absorbance of sample wells were normalized to absorbance of the untreated wells. Statistical comparisons are vs. untreated control (represented by the dotted line at 1). * p<0.05, ** p<0.01, + p<0.001, ++ p<0.0001

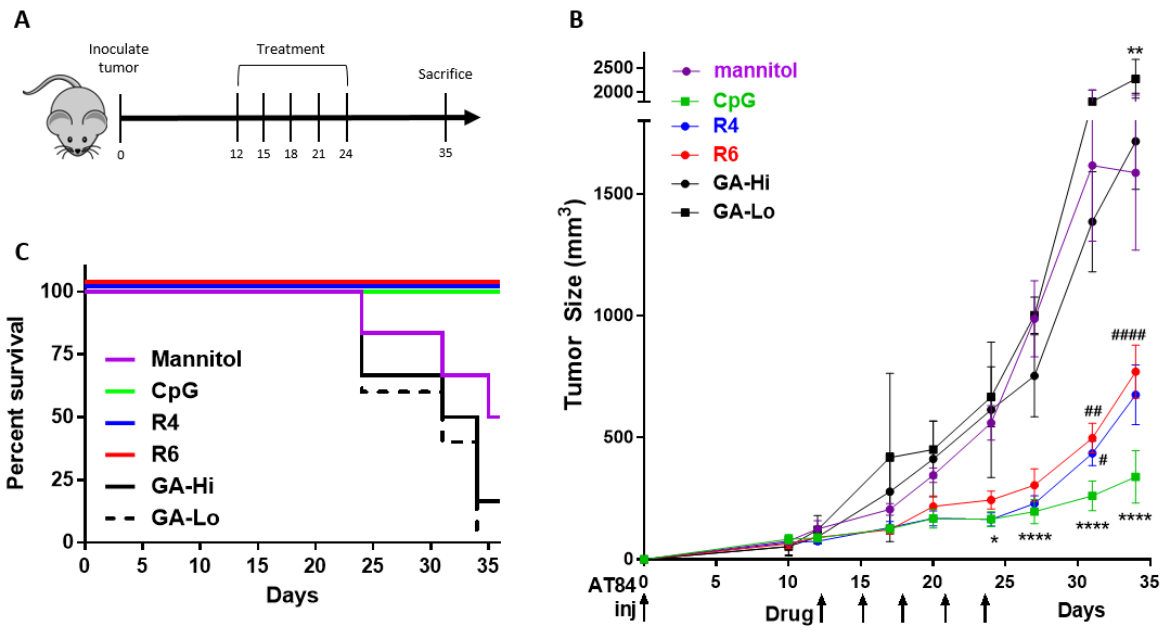

Figure 11. Intratumoral injection of complexes. (A) is a schematic treatment timeline. When tumors reached ~100 mm^3, generally 10-12 days after injection, mice were injected with either 4% mannitol, CpG, GA+CpG R4, GA+CpG R6, GA-high, or GA-low. (B) Survival curves. (C) Tumor burden curves for treatment groups. Statistics performed in relation to 4% mannitol control: **p<0.05, **p<0.01, ****p<0.0001.* Statistics performed between CpG and other treatment groups: *#p<0.05, ##p<0.01, ####p<0.0001.*

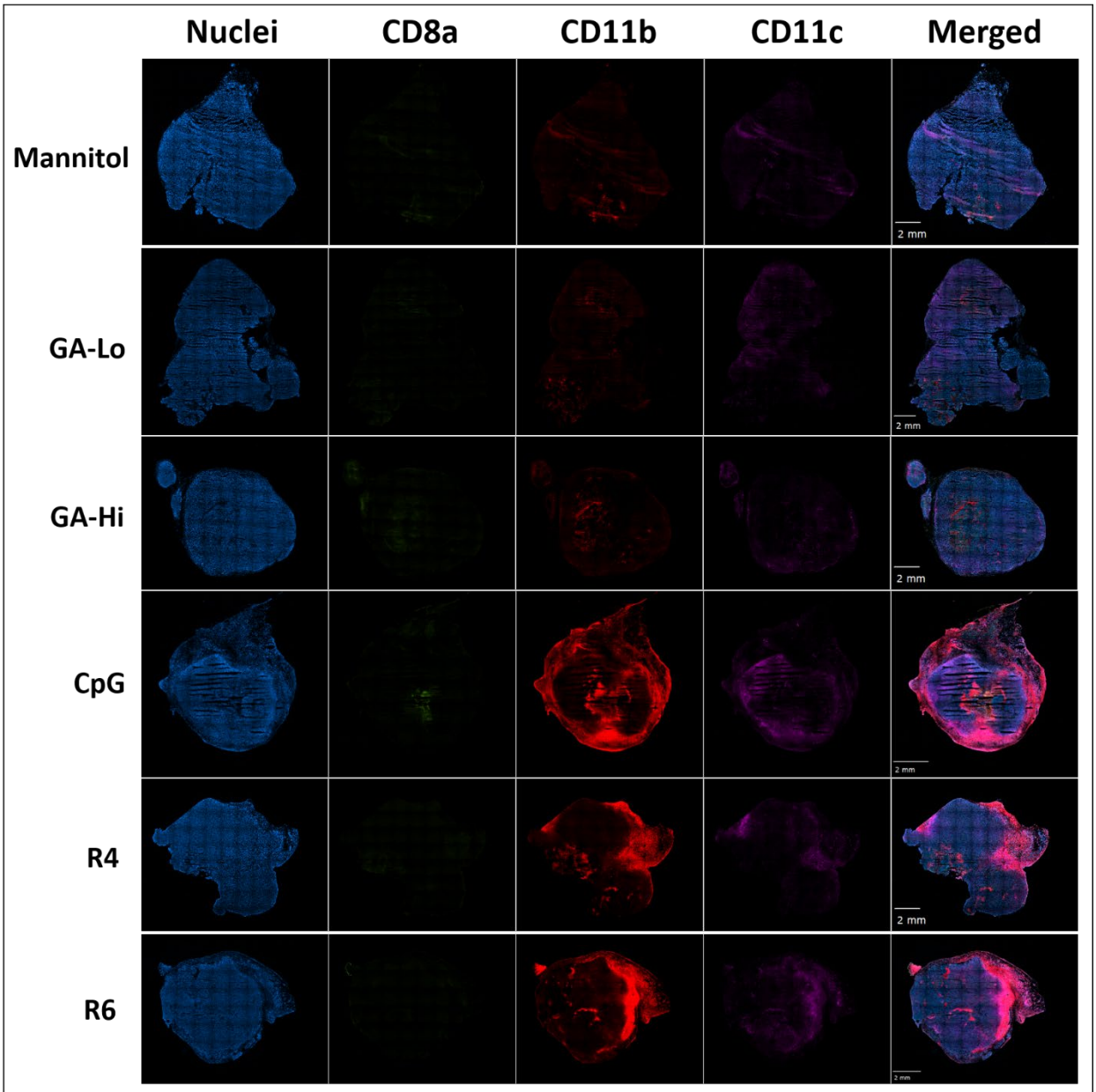

Figure 12. Tumor slices stained for nuclei, CD8a (cytotoxic T lymphocytes), CD11b (monocytes, granulocytes, macrophages, dendritic cells, NK cells, and some T and B cells), or CD11c (dendritic cells)

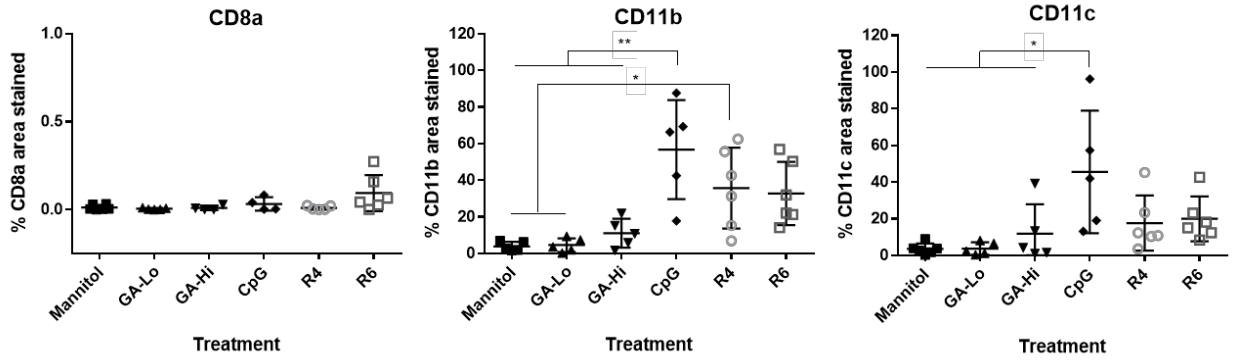

Figure 13. Quantification of tumor slice staining for CD8a (cytotoxic T lymphocytes), CD11b (monocytes, granulocytes, macrophages, dendritic cells, NK cells, and some T and B cells), and CD11c (dendritic cells). * p<0.05, ** p<0.01

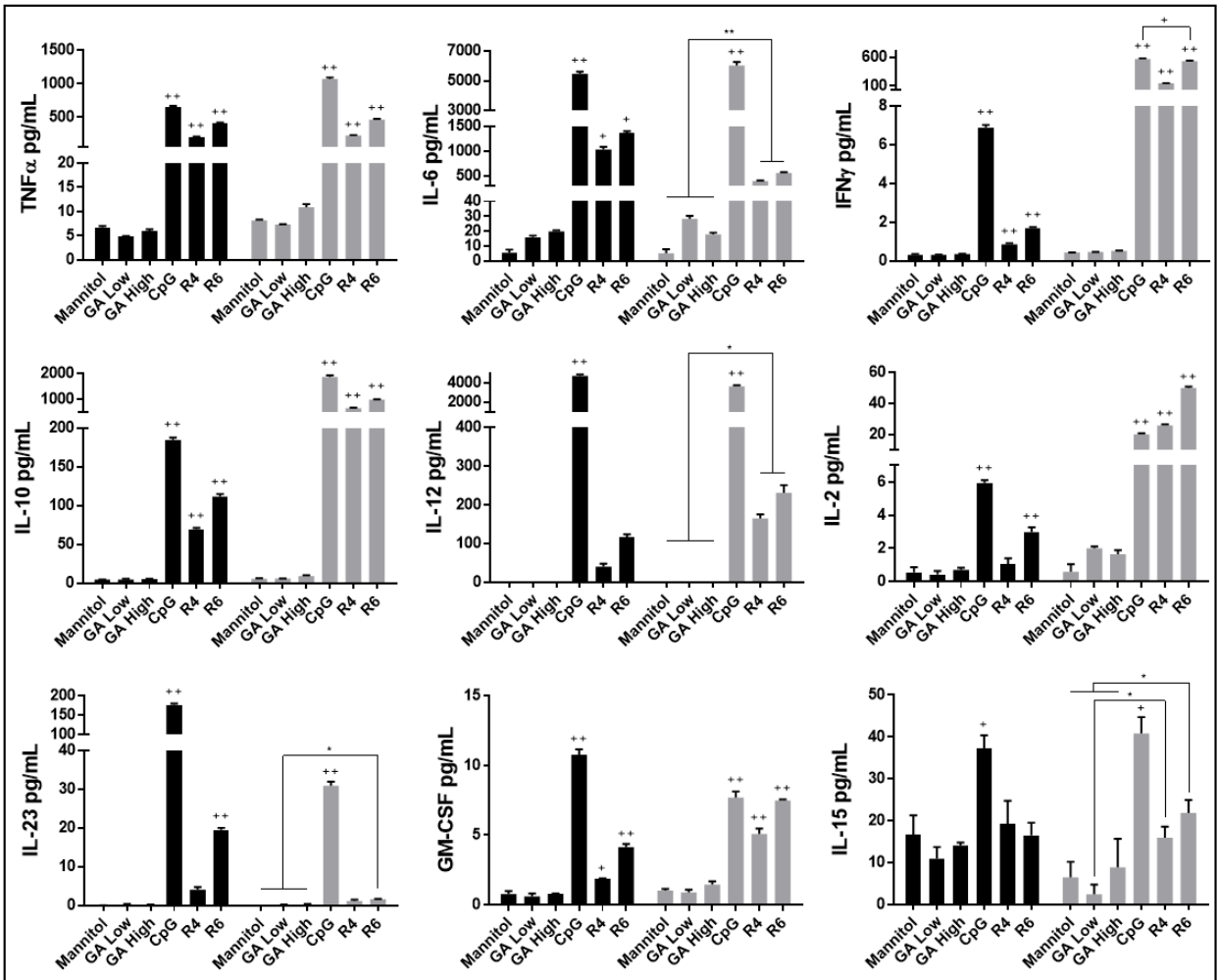

Figure 14. Mouse serum cytokines 2 hours after injection 1 (black bars) and after injection 5 (grey bars). * p<0.05, ** p<0.01, + p<0.001, ++ p<0.0001

7. Supplementary Figures

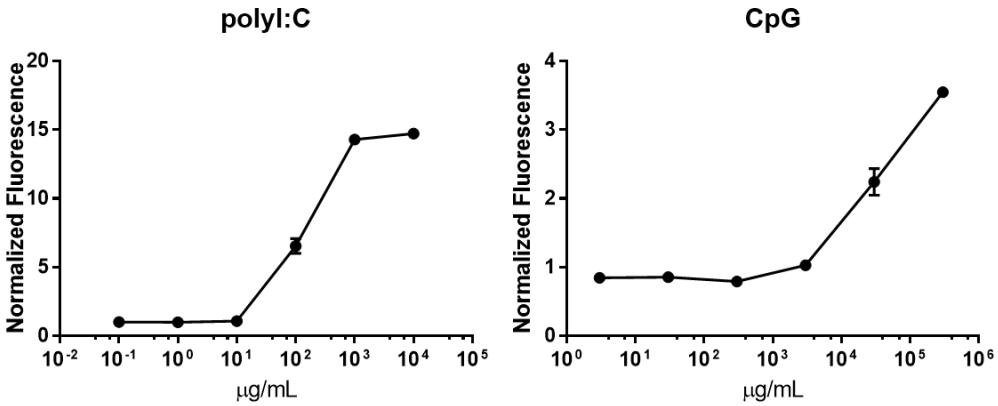

Supp. Figure 1. Concentration curves for polyI:C and CpG in HEK blue TLR3 and TLR9 reporter cells respectively.

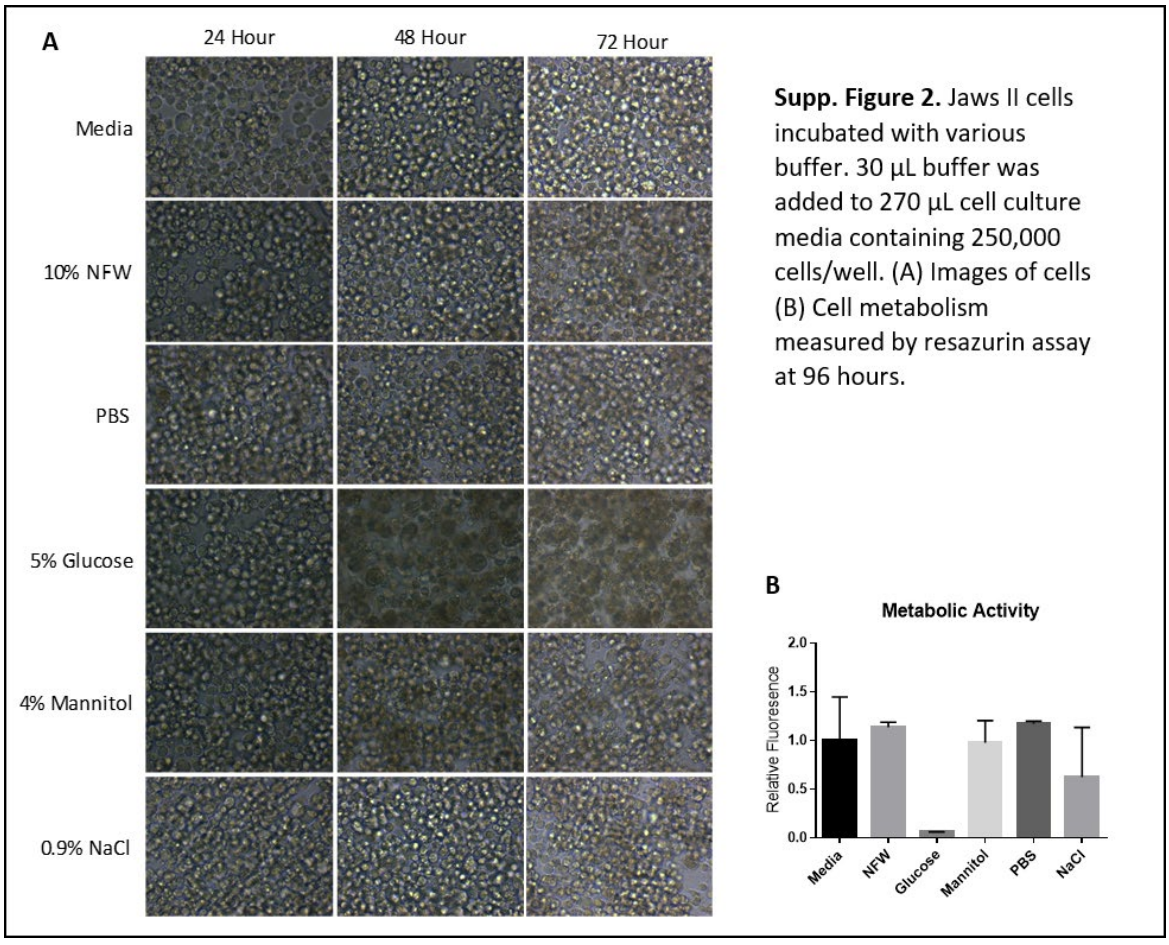

Supp. Figure 2. Jaws II cells incubated with various buffer. 30 µL buffer was added to 270 µL cell culture media containing 250,000 cells/well. (A) Images of cells (B) Cell metabolism measured by resazurin assay at 96 hours.

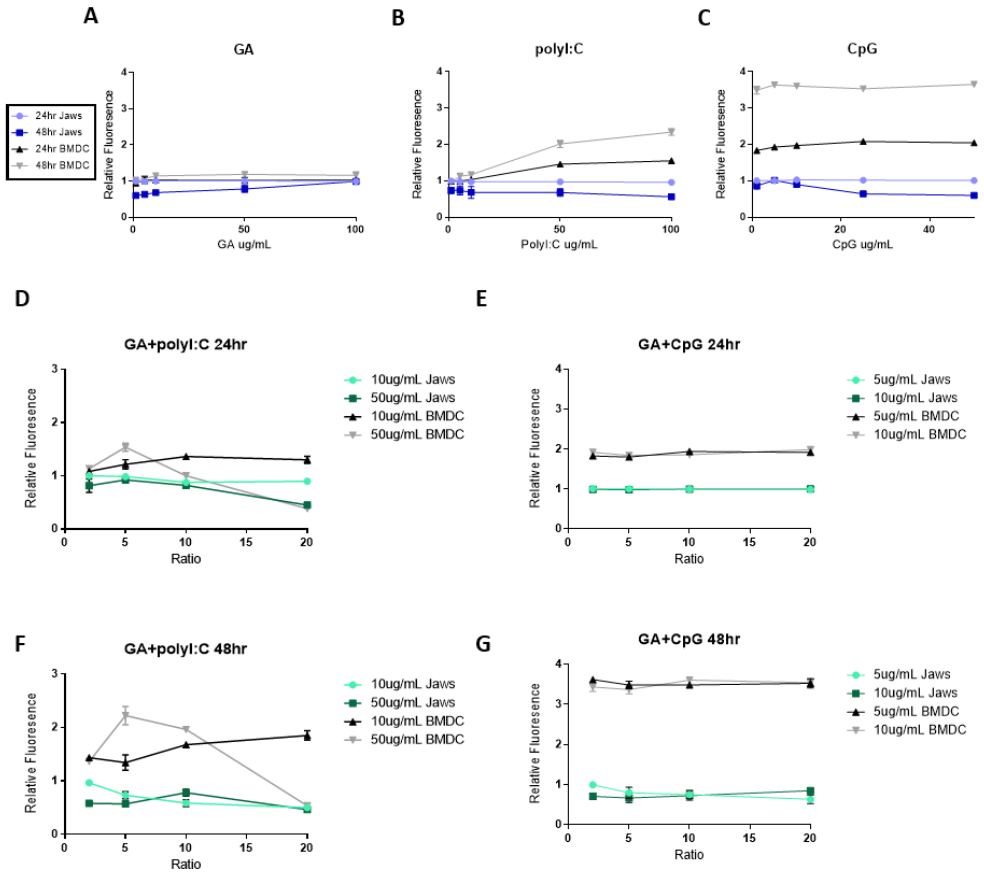

Supp. Figure 3. Normalized metabolic activity of Jaws II and BMDCs at 24 and 48 hours incubated with (A) GA, (B) PolyI:C, (C) CpG, (D) GA+PolyI:C complexes 24 hrs, and (E) GA+CpG complexes 24 hrs, (F) GA+PolyI:C complexes 48 hrs, (G) GA+CpG complexes 48 hrs.

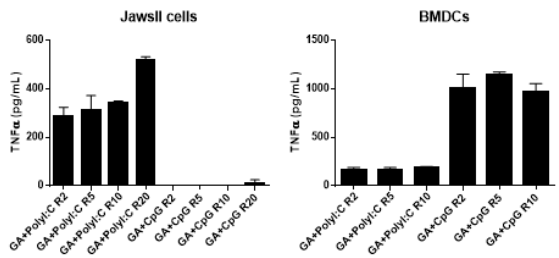

Supp. Figure 4. TNF-α expressions of (A) JawsII cells cultured with complexes for 48 hours, (B) Primary BMDCs cells cultured with complexes for 48 hours.

References

1. Coley, W. B., The Treatment of Inoperable Sarcoma by Bacterial Toxins (the Mixed Toxins of the Streptococcus erysipelas and the Bacillus prodigiosus). *Proceedings of the Royal Society of Medicine* **1910,** *3* (Surg Sect), 1-48.
2. Coley, W. B., THE TREATMENT OF INOPERABLE SARCOMA WITH THE MIXED TOXINS OF ERYSIPELAS AND BACILLUS PRODIGIOSUS.: IMMEDIATE AND FINAL RESULTS IN ONE HUNDRED AND FORTY CASES. *Journal of the American Medical Association* **1898,** *XXXI* (8), 389-395.
3. Institute, N. C. Immunotherapy to Treat Cancer. https://www.cancer.gov/about-cancer/treatment/types/immunotherapy.
4. Alatrash, G.; Jakher, H.; Stafford, P. D.; Mittendorf, E. A., Cancer immunotherapies, their safety and toxicity. *Expert Opinion on Drug Safety* **2013,** *12* (5), 631-645.
5. Mellman, I.; Coukos, G.; Dranoff, G., Cancer immunotherapy comes of age. *Nature* **2011,** *480*, 480.
6. Yang, L.; Yu, H.; Dong, S.; Zhong, Y.; Hu, S., Recognizing and managing on toxicities in cancer immunotherapy. *Tumor Biology* **2017,** *39* (3), 1010428317694542.
7. Schmidt, C., Clinical setbacks for toll-like receptor 9 agonists in cancer. *Nature Biotechnology* **2007,** *25*, 825.
8. Bonaventura, P.; Shekarian, T.; Alcazer, V.; Valladeau-Guilemond, J.; Valsesia-Wittmann, S.; Amigorena, S.; Caux, C.; Depil, S., Cold Tumors: A Therapeutic Challenge for Immunotherapy. *Frontiers in Immunology* **2019,** *10* (168).
9. Trujillo, J. A.; Sweis, R. F.; Bao, R.; Luke, J. J., T Cell–Inflamed versus Non-T Cell–Inflamed Tumors: A Conceptual Framework for Cancer Immunotherapy Drug Development and Combination Therapy Selection. *Cancer Immunology Research* **2018,** *6* (9), 990-1000.
10. Velcheti, V.; Schalper, K., Basic Overview of Current Immunotherapy Approaches in Cancer. *American Society of Clinical Oncology Educational Book* **2016,** (36), 298-308.
11. Junttila, M. R.; De Sauvage, F. J., Influence of tumour micro-environment heterogeneity on therapeutic response. *Nature* **2013,** *501*, 346.
12. Sriraman, S. K.; Aryasomayajula, B.; Torchilin, V. P., Barriers to drug delivery in solid tumors. *Tissue barriers* **2014,** *2*, e29528-e29528.
13. Nierkens, S.; Den Brok, M. H.; Roelofsen, T.; Wagenaars, J. a. L.; Figdor, C. G.; Ruers, T. J.; Adema, G. J., Route of Administration of the TLR9 Agonist CpG Critically Determines the Efficacy of Cancer Immunotherapy in Mice. *PLOS ONE* **2009,** *4* (12), e8368.
14. Temizoz, B.; Kuroda, E.; Ishii, K. J., Vaccine adjuvants as potential cancer immunotherapeutics. *International Immunology* **2016,** *28* (7), 329-338.
15. Ceravarix. https://www.fda.gov/vaccines-blood-biologics/vaccines/cervarix. FDA.
16. Smith, M.; García-Martínez, E.; Pitter, M. R.; Fucikova, J.; Spisek, R.; Zitvogel, L.; Kroemer, G.; Galluzzi, L., Trial Watch: Toll-like receptor agonists in cancer immunotherapy. *OncoImmunology* **2018,** *7* (12), e1526250.
17. Stalberg, C.; Loskog, A.; Klevenfeldt, M.; Essand, M.; Tötterman, T., *CpG Oligonucleotide Therapy Cures Subcutaneous and Orthotopic Tumors and Evokes Protective Immunity in Murine Bladder Cancer*. 2005; Vol. 28, p 20-7.
18. Salem, M. L.; Kadima, A. N.; Cole, D. J.; Gillanders, W. E., Defining the Antigen-Specific T-Cell Response to Vaccination and Poly(I:C)/TLR3 Signaling: Evidence of Enhanced Primary and Memory CD8 T-Cell Responses and Antitumor Immunity. *Journal of Immunotherapy* **2005,** *28* (3), 220-228.
19. Currie, A. J.; Van Der Most, R. G.; Broomfield, S. A.; Prosser, A. C.; Tovey, M. G.; Robinson, B. W. S., Targeting the Effector Site with IFN-αβ-Inducing TLR Ligands Reactivates Tumor-Resident CD8 T Cell Responses to Eradicate Established Solid Tumors. *The Journal of Immunology* **2008,** *180* (3), 1535-1544.
20. Bianchi, F.; Pretto, S.; Tagliabue, E.; Balsari, A.; Sfondrini, L., Exploiting poly(I:C) to induce cancer cell apoptosis. *Cancer Biology & Therapy* **2017,** *18* (10), 747-756.
21. Kumar, A.; Zhang, J.; Yu, F.-S. X., Toll-like receptor 3 agonist poly(I:C)-induced antiviral response in human corneal epithelial cells. *Immunology* **2006,** *117* (1), 11-21.
22. Matsumoto, M.; Tatematsu, M.; Nishikawa, F.; Azuma, M.; Ishii, N.; Morii-Sakai, A.; Shime, H.; Seya, T., Defined TLR3-specific adjuvant that induces NK and CTL activation without significant cytokine production in vivo. *Nature Communications* **2015,** *6*, 6280.
23. Oncovir, I., Oncovir. 2019.
24. Krieg, A. M.; Yi, A.-K.; Matson, S.; Waldschmidt, T. J.; Bishop, G. A.; Teasdale, R.; Koretzky, G. A.; Klinman, D. M., CpG motifs in bacterial DNA trigger direct B-cell activation. *Nature* **1995,** *374* (6522), 546-549.
25. Pharmaceuticals, C., Technology.
26. Ngwa, W.; Irabor, O. C.; Schoenfeld, J. D.; Hesser, J.; Demaria, S.; Formenti, S. C., Using immunotherapy to boost the abscopal effect. *Nature Reviews Cancer* **2018,** *18*, 313.
27. Shmueli, R. B.; Anderson, D. G.; Green, J. J., Electrostatic surface modifications to improve gene delivery. *Expert Opinion on Drug Delivery* **2010,** *7* (4), 535-550.
28. Baoum, A.; Ovcharenko, D.; Berkland, C., Calcium condensed cell penetrating peptide complexes offer highly efficient, low toxicity gene silencing. *International Journal of Pharmaceutics* **2012,** *427* (1), 134-142.
29. Démoulins, T.; Ebensen, T.; Schulze, K.; Englezou, P. C.; Pelliccia, M.; Guzmán, C. A.; Ruggli, N.; Mccullough, K. C., Self-replicating RNA vaccine functionality modulated by fine-tuning of polyplex delivery vehicle structure. *Journal of Controlled Release* **2017,** *266*, 256-271.

30. Peine, K. J.; Bachelder, E. M.; Vangundy, Z.; Papenfuss, T.; Brackman, D. J.; Gallovic, M. D.; Schully, K.; Pesce, J.; Keane-Myers, A.; Ainslie, K. M., Efficient Delivery of the Toll-like Receptor Agonists Polyinosinic:Polycytidylic Acid and CpG to Macrophages by Acetalated Dextran Microparticles. *Molecular Pharmaceutics* **2013,** *10* (8), 2849-2857.
31. Chen, J.; Wang, K.; Wu, J.; Tian, H.; Chen, X., Polycations for Gene Delivery: Dilemmas and Solutions. *Bioconjugate Chemistry* **2019,** *30* (2), 338-349.
32. Alhakamy, N. A.; Berkland, C. J., Glatiramer Acetate (Copaxone) is a Promising Gene Delivery Vector. *Molecular Pharmaceutics* **2019,** *16* (4), 1596-1605.
33. Song, J. Y.; Larson, N. R.; Thati, S.; Torres-Vazquez, I.; Martinez-Rivera, N.; Subelzu, N. J.; Leon, M. A.; Rosa-Molinar, E.; Schöneich, C.; Forrest, M. L.; Middaugh, C. R.; Berkland, C. J., Glatiramer acetate persists at the injection site and draining lymph nodes via electrostatically-induced aggregation. *Journal of Controlled Release* **2019,** *293*, 36-47.
34. Kinnunen, H. M.; Sharma, V.; Contreras-Rojas, L. R.; Yu, Y.; Alleman, C.; Sreedhara, A.; Fischer, S.; Khawli, L.; Yohe, S. T.; Bumbaca, D.; Patapoff, T. W.; Daugherty, A. L.; Mrsny, R. J., A novel in vitro method to model the fate of subcutaneously administered biopharmaceuticals and associated formulation components. *Journal of Controlled Release* **2015,** *214*, 94-102.
35. Kinnunen, H. M.; Mrsny, R. J., Improving the outcomes of biopharmaceutical delivery via the subcutaneous route by understanding the chemical, physical and physiological properties of the subcutaneous injection site. *Journal of Controlled Release* **2014,** *182*, 22-32.
36. Zapała, Ł.; Drela, N.; Bil, J.; Nowis, D.; Basak, G.; Lasek, W., Optimization of activation requirements of immature mouse dendritic JAWSII cells for in vivo application. *Oncology reports* **2011,** *25*, 831-40.
37. Milling, L.; Zhang, Y.; Irvine, D. J., Delivering safer immunotherapies for cancer. *Advanced drug delivery reviews* **2017,** *114*, 79-101.
38. Marabelle, A.; Andtbacka, R.; Harrington, K.; Melero, I.; Leidner, R.; De Baere, T.; Robert, C.; Ascierto, P. A.; Baurain, J. F.; Imperiale, M.; Rahimian, S.; Tersago, D.; Klumper, E.; Hendriks, M.; Kumar, R.; Stern, M.; Öhrling, K.; Massacesi, C.; Tchakov, I.; Tse, A.; Douillard, J. Y.; Tabernero, J.; Haanen, J.; Brody, J., Starting the fight in the tumor: expert recommendations for the development of human intratumoral immunotherapy (HIT-IT). *Annals of Oncology* **2018,** *29* (11), 2163-2174.
39. Lynn, G. M.; Laga, R.; Darrah, P. A.; Ishizuka, A. S.; Balaci, A. J.; Dulcey, A. E.; Pechar, M.; Pola, R.; Gerner, M. Y.; Yamamoto, A.; Buechler, C. R.; Quinn, K. M.; Smelkinson, M. G.; Vanek, O.; Cawood, R.; Hills, T.; Vasalatiy, O.; Kastenmüller, K.; Francica, J. R.; Stutts, L.; Tom, J. K.; Ryu, K. A.; Esser-Kahn, A. P.; Etrych, T.; Fisher, K. D.; Seymour, L. W.; Seder, R. A., In vivo characterization of the physicochemical properties of polymer-linked TLR agonists that enhance vaccine immunogenicity. *Nature Biotechnology* **2015,** *33* (11), 1201-1210.
40. Mullins, S. R.; Vasilakos, J. P.; Deschler, K.; Grigsby, I.; Gillis, P.; John, J.; Elder, M. J.; Swales, J.; Timosenko, E.; Cooper, Z.; Dovedi, S. J.; Leishman, A. J.; Luheshi, N.; Elvecrog, J.; Tilahun, A.; Goodwin, R.; Herbst, R.; Tomai, M. A.; Wilkinson, R. W., Intratumoral immunotherapy with TLR7/8 agonist MEDI9197 modulates the tumor microenvironment leading to enhanced activity when combined with other immunotherapies. *J Immunother Cancer* **2019,** *7* (1), 244.
41. Kim, S.-Y.; Heo, M. B.; Hwang, G.-S.; Jung, Y.; Choi, D. Y.; Park, Y.-M.; Lim, Y. T., Multivalent Polymer Nanocomplex Targeting Endosomal Receptor of Immune Cells for Enhanced Antitumor and Systemic Memory Response. *Angewandte Chemie International Edition* **2015,** *54* (28), 8139-8143.
42. Albershardt, T. C.; Parsons, A. J.; Berglund, P.; Ter Meulen, J., Intratumoral injections of G100 (synthetic TLR4 agonist) increase trafficking of lentiviral vector-induced antigen-specific CD8 T cells to the tumor microenvironment. *J Immunother Cancer* **2015,** *3* (Suppl 2), P290-P290.
43. Schmidt, M.; Hagner, N.; Marco, A.; König-Merediz, S. A.; Schroff, M.; Wittig, B., Design and Structural Requirements of the Potent and Safe TLR-9 Agonistic Immunomodulator MGN1703. *Nucleic Acid Ther* **2015,** *25* (3), 130-140.
44. Cornfield, M. J. In *IMO-2125, an investigational intratumoral tolllike receptor 9 agonist, modulates the tumor microenvironment to enhance anti-tumor immunity*, Society for Immunotherapy of Cancer, National Harbor, MD, November 9, 2016; Pharmaceuticals, I., Ed. National Harbor, MD, 2016.
45. Bioncotech, BO-112: a Potent Immunotherapy.
46. Alhakamy, N. A.; Berkland, C. J., Polyarginine Molecular Weight Determines Transfection Efficiency of Calcium Condensed Complexes. *Molecular Pharmaceutics* **2013,** *10* (5), 1940-1948.
47. Hall, A.; Lächelt, U.; Bartek, J.; Wagner, E.; Moghimi, S. M., Polyplex Evolution: Understanding Biology, Optimizing Performance. *Molecular Therapy* **2017,** *25* (7), 1476-1490.
48. Dow, S., Liposome-nucleic acid immunotherapeutics. *Expert opinion on drug delivery* **2008,** *5* (1), 11-24.
49. Zaks, K.; Jordan, M.; Guth, A.; Sellins, K.; Kedl, R.; Izzo, A.; Bosio, C.; Dow, S., Efficient Immunization and Cross-Priming by Vaccine Adjuvants Containing TLR3 or TLR9 Agonists Complexed to Cationic Liposomes. *The Journal of Immunology* **2006,** *176* (12), 7335-7345.
50. Wiethoff, C. M.; Middaugh, C. R., Barriers to Nonviral Gene Delivery. *Journal of Pharmaceutical Sciences* **2003,** *92* (2), 203-217.
51. Fu, J.; Cai, J.; Ling, G.; Li, A.; Zhao, J.; Guo, X.; Zhang, P., Cationic polymers for enhancing CpG oligodeoxynucleotides-mediated cancer immunotherapy. *European Polymer Journal* **2019,** *113*, 115-132.
52. Han, J.; Kim, S. K.; Cho, T.-S.; Lee, J.-C., Effect of molecular weights of polyethyleneimine on the polyplex formation with calf thymus DNA. *Macromolecular Research* **2004,** *12* (3), 276-281.

53. Monnery, B. D.; Wright, M.; Cavill, R.; Hoogenboom, R.; Shaunak, S.; Steinke, J. H. G.; Thanou, M., Cytotoxicity of polycations: Relationship of molecular weight and the hydrolytic theory of the mechanism of toxicity. *International Journal of Pharmaceutics* **2017,** *521* (1), 249-258.
54. Foged, C.; Brodin, B.; Frokjaer, S.; Sundblad, A., Particle size and surface charge affect particle uptake by human dendritic cells in an in vitro model. *International Journal of Pharmaceutics* **2005,** *298* (2), 315-322.
55. Jia, J.; Zhang, Y.; Xin, Y.; Jiang, C.; Yan, B.; Zhai, S., Interactions Between Nanoparticles and Dendritic Cells: From the Perspective of Cancer Immunotherapy. *Front Oncol* **2018,** *8*, 404-404.
56. Bookstaver, M. L.; Tsai, S. J.; Bromberg, J. S.; Jewell, C. M., Improving Vaccine and Immunotherapy Design Using Biomaterials. *Trends Immunol* **2018,** *39* (2), 135-150.
57. Tang, L.; Yang, X.; Yin, Q.; Cai, K.; Wang, H.; Chaudhury, I.; Yao, C.; Zhou, Q.; Kwon, M.; Hartman, J. A.; Dobrucki, I. T.; Dobrucki, L. W.; Borst, L. B.; Lezmi, S.; Helferich, W. G.; Ferguson, A. L.; Fan, T. M.; Cheng, J., Investigating the optimal size of anticancer nanomedicine. *Proceedings of the National Academy of Sciences* **2014,** *111* (43), 15344-15349.
58. Bao, A.; Phillips, W. T.; Goins, B.; Zheng, X.; Sabour, S.; Natarajan, M.; Ross Woolley, F.; Zavaleta, C.; Otto, R. A., Potential use of drug carried-liposomes for cancer therapy via direct intratumoral injection. *International Journal of Pharmaceutics* **2006,** *316* (1), 162-169.
59. Shang, L.; Nienhaus, K.; Nienhaus, G. U., Engineered nanoparticles interacting with cells: size matters. *J Nanobiotechnology* **2014,** *12*, 5-5.
60. Lee, H.; Fonge, H.; Hoang, B.; Reilly, R. M.; Allen, C., The Effects of Particle Size and Molecular Targeting on the Intratumoral and Subcellular Distribution of Polymeric Nanoparticles. *Molecular Pharmaceutics* **2010,** *7* (4), 1195-1208.
61. Carmona-Ribeiro, A. M., Cationic Nanostructures for Vaccines, Immune Response Activation. Guy Huynh Thien Duc, IntechOpen, 2014.
62. Nomura, T.; Koreeda, N.; Yamashita, F.; Takakura, Y.; Hashida, M., Effect of particle size and charge on the disposition of lipid carriers after intratumoral injection into tissue-isolated tumors. *Pharmaceutical research* **1998,** *15* (1), 128-32.
63. Nomura, T.; Saikawa, A.; Morita, S.; Sakaeda, T.; Yamashita, F.; Honda, K.; Yoshinobu, T.; Hashida, M., Pharmacokinetic characteristics and therapeutic effects of mitomycin C-dextran conjugates after intratumoural injection. *Journal of Controlled Release* **1998,** *52* (3), 239-252.
64. Birch, N. P.; Schiffman, J. D., Characterization of Self-Assembled Polyelectrolyte Complex Nanoparticles Formed from Chitosan and Pectin. *Langmuir* **2014,** *30* (12), 3441-3447.
65. Snapper, C. M., Distinct Immunologic Properties of Soluble Versus Particulate Antigens. *Frontiers in immunology* **2018,** *9*, 598-598.
66. Tsai, S. J.; Andorko, J. I.; Zeng, X.; Gammon, J. M.; Jewell, C. M., Polyplex interaction strength as a driver of potency during cancer immunotherapy. *Nano Research* **2018,** *11* (10), 5642-5656.
67. Tolokh, I. S.; Pabit, S. A.; Katz, A. M.; Chen, Y.; Drozdetski, A.; Baker, N.; Pollack, L.; Onufriev, A. V., Why double-stranded RNA resists condensation. *Nucleic Acids Res* **2014,** *42* (16), 10823-10831.
68. Li, L.; Pabit, S. A.; Meisburger, S. P.; Pollack, L., Double-stranded RNA resists condensation. *Phys Rev Lett* **2011,** *106* (10), 108101-108101.
69. Shimabukuro-Vornhagen, A.; Gödel, P.; Subklewe, M.; Stemmler, H. J.; Schlößer, H. A.; Schlaak, M.; Kochanek, M.; Böll, B.; Von Bergwelt-Baildon, M. S., Cytokine release syndrome. *J Immunother Cancer* **2018,** *6* (1), 56.
70. Teachey, D. T.; Lacey, S. F.; Shaw, P. A.; Melenhorst, J. J.; Maude, S. L.; Frey, N.; Pequignot, E.; Gonzalez, V. E.; Chen, F.; Finklestein, J.; Barrett, D. M.; Weiss, S. L.; Fitzgerald, J. C.; Berg, R. A.; Aplenc, R.; Callahan, C.; Rheingold, S. R.; Zheng, Z.; Rose-John, S.; White, J. C.; Nazimuddin, F.; Wertheim, G.; Levine, B. L.; June, C. H.; Porter, D. L.; Grupp, S. A., Identification of Predictive Biomarkers for Cytokine Release Syndrome after Chimeric Antigen Receptor T-cell Therapy for Acute Lymphoblastic Leukemia. *Cancer Discovery* **2016,** *6* (6), 664-679.
71. Hay, K. A.; Hanafi, L.-A.; Li, D.; Gust, J.; Liles, W. C.; Wurfel, M. M.; López, J. A.; Chen, J.; Chung, D.; Harju-Baker, S.; Cherian, S.; Chen, X.; Riddell, S. R.; Maloney, D. G.; Turtle, C. J., Kinetics and biomarkers of severe cytokine release syndrome after CD19 chimeric antigen receptor-modified T-cell therapy. *Blood* **2017,** *130* (21), 2295-2306.

Chapter 4:
Conclusions and Future Directions

1. Conclusions

While traditional cancer treatments like radiation and chemotherapy directly kill cancer cells, cancer immunotherapy trains the body to fight its own cancer and can create lasting immune responses. Immunotherapy approaches aim to overcome the immune suppression established by the tumor microenvironment by activating an innate immune response. Activation of an innate immune response can be accomplished by delivering PAMPs, cytokines, viruses, targeted mAbs, or autologous engineered immune cells. For most immunostimulant therapies, the activation is non-specific therefore, immunostimulants should be delivered in the presence of tumor antigen so as not to cause improper immune activation towards healthy tissue. Furthermore, the use of local immunostimulants can induce the infiltration of immune cells into the tumor therefore increasing the efficacy of therapies like anti- PD-1 or anti-PD-L1 checkpoint inhibitors whose activity is dependent on interactions between tumor cells and immune cells. Traditional, systemic administration of immunostimulants has generated adverse events associated with systemic toxicity which are most commonly flu like symptoms or symptoms related to cytokine release syndrome (CRS). Local delivery can circumvent trafficking barriers and should reduce the systemic toxicity seen with systemic administration, however, clinical trials with intratumoral immunostimulants indicate that local delivery itself is not enough to prevent systemic toxicity events. Diffusion, or trafficking out of the tumor injection site and into systemic circulation can lead to similar adverse events seen with systemic administration. Many approaches have focused on modifications of therapy or formulations that have led to increased efficacy after IT injection, but few have directed strategies at increasing retention at the injection site.

Chapter 1, reviewed the intratumoral cancer therapies currently in human clinical trials with discussions on the effects of therapy and formulation characteristics on the safety and efficacy. While it was difficult to make correlations, it was concluded that therapies with modified active or therapies formulated into a particle or emulsion tended to have better safety profiles presumably because of increased retention after injection.

This dissertation focuses on delivery strategies for two negatively charged TLR agonists polyI:C and CpG which are highly explored as immunostimulants in cancer immunotherapy. Both compounds exhibit strong induction of interferons, leading to a proinflammatory environment after binding to TLRs, thus generating memory and tumor-specific T cells.[1-3] PolyI:C is a double-stranded (ds) RNA mimic and TLR3 agonist that has shown both antiviral and anticancer activity.[4-5] CpG is a short, single-stranded synthetic oligonucleotide and TLR9 agonist that contains multiple, unmethylated cytosine-phosphate-guanine motifs, which mimic bacterial DNA.[6] Notably, both polyI:C and CpG are agonists to an intracellular TLR and therefore require endocytosis. To achieve both goals of increased retention and intracellular delivery, polycations were selected as a delivery tool. Polycations have historically been employed for intracellular delivery of nucleic acid material[7-10] and this work suggests that electrostatics can aid in injection site retention through interactions with highly negatively charged extracellular matrix (ECM).

Chapter 2 explored the use of poly-L-lysine (PLL) as a polycationic delivery vehicle for negatively charged immunostimulants polyI:C and CpG to aid in injection site retention and for minimized systemic exposure. We evaluated polyplexes of the polycation PLL with polyanionic TLR agonists. Specifically, the relationship between PLL molecular weight and complex formation, TLR activation, and retention in a simulated tumor microenvironment was explored.

TLR activation was largely driven by the MW of PLL followed by the accessibility of the immunostimulant within the polyplex. Retention was also driven by these factors but in an opposite manner. Taken together, there is likely an optimal window of polycation MW and ratio that favors TLR activation and retention without causing toxicity. For CpG polyplexes, K9 through K50 was ideal for limiting cytotoxicity but higher MW was best for retention. Furthermore, this work supported with the hypothesis that particle formation is critical for immune activation and retention.[11] These findings illustrate the potential use of polycations for carrier vehicles that not only aid in intracellular delivery but also contribute to injection site retention. The characterization results in this work suggest that PLL + CpG polyplexes may be a good candidate for increased intracellular delivery and decreased transport away from the tumor.

Chapter 3 developed and researched the novel idea of using an FDA approved, and safe drug called Glatiramer Acetate (GA) or Copaxone® as a delivery tool for negatively charged immunostimulants polyI:C and CpG. The studies found that GA can complex with TLR agonist immunostimulants polyI:C and CpG with consistent size and tunable charge. In a mouse tumor model, these polyplexes mitigated systemic markers of toxicity in comparison to free TLR agonists, demonstrating increased retention. TLR activation and diffusion in model tumor tissue were highly dependent on the TLR agonist accessibility and particle properties, which can be tuned by altering the ratio of GA to the TLR agonist polyanion. While GA formed a polyplex particle with both polyI:C and CpG, CpG polyplexes exhibited higher retention at the simulated injection site and enhanced TLR activation capabilities. These results demonstrate the importance of particle characteristics in terms of efficacy and retention ability. Particle formation and immobilization of immunostimulant are not the only requirements for subsequent TLR activation or retention; interaction strength of the polyplex plays a significant role. This work

displayed a novel method of delivering immunostimulants but also highlighted the design factors that affect the function of polyplexes.

To conclude, the data in this dissertation demonstrates the use of polycations as delivery tools in cancer immunotherapy for not only increasing intracellular delivery, but also for increasing injection site retention through electrostatic interactions with extracellular matrix. These polyplexes offer a promising therapeutic approach for decreasing systemic toxicity generated by immunostimulants. Upon consideration of the results from both chapters, one could speculate that the charge density, and presence of different types of residues on the polycation (the differences between PLL and GA) may have a significant influence on the ability to create a particle, cytotoxicity level, and ability to increase TLR activation *in vitro*. Previous studies from the Berkland lab have suggested a similar hypotheses that the anionic, cationic, and hydrophobic amino acids of GA may aid in transfection efficiency in comparison to PLL.[12] Furthermore, a balance of hydrophobic and positively charged domains has been seen to be important for penetration of cell-penetrating peptides used for intracellular delivery.[13-15] In addition to the type of polycation, polyplex particle formation, retention ability, and TLR activation ability varied based on the type of immunostimulant used. In both chapters this seemed to be driven by different interaction strengths but could also be due to structural arrangement of the polyplex. Overall, the approved and safe drug, GA was a highly effective at complexing and delivering negatively charged immunostimulants in comparison to PLL, a polycation routinely utilized for delivery of nucleic acid material. In tumor studies the GA + CpG polyplexes exhibited marked tumor burden reduction and were able to reduce levels of systemic pro-inflammatory cytokines in comparison to CpG alone suggesting increased injection site retention. Efficient and safe

delivery of immunostimulants will be a powerful tool for cancer immunotherapy and could either be administered alone or in synergy with checkpoint inhibitor mAbs to increase their efficacy.

2. Future Directions

These studies demonstrate the encouraging potential use of polycations in local injection site retention for negatively charged immunostimulants which would otherwise cause systemic toxicity, however, there are many aspects that remain to be explored. Future studies should focus on optimizing the components and composition of the polyplex such that the polyplex interaction strength allows for efficient TLR activation, the biophysical characteristics strengthen the retention and intracellular delivery, and cellular toxicity is minimized. Further, a better understanding of GA polyplexes enhanced ability to activate TLR over PLL polyplexes may aid in design of future polycations for immunostimulant delivery. Finally, more *in vitro* and *in vivo* studies would be needed to evaluate further changes in composition but also to assess the mechanisms involved after local injection of polyplex.

In both chapters, a range of ratios of polycation to immunostimulant were assessed for their different characteristics, ability to retain, and activate TLR. As stated in the conclusions, a larger ratio led to greater retention abilities but lower ratios had enhanced TLR activation. Further work should narrow down the ideal window of ratio that achieves a balance between retention and TLR activation. Other possibilities for future work in terms of the composition of the polyplex would be modifying the individual components to change the physical characteristics of the polyplex, using a different polycation, or using different immunostimulants. One significant factor in cellular uptake and local retention of therapy is particle size.[11] In this work, mixing unmodified polycation and immunostimulant led to the formation of a particle (excluding PLL + polyI:C) between 40-

150 nm in diameter which was not tunable based on ratio. An interesting extension of this work could be examining chemical modifications of the individual components to see if the particle size can be controlled- followed by determination of optimal size for uptake and decreased diffusion away from injection site.

In addition to the physical composition of the polyplex, other work may include using different polycations or different immunostimulants. For example, CpG comes in a few different classes that have different structures and slightly different *in vivo* effects. As discussed in chapter 1, much research has attempted to use modified versions of CpG to increase stability and increase efficacy. Similarly, for this work changing the CpG class or using modified versions could alter the polyplex characteristics but also impact the efficacy. While the use of a safe and approved drug as a delivery tool is attractive, some may argue that GA is difficult to use in this context due to its heterogeneity. Therefore, a great future branch of this work could include the design of an ideal polycation. Comparing both PLL and GA as polycations for delivery led to an interesting idea to design a peptide for delivery that has similar characteristics to GA in terms of the balance of hydrophobic and positive domains.

While the simulation of tissue retention experiments in this work provided information about the polyplex compared to the controls, further work could be done to improve the model. For example, CpG can be degraded *in vivo* by enzymes that cleave the DNA backbone therefore it would be valuable to examine the effect of the addition some of these physiological components to the hyaluronic acid. Additionally, ongoing efforts in the lab are working to create a model tumor using cross-linked hyaluronic acid and collagen with an aim to measure diffusion of therapy. In animals, there are plans to measure retention in HNSCC tumors using radiolabeled polyplexes for the GA + CpG polyplexes. In this study, a different radiolabel would be conjugated to each

component of the polyplex. This study design would be compelling for the evaluation of not only retention *in vivo* but also observing the interaction strength of polyplexes. In the case of some of the polyI:C polyplexes, it was hypothesized that the components were disassociating from each other in cell culture media or in the retention study. It would be very interesting to see after radiolabeling, if *in vivo,* the components separated and trafficked separately.

One critical future animal study would be determination of dose and ratio. As mentioned in Chapter 3, there may have been some anaphylaxis reactions for animals dosed with GA, which highlights the importance of optimizing the dose required. In chapter 3, CpG alone had enhanced tumor burden reduction than the two polyplexes but showed drastically increased systemic cytokines. One question raised with these results was whether the differences were a result of increased retention *in vivo* or rather availability of the immunostimulant within the polyplex-meaning in a polyplex of sufficient interaction strength, was the dose effectively lowered? Further, optimization of ratio has the same justifications as mentioned previously, balancing charge and interaction strength for optimized retention and efficacy. To elucidate mechanisms of retention after injection, another *in vivo* study could use electron microscopy to image tumor issue after injection. Previous work in the lab captured images of GA aggregating into spherical particles and sticking to muscle tissue upon injection, thus it would be curious to observe what occurs after injection of particles that are formed pre-injection as in the polyplexes. Finally, future studies should evaluate the use of these polyplexes in synergy with established immunotherapies like checkpoint inhibitors. While checkpoint inhibitors have had an enormous impact on cancer immunotherapy, it is estimated that only 12.46% of patients are receptive to the therapy.[16] Patients who have tumors with excluded immune cells, or ‘cold’ tumors, are much less likely to be have success with checkpoint inhibitors. Local administration of immunostimulants like polyI:C and

CpG can induce recruitment of immune cells to the tumor by activating an innate immune response and therefore could expand the reach of the checkpoint inhibitors.

References

1. Stalberg, C.; Loskog, A.; Klevenfeldt, M.; Essand, M.; Tötterman, T., *CpG Oligonucleotide Therapy Cures Subcutaneous and Orthotopic Tumors and Evokes Protective Immunity in Murine Bladder Cancer*. 2005; Vol. 28, p 20-7.
2. Salem, M. L.; Kadima, A. N.; Cole, D. J.; Gillanders, W. E., Defining the Antigen-Specific T-Cell Response to Vaccination and Poly(I:C)/TLR3 Signaling: Evidence of Enhanced Primary and Memory CD8 T-Cell Responses and Antitumor Immunity. *Journal of Immunotherapy* **2005,** *28* (3), 220-228.
3. Currie, A. J.; Van Der Most, R. G.; Broomfield, S. A.; Prosser, A. C.; Tovey, M. G.; Robinson, B. W. S., Targeting the Effector Site with IFN-αβ-Inducing TLR Ligands Reactivates Tumor-Resident CD8 T Cell Responses to Eradicate Established Solid Tumors. *The Journal of Immunology* **2008,** *180* (3), 1535-1544.
4. Bianchi, F.; Pretto, S.; Tagliabue, E.; Balsari, A.; Sfondrini, L., Exploiting poly(I:C) to induce cancer cell apoptosis. *Cancer Biology & Therapy* **2017,** *18* (10), 747-756.
5. Kumar, A.; Zhang, J.; Yu, F.-S. X., Toll-like receptor 3 agonist poly(I:C)-induced antiviral response in human corneal epithelial cells. *Immunology* **2006,** *117* (1), 11-21.
6. Krieg, A. M.; Yi, A.-K.; Matson, S.; Waldschmidt, T. J.; Bishop, G. A.; Teasdale, R.; Koretzky, G. A.; Klinman, D. M., CpG motifs in bacterial DNA trigger direct B-cell activation. *Nature* **1995,** *374* (6522), 546-549.
7. Wiethoff, C. M.; Middaugh, C. R., Barriers to Nonviral Gene Delivery. *Journal of Pharmaceutical Sciences* **2003,** *92* (2), 203-217.
8. Baoum, A. A.; Berkland, C., Calcium Condensation of DNA Complexed with Cell-Penetrating Peptides Offers Efficient, Noncytotoxic Gene Delivery. *Journal of Pharmaceutical Sciences* **2011,** *100* (5), 1637-1642.
9. Fu, J.; Cai, J.; Ling, G.; Li, A.; Zhao, J.; Guo, X.; Zhang, P., Cationic polymers for enhancing CpG oligodeoxynucleotides-mediated cancer immunotherapy. *European Polymer Journal* **2019,** *113*, 115-132.
10. Midoux, P.; Monsigny, M., Efficient Gene Transfer by Histidylated Polylysine/pDNA Complexes. *Bioconjugate Chemistry* **1999,** *10* (3), 406-411.
11. Lynn, G. M.; Laga, R.; Darrah, P. A.; Ishizuka, A. S.; Balaci, A. J.; Dulcey, A. E.; Pechar, M.; Pola, R.; Gerner, M. Y.; Yamamoto, A.; Buechler, C. R.; Quinn, K. M.; Smelkinson, M. G.; Vanek, O.; Cawood, R.; Hills, T.; Vasalatiy, O.; Kastenmüller, K.; Francica, J. R.; Stutts, L.; Tom, J. K.; Ryu, K. A.; Esser-Kahn, A. P.; Etrych, T.; Fisher, K. D.; Seymour, L. W.; Seder, R. A., In vivo characterization of the physicochemical properties of polymer-linked TLR agonists that enhance vaccine immunogenicity. *Nature Biotechnology* **2015,** *33* (11), 1201-1210.
12. Alhakamy, N. A.; Berkland, C. J., Glatiramer Acetate (Copaxone) is a Promising Gene Delivery Vector. *Molecular Pharmaceutics* **2019,** *16* (4), 1596-1605.
13. Alhakamy, N. A.; Kaviratna, A.; Berkland, C. J.; Dhar, P., Dynamic Measurements of Membrane Insertion Potential of Synthetic Cell Penetrating Peptides. *Langmuir* **2013,** *29* (49), 15336-15349.
14. Alhakamy, N. A.; Dhar, P.; Berkland, C. J., Charge Type, Charge Spacing, and Hydrophobicity of Arginine-Rich Cell-Penetrating Peptides Dictate Gene Transfection. *Molecular Pharmaceutics* **2016,** *13* (3), 1047-1057.
15. Alhakamy, N. A.; Elandaloussi, I.; Ghazvini, S.; Berkland, C. J.; Dhar, P., Effect of Lipid Headgroup Charge and pH on the Stability and Membrane Insertion Potential of Calcium Condensed Gene Complexes. *Langmuir* **2015,** *31* (14), 4232-4245.
16. Haslam, A.; Prasad, V., Estimation of the Percentage of US Patients With Cancer Who Are Eligible for and Respond to Checkpoint Inhibitor Immunotherapy Drugs. *JAMA Netw Open* **2019,** *2* (5), e192535-e192535.